Unveiling the role of Rhizaria in the silicon cycle

Natalia Llopis Monferrer

DOCTORAT SCIENCES BRETAGNE DE LA MER LOIRE ET DU LITTORAL

UBO Université de Bretagne Occidentale

THESE DE DOCTORAT DE

L'UNIVERSITE
DE BRETAGNE OCCIDENTALE

ECOLE DOCTORALE N° 598
Sciences de la Mer et du littoral
Spécialité : *Chimie Marine*

Par
Natalia LLOPIS MONFERRER

Unveiling the role of Rhizaria in the silicon cycle (Rôle des Rhizaria dans le cycle du silicium)

Thèse présentée et soutenue à PLouzané, le 18 septembre 2020
Unité de recherche : Laboratoire de Sciences de l'Environnement Marin

Rapporteurs avant soutenance :

Diana VARELA	Professor, Université de Victoria, Canada
Giuseppe CORTESE	Senior Scientist, GNS Science, Nouvelle Zélande

Composition du Jury :

Président :	Géraldine SARTHOU	Directrice de recherche, CNRS, LEMAR, Brest, France
Examinateurs :	Diana VARELA	Professor, Université de Victoria, Canada
	Giuseppe CORTESE	Senior Scientist, GNS Science, Nouvelle Zélande
	Colleen DURKIN	Research Faculty, Moss Landing Marine Laboratories, Etats Unis
	Tristan BIARD	Maître de Conférences, Université du Littoral Côte d'Opale, France
Dir. de thèse :	Paul TREGUER	Professeur des Universités, Université de Bretagne Occidentale, France
Co-dir. de thèse :	Aude LEYNAERT	Directrice de recherche, CNRS, LEMAR, Brest, France
Co-dir. de thèse :	Fabrice NOT	Directeur de recherche, CNRS, Station Biologique de Roscoff, France

Invité(s)
Jill SUTTON — Maîtresse de Conférences, Université de Bretagne Occidentale, Brest, France


UBO
Université de Bretagne Occidentale


Région
BRETAGNE


labex
MER


ISblue
The interdisciplinary
graduate school
for the blue planet


LEMAR
laboratoire des sciences
de l'environnement marin
UBO | CNRS | IRD | Ifremer


IRD
CNRS
UBO
IFREMER
iuem


1872
CNRS • SORBONNE UNIVERSITÉ
Station Biologique
de Roscoff

Unveiling the role of Rhizaria in the Silicon cycle

Natalia Llopis Monferrer

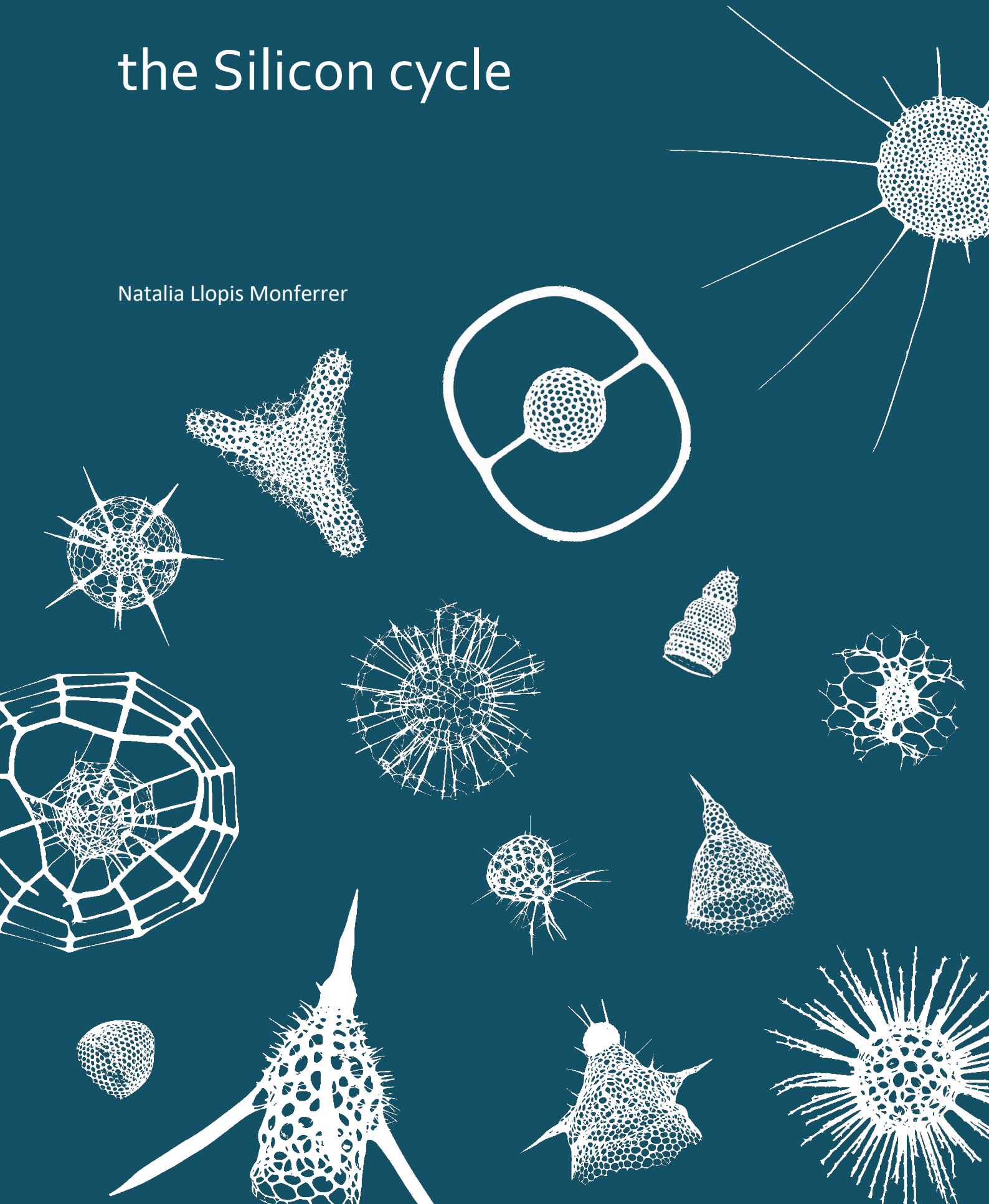

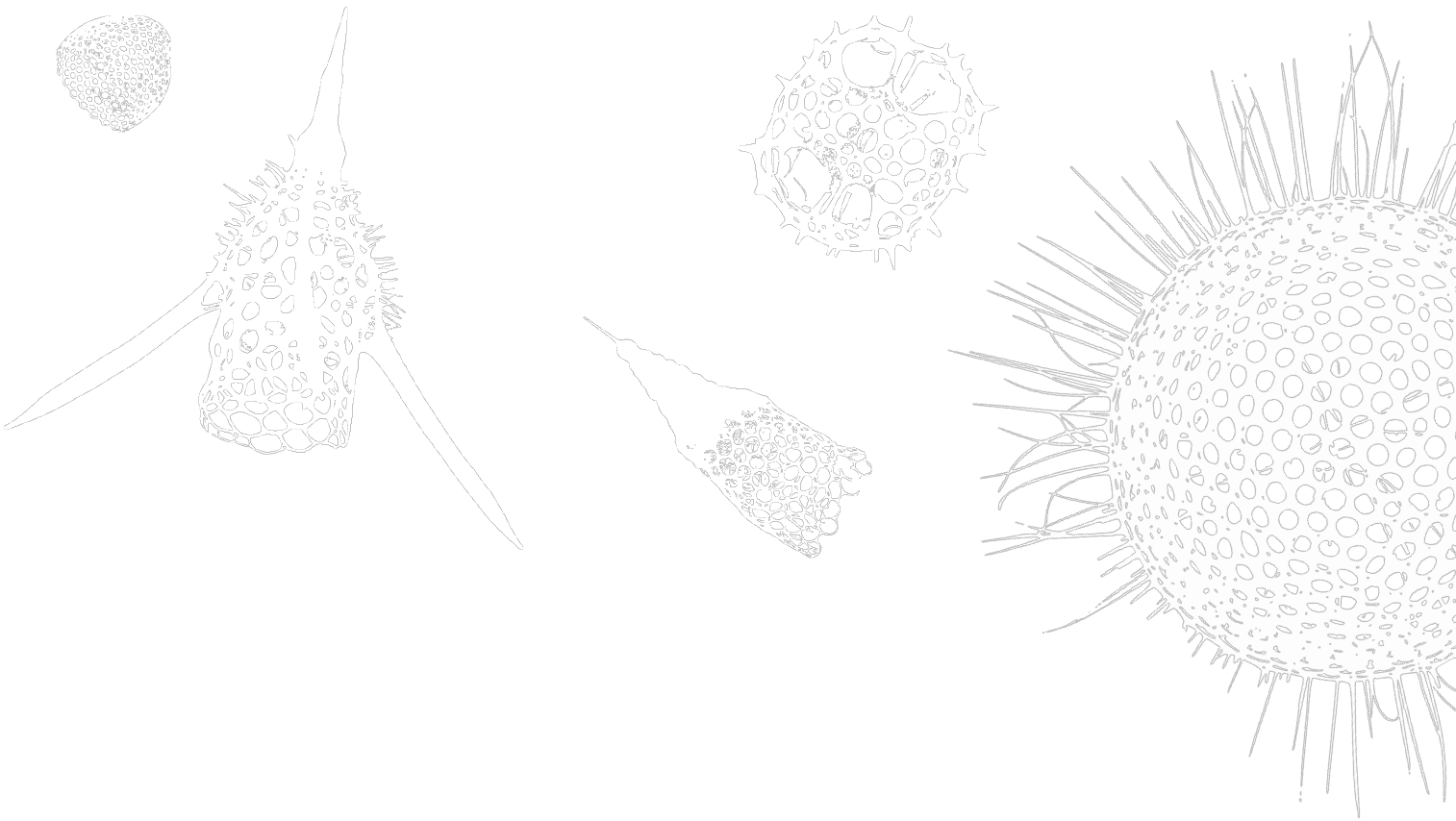

Drawings of Nassellaria and Spumellaria specimens from Miguel Méndez-Sandin pictures.

A mi familia

Acknowledgements

I would like to thank l'Université de Bretagne Occidentale and the LabexMer for funding these three years of PhD. I also thank Luis Tito de Morais, director of the Laboratoire des Sciences de l'environnement marin for hosting me in his laboratory.

I would like to extend my gratitude to the members of my committee, Diana Varela, Giuseppe Cortese, Colleen Durkin, Tristan Biard and Jill Sutton for accepting to evaluate my PhD thesis as well as the inclement timing of the presentation.

I would like to warmly thank all my supervisors, Paul, Aude et Fabrice. Merci beaucoup Aude de m'avoir fait confiance depuis notre premier Skype, quand je ne connaissais pas grand-chose sur les Rhizaria ni la silice. Merci d'avoir été là dès j'avais des questions, scientifiques et pas scientifiques. Merci pour ta bonne humeur sans limite, même quand j'oubliais les unités sur mes fichiers. Ça été un plaisir de partir à l'aventure avec toi et d'unifier les fabuleux mondes des Rhizaria et de la silice. Merci Paul de m'avoir ouvert les portes de l'univers de la silice et pour votre insatiable soif de connaissances, je n'aurais pas pu espérer meilleur mentor. Merci également d'avoir enrichi mon dictionnaire d'expressions françaises et brestoises. Fabrice, malgré l'encadrement à distance, je me suis toujours sentie soutenue. Ton esprit scientifique critique a vraiment marqué une différence dans mes travaux, bref, merci de m'avoir introduit au monde magnifique des Rhizaria. Merci à tous de m'avoir donné l'opportunité de voyager et découvrir des Rhizaria autour du globe. Je me rappellerai grâce à vous avec émotion de la traversée de l'équateur et des manchots de la mer de Ross.

Quería agradecer a Demetrio Boltovskoy toda su ayuda y paciencia y porque ha sido una gran fuente de inspiración. Merci Tristan pour ton aide et tes retours, grâce à toi, le monde de l'imagerie n'a (presque) plus de secrets pour moi. Mais je crois que je vais encore avoir besoin de ton aide pendant un petit moment.

Je voulais remercier le LEMAR et toutes les personnes que j'ai pu côtoyer quotidiennement pendant ces trois années. Je veux notamment remercier Morgane Gallinari, d'avoir égayé mes heures au laboratoire, qui auraient été bien moins sympas sans elle. Merci Manon pour l'aide avec les analyses et les petits footings du midi (il va falloir les reprendre). Merci beaucoup Jill pour tes conseils et ton soutien. Merci à Gene, Anne-So, Yves, Natalie, Elodie[2], Elisabeth pour

l'aide avec la paperasse. Muchas gracias Bea, por ser tan linda y haberme enseñado la belleza del plancton.

Merci aux roskovites et l'équipe ECOMAP. Merci à Éric Thiébaut pour son aide en stats, Christian Jeanthon, Florence, Pris, Fabienne, Joost, Mathilde, Miguel, Morgane et plein d'autres !

I cannot forget to thank people with who I shared valuable time at sea. Many thanks to Chata, Hans, Andreia, Afonso, Cecilia, Carol, Wade, John, Giorgio, Igor, Glen, Karl, Mark, Pablo Escobar (yes, I can say I've been on a cruise with him!), Magali and so many other people I had the pleasure to sail with. Muchas gracias a Miguel, quien ha compartido todo, desde sus mejores fotos de radiolarios hasta las mejores pistas para diferenciar un spumellaria de una diatomea. Muchas gracias a Andrés por haber confiado en mí y por haberme ayudado a subirme, junto con mis cajas en el Tangaroa. Et bien sûr Briva, c'était un vrai plaisir de partager une belle campagne avec toi, sans oublier (même si ça peut arriver d'être tête en l'air), toutes les heures passées à sucer des radiolaires.

J'ai fait mes premiers pas d'océanographe en herbe à Villefranche-sur-Mer grâce à une très belle équipe. Merci Lars, Lionel, Fabien, Marc, Amanda, Baptiste, Corinne et Simon, qui m'ont aidé il y déjà quelques années et qui ont continué à m'aider durant ma thèse.

A huge thanks to my office mates, Hannah, Natasha, David, Marie, Debany, Manu, Wen-Hsuan and María to have shared all those wonderful times everywhere and always. Thanks for the patience, for correcting my English and listening to my scientific dramas, you are the best.

Je ne peux pas oublier mes amis doctorants. Chloé et Nico qui m'ont montré que coder peut être facile (pour eux), Jordon, qui m'a aidé à organiser mes campagnes et à renforcer mon psoas. Merci à tous les autres, Elyne, Pauline, Sarah, Julien, Justine^2, Leslie, Gabin, Mariana, Romina, José, Will, Aurélien, Anaïs, Kevin et un long etcétéra pour les bons moments de rigolade.

Muchas gracias a mis amigos, que a pesar de estar lejos, los siento siempre cerca. Palo y Lidia por seguirme hasta al polo norte si hace falta. Auro, por tus consejos, echo de menos las charlas después de la piscina. A Mau, Álvaro, Candel y todos los de la playa, por seguir siendo como sois, no cambiéis nunca. A todos los saguntinos, pero sobre todo a Paloma, por ser siempre la más luchadora, un verdadero ejemplo a seguir. No me puedo olvidar de mis

queridas gaditanas, Nora, Zo, Meli y Arlet, que aunque elegimos caminos distintos hace mucho tiempo, adoro esos momentos en los que se vuelven a juntar.

Merci à Marc, pour toute la patience. Gracias por haber convertido el confinamiento y el final de la tesis en momentos inolvidables, el mejor compañero de viaje.

Por supuesto no me olvido de mi familia (la de Llopis y la de Monferrer). Si estoy aquí es gracias a vosotros, que siempre me habéis apoyado, desde el primer momento en que decidí embarcarme en esta aventura de oceanógrafa. Al tete, por aguantarme cada vez que le pido un dibujo o cualquier otra cosa que se le pueda ocurrir a mi cabecita. A Miguel, por haber conseguido sin saberlo, hacer de mi la tía más feliz del mundo.

Enfin, je voulais remercier toutes les personnes que je n'ai pas cité précédemment mais qui m'ont aidé de près ou de loin dans cette aventure.

Résumé

Les radiolaires polycystines et les phaeodaires sont des organismes unicellulaires eucaryotes (*i.e.*, protistes) hétérotrophes marins appartenant au super-groupe des Rhizaria. Ces protistes, qui présentent des tailles allant de quelques micromètres à quelques millimètres, sont présents à la surface et dans les profondeurs de l'ensemble des océans. De nombreux Rhizaria utilisent le silicium dissous dans l'eau de mer pour construire un squelette de silice. Les squelettes robustes des Rhizaria préservés dans les sédiments sont particulièrement précieux pour les micro-paléontologues pour la reconstitution des paléo-environnements. Bien qu'ils soient largement étudiés par les micro-paléontologues, l'écologie et la contribution des Rhizaria au fonctionnement des écosystèmes marins actuels sont demeurés jusqu'à présent largement inexplorés.

La première partie de cette thèse est dédiée à la mesure des taux d'absorption du silicium par les Rhizaria à l'aide du radio-isotope ^{32}Si et à la mesure de la composition élémentaire (C ; N ; Si) d'organismes appartenant à plusieurs groupes taxinomiques. Les différents spécimens ont été collectés en 2017, 2018 et 2019, lors de trois campagnes océanographiques (MOOSE-GE 17, AMT28, TAN1901) en mer Méditerranée, océan Atlantique et mer de Ross. Nous avons observé une production de silice biogène par cellule très élevée chez les Rhizaria (jusqu'à 11.9 nmol de Si cellule^{-1}j^{-1}) en comparaison avec les diatomées (0.001-21 pmol-Si cellule^{-1}j^{-1}). Avec des teneurs en silicium allant jusqu'à 9 nmol-Si cellule^{-1}, ces organismes apparaissent parmi les plus silicifiés des organismes planctoniques. Une première évaluation de leur contribution au cycle biogéochimique de la silice dans l'océan mondial a été réalisée en combinant les résultats de nos expériences avec des données d'abondance publiées précédemment. Les Rhizaria pourraient contribuer de 4 à 22% à la production de silice biogène de l'ensemble des océans.

L'abondance, la biomasse et la diversité des Rhizaria ont été quantifiées dans le bassin nord-ouest de la Mer Méditerranée en combinant simultanément des techniques innovantes d'imagerie (FlowCAM, Zooscan et UVP) et des techniques metabarcode afin de couvrir la large gamme de taille de ces organismes. Cette approche a révélé que les petites cellules sont les plus nombreuses mais les grosses cellules constituent l'essentiel de la biomasse. L'ensemble représente jusqu'à 6% de la silice biogène des 500 premiers mètres de la colonne d'eau en Méditerranée.

Cette thèse fournit des données quantitatives uniques mettant en évidence le rôle fondamental des Rhizaria siliceux dans les océans contemporains. Elle souligne également la nécessité d'explorer davantage les profondeurs de l'océan pour affiner notre première estimation de la contribution des Rhizaria au cycle biogéochimique du Si à l'échelle locale et mondiale.

Abstract

Polycystine radiolaria and phaeodarians are unicellular eukaryotic (*i.e.*, protist) heterotrophic marine organisms belonging to the Rhizaria supergroup. These protists, which range in size from a few micrometers to a few millimeters, are present from the surface to the bathypelagic waters of all oceans. Many Rhizaria use dissolved silicic acid in seawater to build a silica skeleton. The robust skeletons of Rhizaria preserved in sediments are particularly valuable for paleoceanographic reconstructions. Although widely studied by micro-paleontologists, the ecology and contribution of Rhizaria to the functioning of contemporary marine ecosystems has remained largely unexplored so far.

The first part of this thesis is dedicated to the measurement of silicic acid uptake rates by Rhizaria using the ^{32}Si radioisotope and the elementary composition (C; N; Si) of organisms belonging to several taxonomic groups. The different specimens were collected in 2017, 2018 and 2019 during three oceanographic expeditions (MOOSE-GE 17, AMT28, TAN1901) in the Mediterranean Sea, Atlantic Ocean and Ross Sea. We observed a very high production of biogenic silica per individual in Rhizaria (up to 11.9 nmol-Si $cell^{-1}d^{-1}$) compared to diatoms. With biogenic silica cellular contents up to 9 nmol-Si $cell^{-1}$, Rhizaria appear among the most silicified of planktonic organisms. A first assessment of their contribution to the biogeochemical cycling of silica in the world ocean has been made by combining the results of our experiments with previously published abundance data. Rhizaria could contribute between 4 and 22% to the biogenic silica production of the global ocean.

The abundance, biomass and diversity of Rhizaria have been quantified in the north-western basin of the Mediterranean Sea by simultaneously combining innovative imaging techniques (FlowCAM, Zooscan and UVP) and metabarcode techniques to cover the wide size range of these organisms. This approach has revealed that small cells are the most numerous but large cells constitute the bulk of the biomass. Together they account for up to 6% of the biogenic silica in the first 500 metres of the Mediterranean water column. This work provides unique quantitative data that highlight the impact of Rhizaria in the cycling of Si in contemporary oceans. This thesis also reveals the need to explore further the deep ocean to refine our first estimates of Rhizaria contribution to the Si biogeochemical cycle at local and global scales.

Contents

Introduction

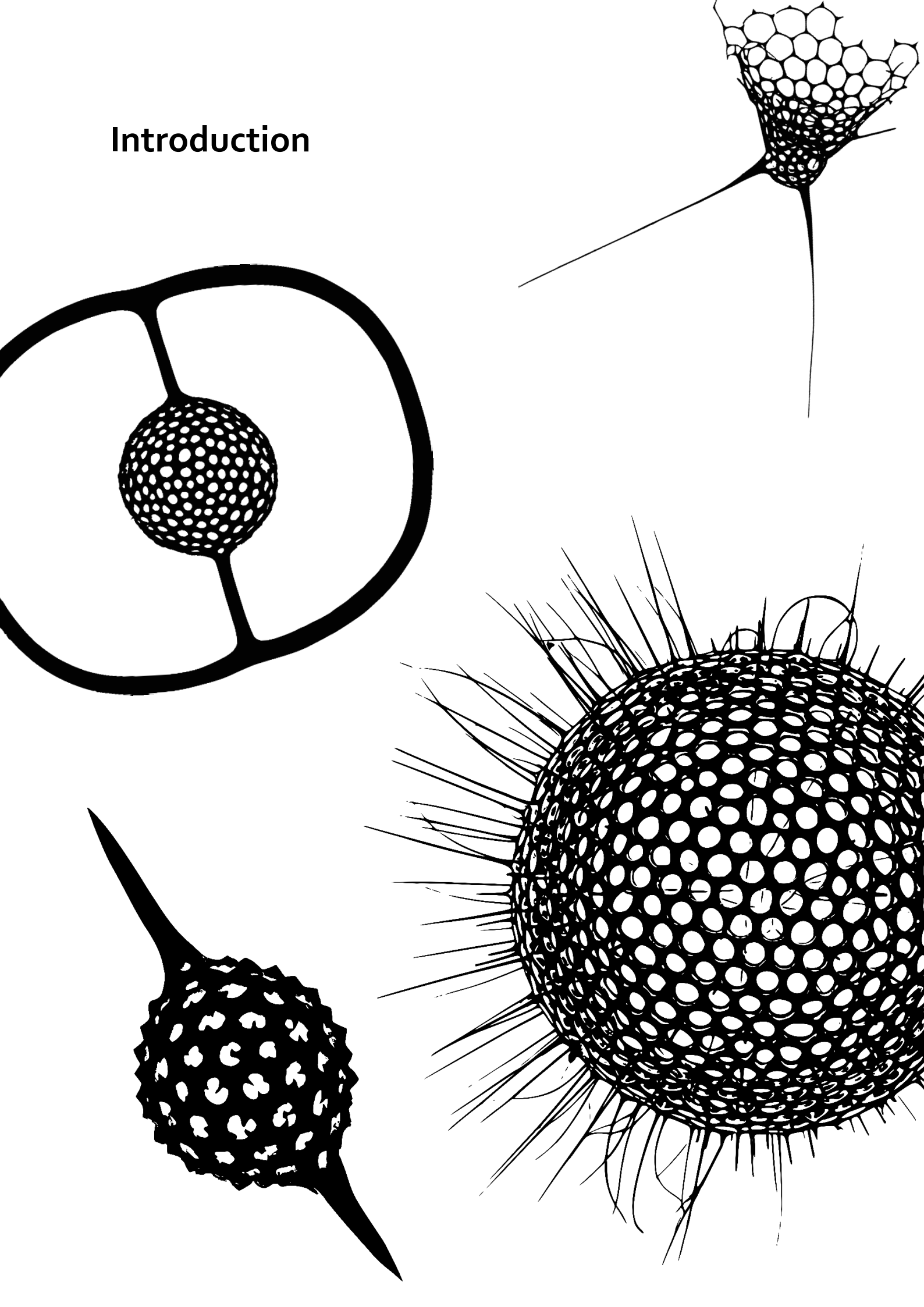

Drawings of Nassellaria and Spumellaria specimens from Miguel Méndez-Sandin pictures.

1. Silica and the marine silicon cycle

Silicon (Si) is the second most abundant element in Earth's crust. Silicon atoms bond with oxygen (O) atoms to create silicon dioxide (SiO_2), also known as silica, which may be either crystalline or amorphous. This element cycles through the marine environment (Figure 1), entering the ocean primarily from rivers. Other secondary sources include submarine groundwater, erosion of marine soils, hydrothermal vents and aeolian inputs. In the ocean, Si is essentially found as dissolved silicic acid (dSi), which is required for the growth of some phytoplankton groups like diatoms and other silicified planktons, such as radiolarians and phaeodarians, sponges, silicoflagellates and several species of choanoflagellates. These organisms, commonly called "silicifiers", remove dSi from the ocean to build their cell tests. After they die, their test acts as ballast, thus causing themto sink toward the ocean floor. While sinking, most of the Si recycles throughout the water column, being again available as dSi for other silicifiers. The fraction of the cells that resists dissolution reaches the sea-floor, where they can either remain, forming a siliceous ooze, or dissolve and return to the upper layers of the ocean through upwelling processes.

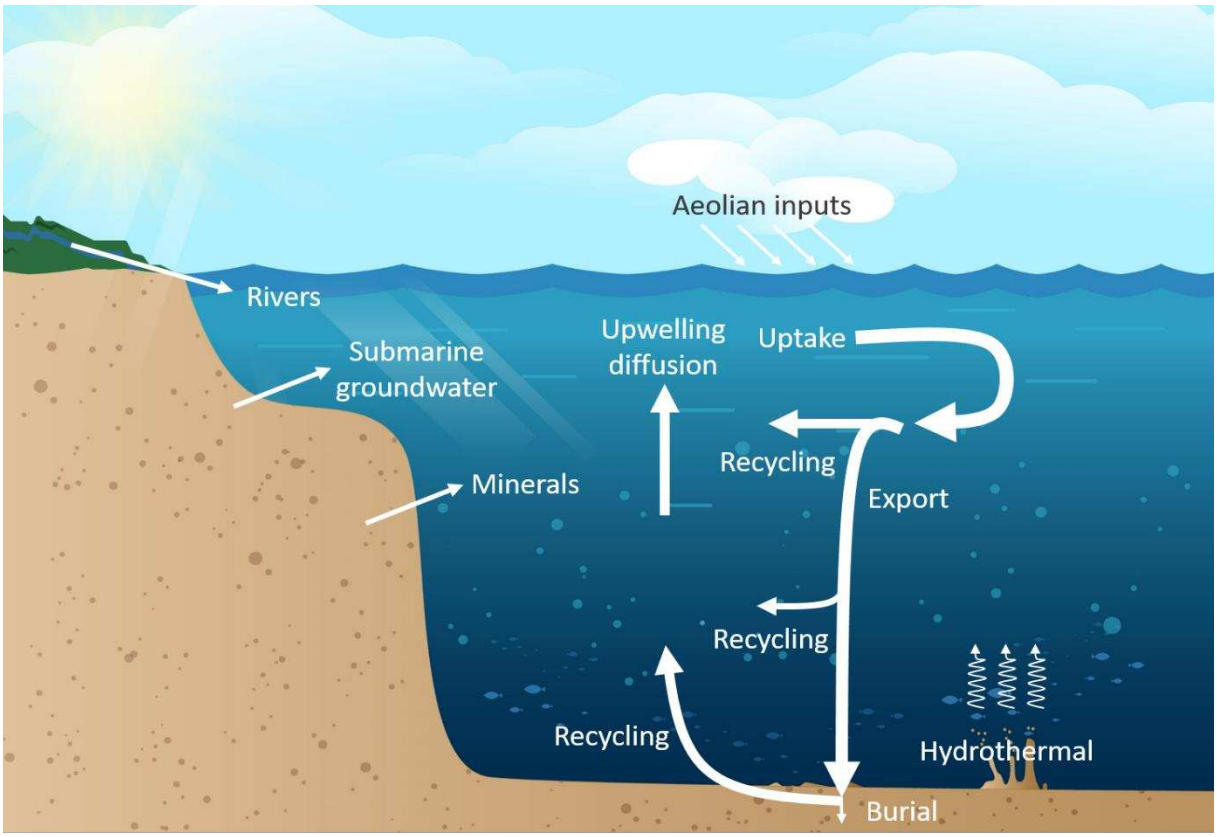

Figure 1. Cycling of silica in the marine environment. Adapted from Tréguer and De La Rocha (2013).

The Si cycle is intimately connected to other biogeochemical cycles, like those of carbon and nitrogen. These cycles interact via marine primary production, which drives atmospheric CO_2 sequestration to the deep ocean via the biological pump and, ultimately, exerts control over the Earth's climate (*e.g.*, Buitenhuis et al., 2006; Reynolds, 2001).

Among organisms that require Si to grow, diatoms have been the main focus so far. The production of bSi in the oceans by diatoms has been estimated to 240 Tmol Si yr^{-1} (Nelson et al., 1995). Diatoms largely dominates all other biogeochemical fluxes in the Si cycle (Tréguer and De La Rocha, 2013). However, the contribution of other silicifiers, like sponges and Rhizaria, is poorly documented.

Since the late 20th century, silicified rhizarians have drawn attention for their role in the marine Si cycle (Heath, 1974). Takahashi (1983) suggested that, in some oceanic areas, the daily flux of rhizarian biogenic silica (bSi) ranges around 20% to 30% of the overall bSi.

Recent studies combining genomic and *in situ* imaging data have evidenced that densities of siliceous Rhizaria, have so far been underestimated. Biard et al. (2016) reported that some Rhizaria taxa represent approximately 33% of the large zooplankton (>600 µm) in the upper water column. Guidi et al. (2016) pointed out Rhizaria's significant involvement in the export of C to the deep ocean, with their abundances correlating with export C fluxes at 150-m depth in oligotrophic oceanic regions. These studies have raised awareness of the global significance of Rhizaria in the biological pump, as well as in the Si cycle.

2. Rhizaria, conspicuous organisms in the ocean

Oceanic Rhizaria are a very diverse microplankton group that have existed at least since the Cambrian era (~500 million years ago). This group of protists is a major lineage of eukaryotes, including Cercozoa and Retaria (Cavalier-Smith, 2002), with the latter grouping Radiolaria and Foraminifera (Figure 2).

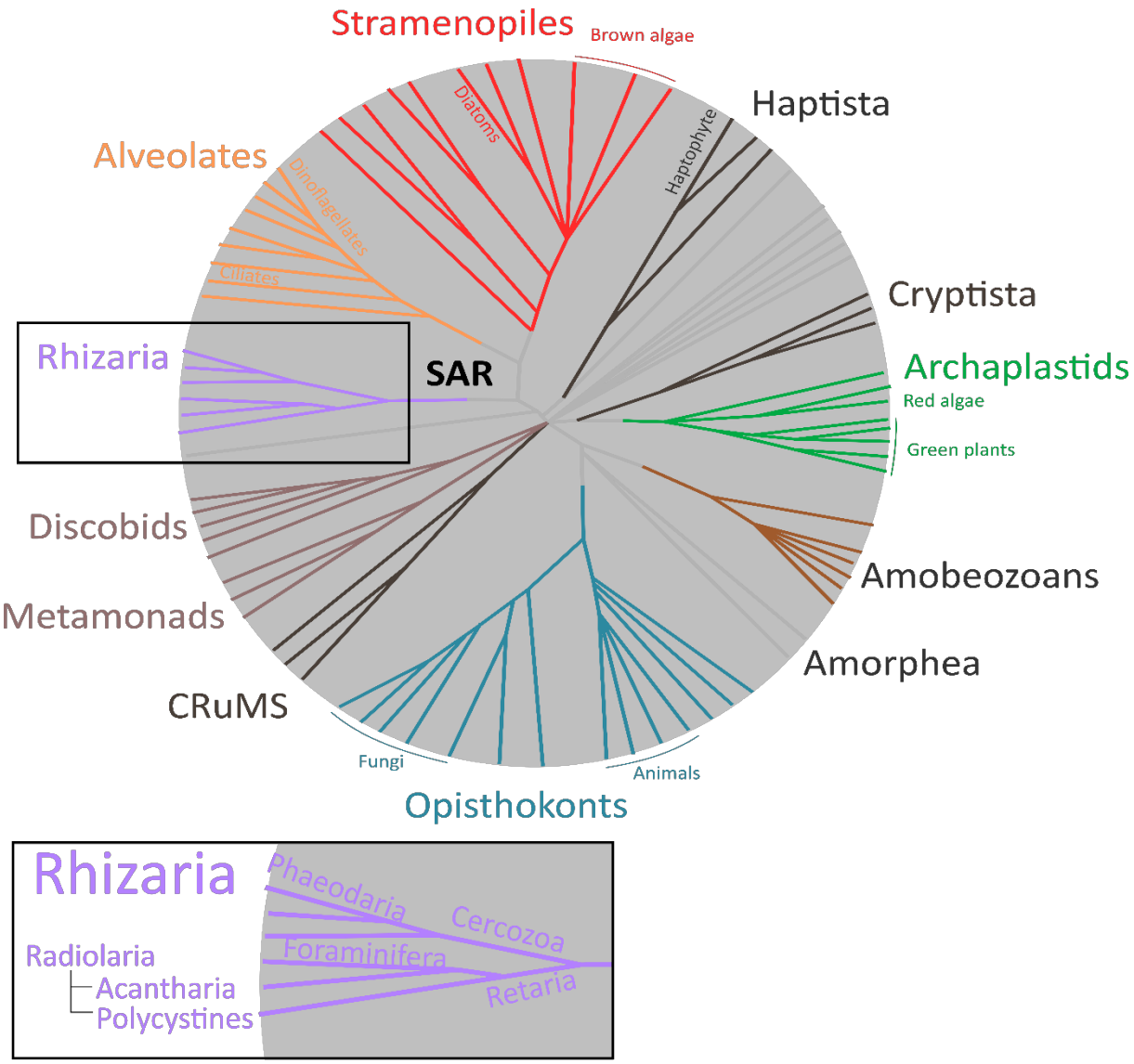

Figure 2. Schematic of the eukaryotic tree based on a consensus of phylogenomic together with morphological and cell biological information. SAR is the conglomerate of Stramenopiles, Alveolates, and Rhizaria, which together make an assemblage encompassing perhaps half of all eukaryote diversity. CRuMS is an amalgamation of several 'orphan' taxa: the Collodictyonids, Rigifilida, and Mantamonas. Adapted from Keeling and Burki (2019).

Essentially unicellular though some are capable of forming colonies up to over 1 m in length, Retaria span a wide range of sizes, from tens to hundreds of micrometers (Boltovskoy et al., 2017).

Some species of Retaria have elaborate mineral skeletons of strontium sulfate (Acantharia), calcium carbonate (Foraminifera) and opaline silica (Nassellaria, Spumellaria and Phaeodaria). Radiolaria are divided into two major lineages: the Polycystinea (including the three orders: Nassellaria, Spumellaria and Collodaria) and the Spasmaria (including Acantharia and

Taxopodida; Krabberød et al., 2011). Phaeodaria, initially classified in Radiolaria, is now placed among the Cercozoa as revealed by molecular phylogeny (Polet, 2004).

The work performed during this thesis focuses on the silicifying Rhizaria (polycystine Radiolaria and Phaeodaria). The study of these planktonic protists has been essentially used for paleoceanographic reconstructions, based on the fossil record left by their silicified skeletons in oceanic sediments (Matsuzaki et al., 2014; Moore, 1978). Almost all polycystine species preserve well in the bottom sediments while most Phaeodaria skeletons dissolve more readily before reaching the sea-floor (Takahashi, 1983).

Despite their potential role as Si consumers and C exporters (*e.g.*, Lampitt et al., 2009; Takahashi, 1983) in the marine environment, very little is known about their physiology, life cycle and ecology, particularly regarding silica. This is essentially due to the difficulty of culturing Rhizaria, as well as the delicate morphologies of living specimens which make them liable to collapse when using conventional sampling methods.

2.1. Cell structure

Polycystine radiolarian and Phaeodaria skeletal morphology can be very variable depending on the taxa considered (Figure 3). Generally, their ornamented skeletons surround a central and porous capsule from which pseudopodia (long and slender cytoplasmic projections) radiate.

Skeletons in protists are believed to play a role in essential functions. For instance, for the microalgae diatoms it has been proven that the skeleton provide mechanical protection for the cell against predators (Finkel and Kotrc, 2010; Hamm et al., 2003), as well as an effective pH buffer (Milligan, 2002). Less is known about the role of the Rhizaria's skeletons, but it is likely to improve the uptake or storage of bio-essential elements (Suzuki and Not, 2015).

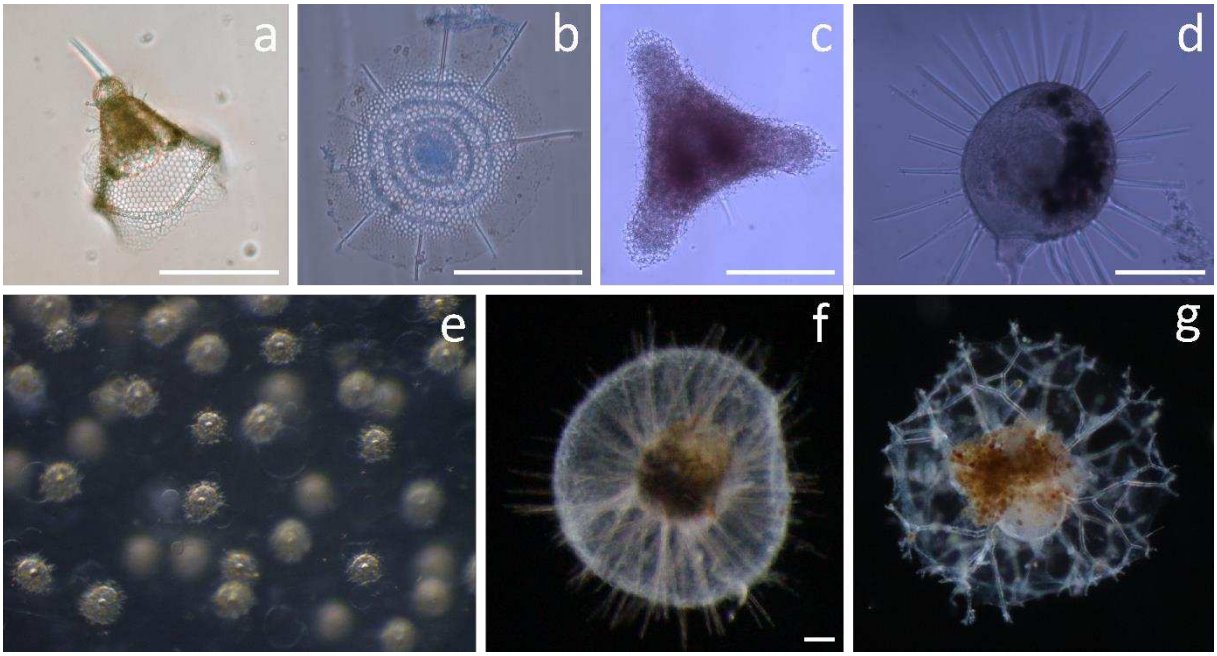

Figure 3. Representative examples of taxonomic groups analyzed in this thesis (scale bar when available 100 µm). (a) Nassellarian of the family Plagiacanthidae, (b) Spumellarian of the superfamily Stylodictytoidea, (c) Spumellarian of the superfamily Spongodiscidae, (d) Phaeodarian of the family Challengeridae (*Challengeron sp.*), (e) Detail of central capsule of a colonie of Collodarian, family Sphaerozoidea, (f) Phaeodarian of the family Aulacanthidae (*Aulacantha scolymanta*), (g) Phaeodarian of the family Coelodendridae (*Coelechinus sp.*). Pictures N. Llopis Monferrer except picture (e), taken by A. Leynaert.

Polycystine Radiolaria. Most Nassellaria, Spumellaria and siliceous Collodaria possess solid and dense skeletons of amorphous silica, so-called opal (SiO_2) (Figure 4).

Nassellaria present a heteropolar skeleton with one or more sections aligned along an axis. From the narrower end, the cephalis, which is the first to be formed, several segments succeed: cephalis, thorax and abdomen (Boltovskoy et al., 2017). Skeletons vary from simple tripods to elaborate, helmet-shaped structure, often with spines or other ornamentations (Boltovskoy et al., 1990).

Most Spumellaria have radial or spherical symmetry with centrifugal shell-growth, but their skeleton can also be flat or elliptical (Suzuki and Not, 2015). The nucleus is located in the central capsule and it is surrounded by radially arranged lobes of cytoplasm, enclosed by a porous capsular wall.

Collodaria is the only taxon with colonial representatives, which can be composed of tens to thousand cells. Each colony consists of a spheroidal, hollow, gelatinous envelope containing numerous interconnected cells embedded within a gelatinous matrix (Anderson et al., 1987). Cells can be either naked (*e.g.*, *Collozoum* sp.), or surrounded by a porous, spherical Si skeleton

(*e.g.*, *Collosphaera globularis*) or provided with siliceous spines embedded in the cytoplasm (*e.g.*, *Sphaerozoum* sp.).

Phaeodaria. Phaeodarians are often larger than polycystine individuals. Their cell size ranges from several hundreds of micrometres up to several millimetres. Phaeodaria's skeleton is also composed of amorphous silica but is more porous and less solid than polycystine's skeletons (Nakamura et al., 2018). The porosity of their skeleton and the organic matter content in their test is presumably responsible for the poor preservation of these organisms in the fossil record (Takahashi et al., 1983). As for Radiolaria, their geometry is complex and varies among families. This group is mainly defined by a central capsule containing the phaeodium, a mass of partially digested food, generally darkly coloured that emanates from the astropyle, which resembles an oral aperture (Figure 4). Phaeodarians possess a double-walled central capsule and the skeletal network can be surrounded by filopods.

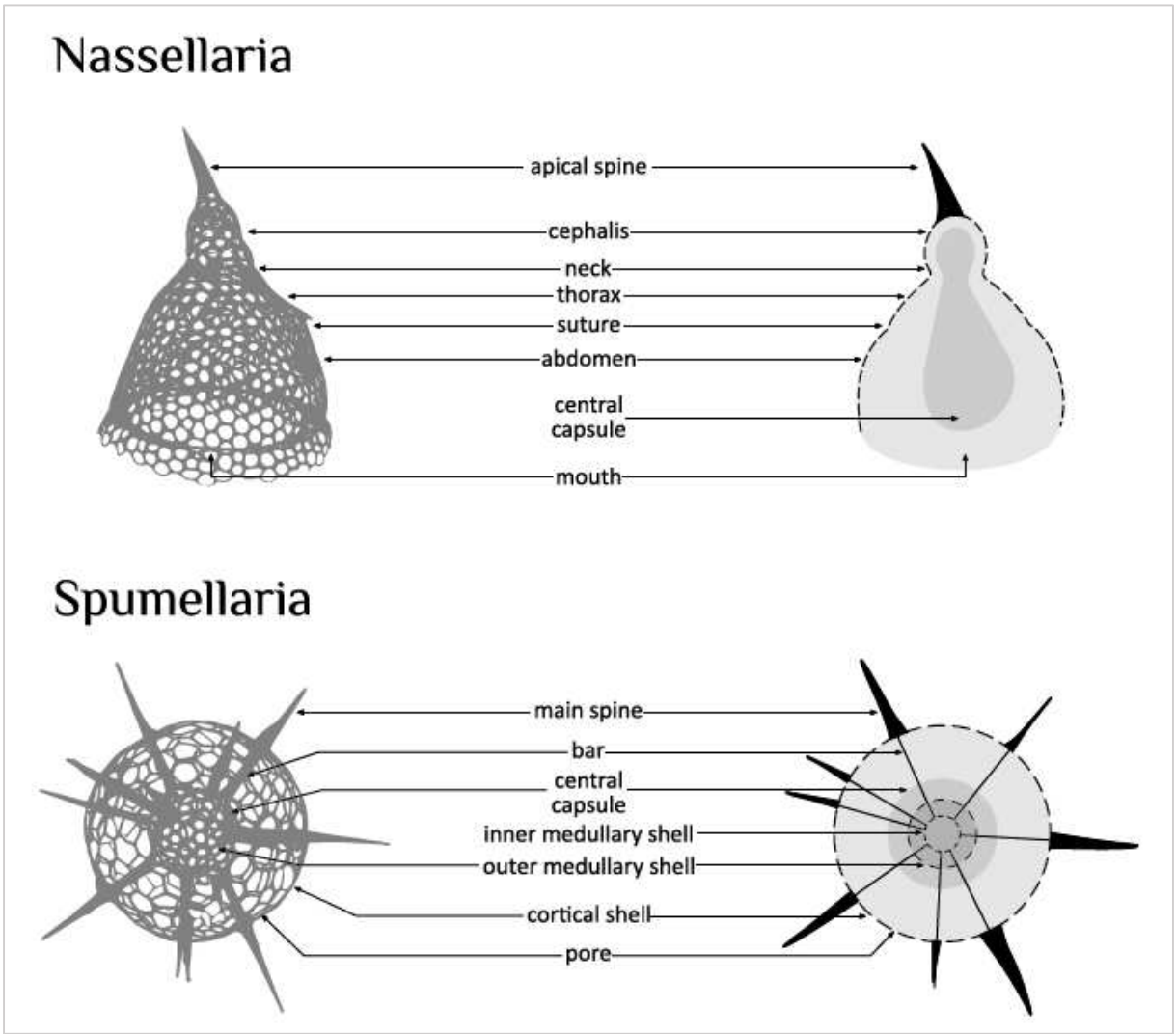

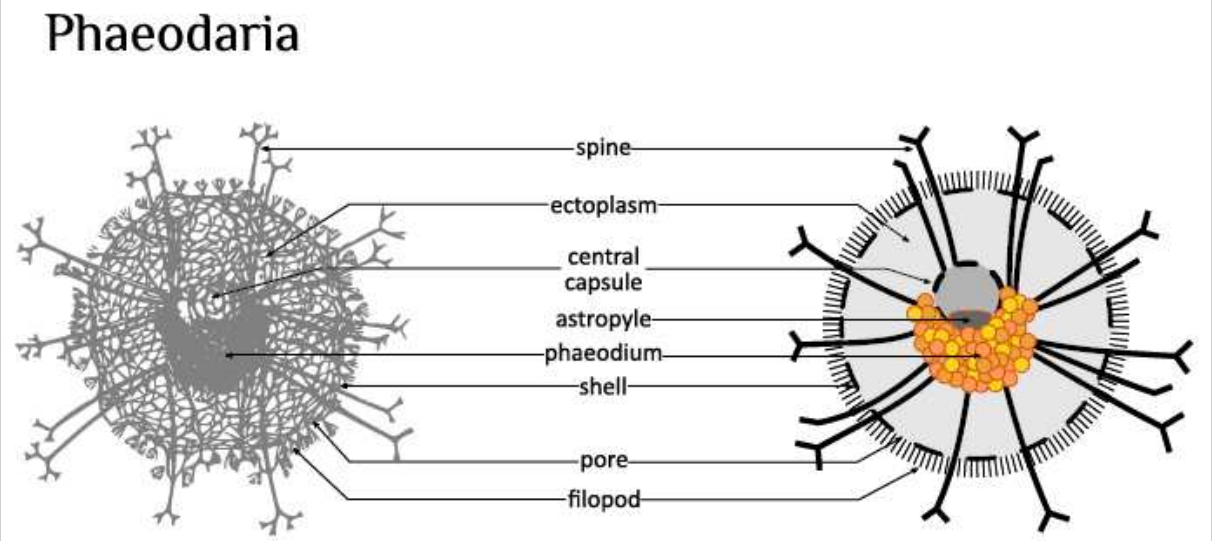

Figure 4. Scheme of the skeletal elements of the shell of a typical Nassellaria, Spumellaria and Phaeodaria (Adapted from Boltovskoy et al., 2017). The right-hand scheme refers to the soft parts compared to the left-hand one, which refers to the skeleton alone.

2.2. General biology and ecology

Place in the trophic network. Despite the ubiquity of these organisms in the oceans, fundamental information about their feeding behaviour is poor. These protists are mainly heterotrophic, as they can capture preys through adhesion to their pseudopodia.

Polycystine consume a wide variety of prey, from bacteria and algae up to small invertebrates (Gowing and Coale, 1989). Beside the heterotrophic behaviour, many polycystine inhabiting surface waters, exhibit symbiotic microalgae providing nutrients to the host (Decelle et al., 2015). Phaeodarians are omnivorous, they can feed on other plankton or on organic suspended matter in the water column (Gowing, 1986). Unlike many polycystine, no Phaeodaria have been reported harbouring microalgal symbiont so far.

Very little is known about the predatory pressure on Rhizaria, although there are evidences of other plankton such as Foraminifera, salps and small crustaceans preying on Rhizaria (Gowing 1989; Swanberg, 1979).

Reproduction. Rhizaria are difficult to keep alive in cultures and our knowledge about their life cycle is incomplete (Suzuki and Not, 2015).

For several species of Nassellaria, Spumellaria and Collodaria it has been observed that after organisms have turned whitish, they release small bi-flagellated cells generally called swarmers (Suzuki and Not, 2015).

For Collodaria, binary fission within the central capsule has been reported as well as swarmer production (Anderson and Gupta, 1998; Biard et al., 2015).
Phaeodaria species have also been observed to reproduce by cell division and swarmer production (Hughes et al., 1989), but the entire life cycle has never been replicated in the laboratory.
Data about the longevity of Rhizaria is limited. Based on laboratory observations, it seems that Rhizaria can live from several weeks to several months, likely depending on the taxa, before reproducing (Boltovskoy et al., 2017).

2.3. Silicification

The general process of silicification has been essentially studied for diatoms. This complex process involves the transport of Si (mediated by Si transporters or by diffusion) across the cell membrane and then through the cytoplasm to the site of polymerisation within the silica deposition vesicle (SDV) (Martin-Jezequel et al., 2000; Thamatrakoln and Hildebrand, 2008). Although the presence of Si transporters that enable the uptake of dSi from the environment have recently been reported in rhizarians (Marron et al., 2016), the physiological and morphological factors regulating Rhizaria skeleton morphogenesis are poorly documented.

One of the first statements about the Rhizaria skeletal secretion was made by Haeckel in the 19th century:

> *"It may indeed be assumed that these skeletons arise directly by a chemical metamorphosis (silicification, acanthinosis, etc.) of the pseudopodia and protoplasmic network; and this view seems especially justified in the case of the Astroid skeleton of the Acantharia, the Spongoid skeleton of the Spumellaria, the Plectoid skeleton of the Nassellaria, the Cannoid skeleton of the Phaeodaria, and several other types. On closer investigation, however, it appears yet more probable that the skeleton does not arise by direct chemical metamorphosis of the protoplasm, but by secretion from it; for when the dissolved skeletal material (silica, acanthin) passes from the fluid into the solid state, it does not appear as imbedded in the plasma, but as deposited from it However, it must be borne in mind that a hard line of demarcation can scarcely, if at all, be drawn between these two processes." [Haeckel, 1887, p.CXXXIV]*

Anderson (1981, 1994) suggested the presence of SDV in polycystine radiolarians, similar to that found in diatoms. Recent studies have used a fluorescence compound, the PDMPO ((2-(4-pyridyl)-5-[(4-(2-dimethylaminoethylaminocarbamoyl) methoxy)-phenyl] oxazole) to elucidate the silicification process in Rhizaria. This compound binds with Si under acidic conditions, emitting a green fluorescence under ultraviolet light, that allows the imaging of newly deposited Si. These studies have also suggested the deposition of Si in an acidic compartment, likely a SDV (Ogane et al., 2010, 2009).

So far, three silicification processes have been reported for Polycystine radiolarians (Anderson et al., 1987; Boltovskoy et al., 1990) (i) Rim growth: which is found in porous shells. The Si deposition occurs on the rims/edges of the pores which become smaller in diameter during maturation. (ii) Bridge growth, which consists of the production of rod like elements that grow from one node of the cell to another resulting in a more complex skeleton (Anderson, 1983). (iii) Intermittent growth: polycystines intermittently assimilate siliceous matter within pseudopodia. This Si is quickly transferred to the cytokalimma —which is a cytoplasmic sheath— where it is deposited on the skeleton (Ogane et al., 2014).

For Collodaria and Phaeodaria, the silicification processes are less known; further application of the PDMPO method could solve this problem.

The porosity of the skeletons depends on the species considered. This is an important feature with respect to the Si biogeochemical cycle as it affects the sinking rate, the dissolution rate of the cell's skeleton in the water column as well as in sediments after reaching the sea-floor (Takahashi, 1983).

2.4. Distribution and biogeography

Rhizaria are exclusively marine organisms, with the exception of the Nassellaria species *Lophophaera rioplatensis*, whose presence has been reported in low salinity waters of Río de la Plata in Argentina (Boltovskoy, 2003). In contrast to the diatoms, which are photosynthetic and reside in the upper layers of the ocean, Rhizaria live throughout the water column, from the surface waters to the deep sea (Suzuki and Not, 2015).

Latitudinal distribution and biogeography. Although Rhizaria can be found in every ocean, they are generally absent in shallow coastal areas. However, they are present in some

coastal regions with narrow continental shelf and abrupt depth changes, influenced by oceanic waters and upwelling systems, such as Villefranche-sur-mer at the Côte d'Azur (France), off the coast of California (USA) and in Norwegian fjords. Boltovskoy and Correa (2016) recently defined six major geographic provinces based on different polycystine assemblages collected using plankton net, sediment trap and surface sediment samples (Figure 5).

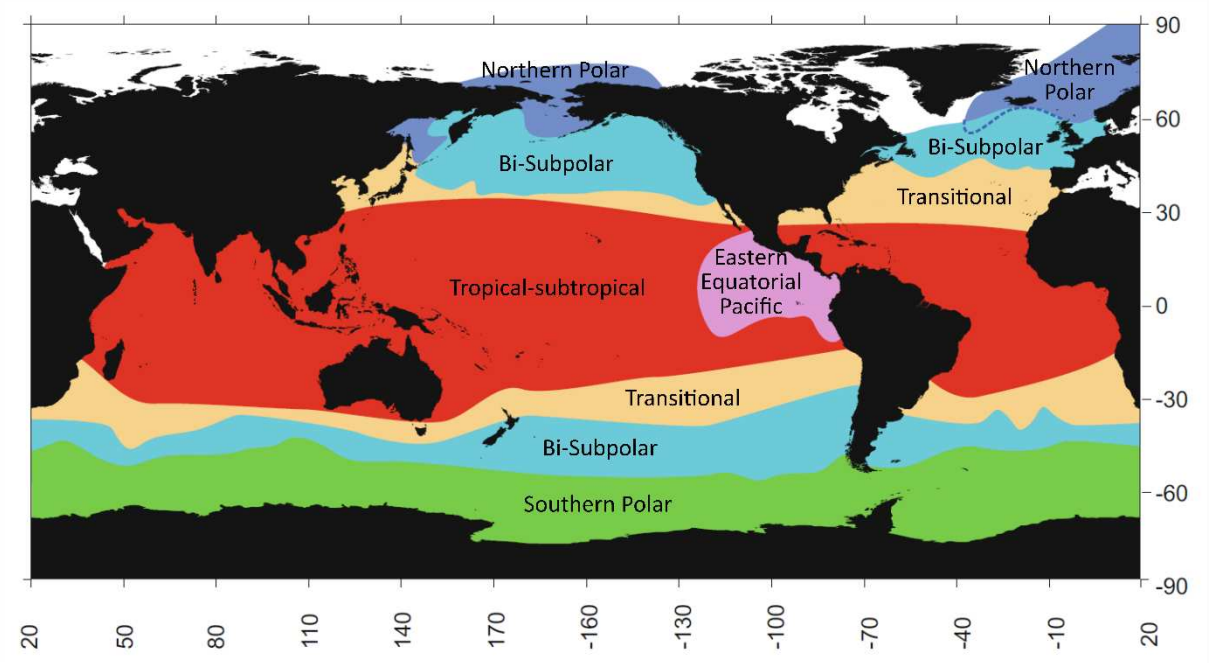

Figure 5. Major biogeographic provinces based on the distribution of polycystine radiolarians from plankton, sediment trap and surface sediment samples. (Adapted from Boltovskoy and Correa (2016)).

Some of the major controlling factors of Rhizaria distribution seem to be water temperature and salinity. Numerous studies in laboratory conditions have demonstrated the broad tolerance of these organisms to changes in several parameters such as salinity, temperature and silica concentration (Anderson et al., 1989). Polycystine abundances peak at the equator (Boltovskoy et al., 2010). Nutrients and primary productivity seem also to affect distribution patterns of polycystine. Phaeodaria distribution is not clearly associated with temperature (Boltovskoy et al., 2017).

Vertical distribution. So far, the distribution of Rhizaria in the ocean has mostly been derived from sediment data. In the last few decades, the development of new imaging and metabarcoding technologies has successfully revealed fine-scale distribution patterns of Rhizaria communities (Biard and Ohman, 2020). A substantial fraction of Polycystine

radiolarians harbour symbionts and therefore occur in the euphotic layer, especially in oligotrophic tropical and subtropical waters. In these waters polycystines are usually concentrated in the upper 50–100 m (Boltovskoy et al. 2010). In polar waters, however, peak abundances seem to be associated with deeper and warmer layers, at around 200–400 m (Boltovskoy and Alder 1992; Nimmergut and Abelmann 2002; Petrushevskaya 1967).
Regarding phaeodarians vertical distribution, it seems that they prefer to inhabit deep-waters, peaking in both abundances and diversity below 100 m (Boltovskoy et al., 2017). A vertical niche zonation was observed by Biard and Ohman (2020), with specific rhizarian taxa associated to each defined water layer. Phaeodarians preferentially inhabiting deeper waters may be due to their omnivorous nature, as these organisms feed on particulate organic matter which settles from the upper layers of the ocean.

Rhizaria abundances. In surface sediment samples, hundreds to thousands radiolarian skeletons can be found in one gram of sediment (Boltovskoy et al., 1993). Phaeodarians, as mentioned above, are not well preserved in the sediment. In the water column, Rhizaria abundances rarely reach 5 cells per liter (Caron 1990), with lower values for phaeodarians (Gowing, 1989). Some studies reveal that densities of the Rhizaria group can be higher than expected in specific regions of the ocean in certain seasons. In the Japan Sea and the North Pacific Ocean high abundances for Phaeodaria and Nassellaria groups were reported, 208 and 234 cells m^{-3}, respectively (Ishitani and Takahashi, 2007). Considering their occasional high biomass and the fact that their skeleton is made of Si, Rhizaria can play an essential role in regional ecosystems and have an important impact in the global marine Si cycle.

PhD Objectives

Very little is known regarding the biology and ecology of Rhizaria. The general objective of this thesis is to better understand the role of silicifying Rhizaria in oceanic ecosystems and in the Si biogeochemical cycle. We developed a multidisciplinary approach merging marine ecology, ecophysiology, biogeochemistry and imaging (including laboratory tools and *in situ* instruments). We applied techniques previously used for diatoms in order to measure Rhizaria dSi consumption rates *in situ* in contrasted ecosystems' settings.

The specific objectives of this thesis are:

1. To determine the elementary composition and the silicic acid uptake rates of a variety of taxonomic groups of siliceous Rhizaria. From these results and a compilation from the literature of rhizarians abundance data, we will estimate the potential role of Rhizaria in the Si cycle of the global Ocean.

2. To determine the relative importance in terms of biomass of siliceous Rhizaria planktonic community compared to diatoms, in contrasted oceanic regions (Mediterranean Sea, the Ross Sea and the Atlantic Ocean).

3. To obtain a holistic view of the Rhizaria community (*i.e*., considering the entire size spectra), and study more into detail, the relative abundance and biomasses of different taxonomic groups. To address this, optical and imaging tools (FlowCam, Zooscan and Underwater Vision Profiler-UVP) and metabarcoding methods are combined.

Chapter 1 – Estimating biogenic silica in the global ocean

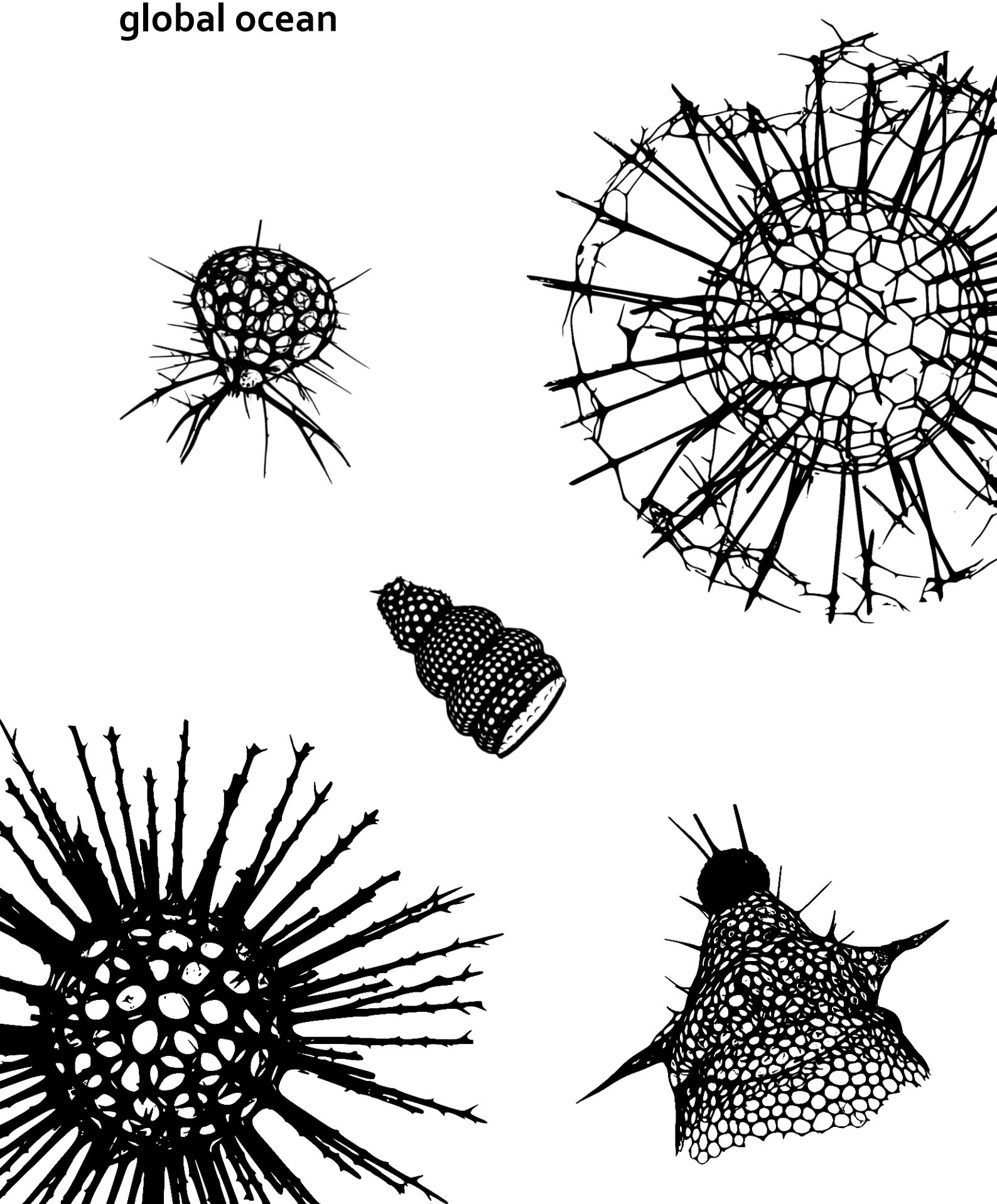

Drawings of Nassellaria and Spumellaria specimens from Miguel Méndez-Sandin pictures.

Context of the work

The first chapter of this thesis is dedicated to the determination of the elementary composition (biogenic silica, carbon and nitrogen) as well as the quantification of the rates of silicic acid uptake of living Rhizaria.

To carry out this objective, I participated in the 2017 Mediterranean Ocean Observing System for the Environment – Grande Echelle (MOOSE-GE) oceanographic cruise. During this cruise I collected Rhizaria specimens in the northwestern Mediterranean Sea and I conducted experiments using radioactive labeled silicon to measure the organisms' biogenic silica production rates. We also analysed the elementary composition of several taxonomic groups. The results of these experiments were combined with previously published data on the abundance of polycystines and phaeodarians in the global ocean to generate the first estimates of the contribution of Rhizaria to the world's biogenic silica production.

These findings challenge the view that diatoms have total control over oceanic silicon cycling in the modern ocean, a process that is coupled with other biogeochemical cycles, such as the carbon and nitrogen cycles.

Estimating Biogenic Silica Production of Rhizaria in the Global Ocean

Natalia Llopis Monferrer[1,2], Demetrio Boltovskoy[3], Paul Tréguer[1], Miguel Méndez Sandin[2], Fabrice Not[2], Aude Leynaert[1]

[1]Univ Brest, CNRS, IRD, Ifremer, LEMAR, F-29280 Plouzane, France

[2]Sorbonne University, CNRS, UMR7144, Ecology of Marine Plankton Team, Station Biologique de Roscoff, Roscoff, France

[3]University of Buenos Aires-CONICET · Institute of Ecology, Genetics and Evolution of Buenos Aires, Argentina

Published in Global Biogeochemical Cycles - February 2020

https://doi.org/10.1029/2019GB006286

Abstract

Siliceous polycystines and phaeodarians are open-ocean planktonic protists found throughout the water column and characterized by complex siliceous skeletons that are formed, at least partly, through the uptake of silicic acid. These protists contribute to the marine organic carbon (C) and biogenic silica (bSi) pools but little is known about their contribution to the silica (Si) biogeochemical cycle. Here we report the first measurements of the Si uptake rate of polycystine and phaeodarian cells from samples collected in the Mediterranean Sea using the ^{32}Si based method. The elementary composition (bSi, particulate organic carbon and nitrogen) of these organisms was also measured. Combining our results with published data on the distribution and abundance of Polycystina and Phaeodaria in the global ocean, we conclude that these organisms could contribute from 0.2 to 2.2 mmol Si m^{-2} of the marine standing stock of bSi and from 2 to 58 Tmol Si yr^{-1} (1 to 19%) of the global oceanic biogenic silica production. The implications for the global marine Si cycle are discussed.

Key words: silica cycle, silicic acid uptake, Rhizaria, Polycystina, Phaeodaria, Radiolaria

1. Introduction

Rhizarians are eukaryotic, mostly heterotrophic single-celled organisms, ranging in size from tens to hundreds of micrometers, although some are capable of forming gelatinous colonies up to over 1 m in length (Boltovskoy et al., 2017; Suzuki & Not, 2015). These protists are globally distributed, dwelling chiefly in the open ocean, from the surface down to bathypelagic depths. Their distribution and abundance are controlled by environmental factors, such as temperature, salinity, productivity, and nutrient availability (Boltovskoy, 2017a, 2017b; Boltovskoy et al., 2017; Boltovskoy & Correa, 2016). Some rhizarian taxa produce mineral skeletons of strontium sulfate (*e.g.*, subclass Acantharia), calcium carbonate (*e.g.*, order Foraminifera), and opaline silica (*e.g.*, orders Spumellaria and Nassellaria and superorder Phaeodaria).

Silicifying organisms are a critical component of the global oceanic Si cycle. Diatoms, silicoflagellates, sponges, and siliceous rhizarians are all capable of using the silicic acid available in seawater to build elaborated skeletons that are believed to improve essential functions, such as mechanical protection for the cell (Hamm et al., 2003), an armor against predators (Finkel & Kotrc, 2010), an effective pH buffer (Milligan, 2002), or an improvement for the uptake or storage of bioessential elements (Suzuki & Not, 2015). Other studies have suggested that the frustule could confer diatoms an advantage due to its peculiar optical properties (Leynaert et al., 2018). Diatoms are considered the world's largest contributors to the Si cycle, dominating both the standing stock of water column biogenic silica (bSi) and its production rate (Ragueneau et al., 2000, 2006; Tréguer & De La Rocha, 2013). A number of studies ranging from sediment traps to environmental molecular surveys have emphasized the importance of rhizarians in biogeochemical cycles and export of C and bSi to the deep ocean (Biard et al., 2018; Guidi et al., 2016; Gutierrez-Rodriguez et al., 2019; Lampitt et al., 2009). Moreover, recent studies combining genomic and *in situ* imaging approaches have shown that the contribution of large Rhizaria to the biomass of zooplankton has been largely underestimated (Biard et al., 2016), with their abundance correlating with carbon export fluxes at 150-m depth in oligotrophic oceanic regions (Guidi et al., 2016). Globally, in terms of numbers, some rhizarian taxa can represent approximately 33% of large zooplankton (>600 µm) in the upper water column and up to 5% of the overall oceanic biota carbon reservoir (Biard et al., 2016; Stukel et al., 2018). These new findings suggest an unsuspected role of

these organisms in the biological carbon pump, as well as in the Si cycle, especially in oligotrophic areas where diatoms are poorly represented while siliceous rhizarians may be dominant in the tropical sediments (Dutkiewicz et al., 2015; Lisitzin, 1974).

The major taxa of silicifying rhizarians are represented by the Phaeodaria (Cercozoa, Thecofilosea) and by Spumellaria, Nassellaria, and Collodaria (Retaria, Radiolaria, Polycystinea) (Adl et al., 2018). The two groups differ in the robustness of their skeletal structures. While most polycystines possess solid and dense skeletons (Takahashi, 1983), phaeodarian skeletons are porous (Nakamura et al., 2018). The ballast produced by this skeleton causes them to sink toward the ocean floor where they can be incorporated into the sediment if their bSi has not been affected by the dissolution and recycling into $Si(OH)_4$. Polycystine bSi is more resistant to dissolution and often remains well preserved in the sediment, whereas that of Phaeodaria is rarely found in bottom deposits (Takahashi, 1983). Among Polycystina, Spumellaria and Nassellaria have been widely used for paleoceanographic reconstructions (Matsuzaki et al., 2014; Moore, 1978). However, essentially due to the difficulty of culturing planktonic rhizarians, our knowledge of their ecology, physiology, and biogeochemistry is very limited, especially with regard to the processes associated with Si sources, uses, stocks, and fluxes. Marron et al. (2016) reported the presence of Si transporters in rhizarians, which enable the uptake of Si (mainly in the form of silicic acid) from the environment.

In this study, we analyze the Si, carbon (C), and nitrogen (N) content of isolated rhizarian cells collected during two oceanographic cruises in the Mediterranean Sea (Mediterranean Ocean Observing System on Environment Grande Echelle, MOOSE-GE) and from the Atlantic Ocean (Atlantic Meridional Transect, AMT28) cruise. We also measured their bSi production rates using the 32Si isotope, an approach successfully applied until now only to estimate diatom bSi production rates. We first discuss the relationship between rhizarians elemental composition and their cell size, and combining these measurements with available data on rhizarian abundances worldwide, we assess their potential contribution to the global marine Si cycle.

2. Material and Methods

2.1. Sampling

Samples were collected at 22 sampling sites in the western Mediterranean basin (Figure 1) during the MOOSE-GE expedition in September 2017 and June 2018 aboard the R/V *Atalante* and at one site during the AMT28 in October 2018 aboard the RRS James Clark Ross.

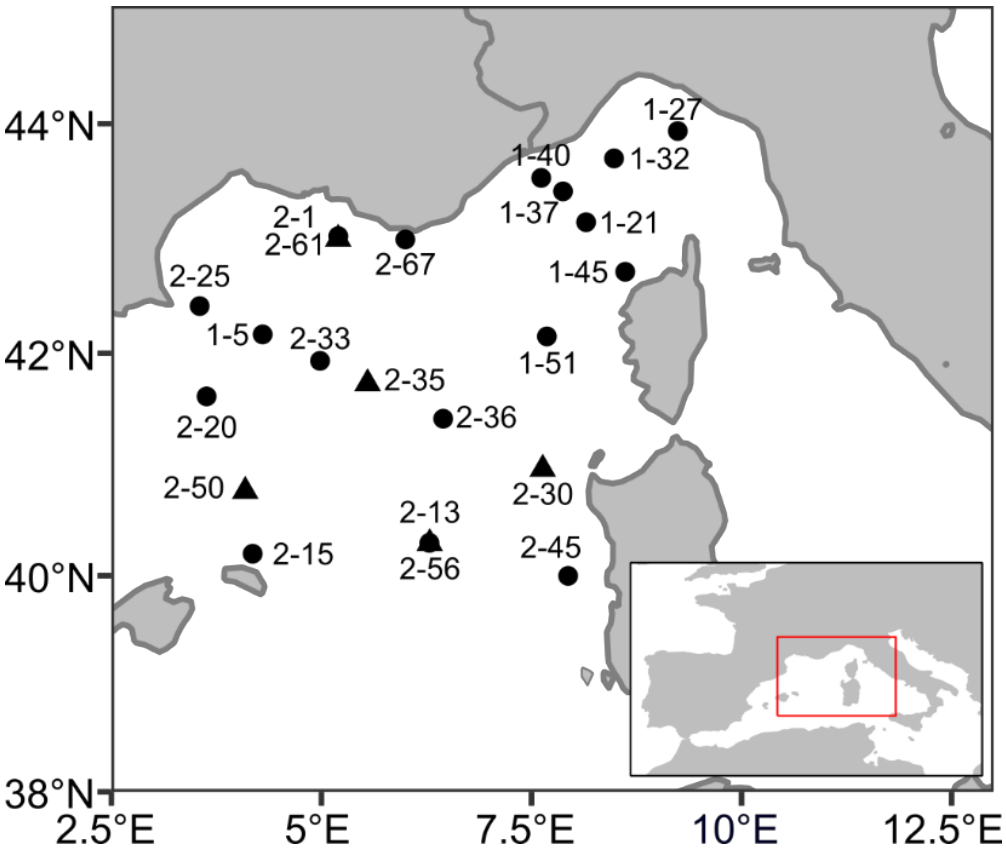

Figure 1. Sampling sites (Leg-Station) of the MOOSE-GE cruises, ● sites sampled in 2017 and ▲ sites sampled in 2018. Net was deployed between 0 and 500 m. The samples of the AMT cruise were collected at 3.69°S 24.98°W at depths between 0 and 200m.

Plankton samples were obtained at discrete depth-intervals, using vertical tows. Upon recovery, samples were immediately diluted in 0.2 µm filtered seawater and observed on-board under a stereomicroscope or an inverted microscope. Rhizarians were handpicked using a Pasteur pipette and transferred to 20 mL glass vials filled with filtered seawater. Cells were sorted according to targeted taxonomic groups, namely Nassellaria, Spumellaria and Collodaria, chiefly represented by Pterocorythidae, Hexastyloidea and Sphaerozoidae

respectively. Among the Phaeodaria, because of their high abundances, we differentiated the genera *Aulacantha*, primarily represented by *Aulacantha scolymantha,* and *Challengeria*.

In each glass vial, we stored from 1 to 50 individuals, depending on cell size and abundance of the target organisms in the sample. Individual pictures were taken prior the experiments to obtain morphometric measurements using the ImageJ software. For each specimen, we measured length, width, and area, and subsequently calculated the biovolume associated using the most similar simple geometric shape (*e.g*., sphere, ellipsoid, cone). Due to logistic problems, for some of the stations, no pictures were available for biovolume estimates. However, samples from all the stations were analysed using the Flowcam (preserved with lugol's solution) and the Zooscan (preserved with formaldehyde) immediately after the cruise. We also compared cell size from living and preserved individuals and we did not observed differences in cells dimensions between them. Therefore, we used the vignettes obtained with these imaging technologies to complete our set of measurements. For Collodaria (mostly colonial radiolarians comprising hundreds to thousands of siliceous shells or spicules embedded in a gelatinous matrix), the entire colony was measured, but the results are reported per individual. Capsules were counted and measured using ImageJ software.

Seawater samples for the incubations were collected at each sampling location and at different depths using Niskin bottles.

2.2. Elementary composition

We analysed the bSi (in nmol Si cell^{-1}) and the particulate organic carbon and nitrogen (POC/PON in µmol cell^{-1}) in 35 and 24 samples respectively (Table 1). In total, 1339 cells were isolated and analysed.

Table 1. Biogenic Silica Stocks, Production Rates and POC content of the rhizarians analyzed. Note: ESD denotes equivalent spherical diameter, n denotes the number of samples analyzed and ^{a}n the number of specimens analyzed. SD: Standard Deviation.

	bSi					bSi Production						POC			Si:C
	n	^{a}n	ESD±SD (µm)	mean±SD (nmol Si cell^{-1})	mean±SD (mg bSi mm^{-3})	n	^{a}n	mean±SD (nmol Si cell^{-1} d^{-1})	n	^{a}n	ESD±SD (µm)	mean±SD (µmolC cell^{-1})	mean±SD (mgC mm^{-3})	
Polycystina															
Collodaria	6	378	150±34	1.24±0.79	0.05±0.04	6	378	0.60±0.72	-	-	-	-	-		
Nassellaria	3	64	80±1	2.16±1.07	0.53±0.25	3	64	0.17±0.05	1	33	102	0.07	1.56		0.03
Spumellaria	4	44	143±51	6.09±5.80	0.20±0.09	4	44	1.59±1.35	3	99	144±38	0.09±0.05	1.00±1.03		0.07
Phaeodaria															
Aulacantha	17	249	835±119	26.09±11.80	0.01±0.01	13	198	1.78±3.10	17	302	695±122	0.26±0.13	0.02±0.02		0.10
Challengeria	5	97	124±66	3.09±3.34	0.24±0.19	5	97	0.34±0.23	3	73	151±39	0.09±0.08	1.62±1.35		0.03

The entire content of each vial with isolated cells in filtered seawater was filtered onto polycarbonate membrane (Nuclepore 47mm, 0.6 µm pore size) for bSi determination and onto 25 mm GF/F precombusted filters (at 450 °C during 4 h) for POC and PON analysis. Nuclepore membranes were 4-folded in a petri dish, dried and stored at ambient temperature until later analysis in the laboratory. GF/F filters were folded in a petri dish and stored at -20 °C until analysis.

The bSi of Polycystina and Phaeodaria was quantified by colorimetric determination of the orthosilicic acid after leaching. A single digestion in hydrofluoric acid (HF) was performed, since the samples only contained isolated rhizarians, *i.e*., there was no possible interference with lithogenic Si as there might be when filtering raw seawater (see Ragueneau et al., 2005). We added 0.2 ml of HF 2.5N to the polymethylpentene (PMP) tubes containing the filters. The filter was then compressed until submerged in HF and air bubbles were removed. The tube was tightly covered with a cap and kept under a fume hood, at room temperature for 48 h to allow for digestion of the bSi. We then added 9.8 ml of saturated H_3BO_3 solution. The standards used for calibration were prepared with the same matrix as for the samples (HF/H_3BO_3), before analysis by colorimetric methods on a Technicon Auto-Analyzer II (Aminot and Kérouel, 2007; Brzezinski and Nelson, 1989).

Concentrations of POC and PON were measured with a mass spectrometer (Delta plus, ThermoFisher Scientfic) coupled to a C/N analyser (Flash EA, ThermoFisher Scientifc). Standard deviations (SD) were 0.009 µM and 0.004 µM for POC and PON respectively. In order to avoid false positives, the detection limit was set at the control level plus ten times the standard deviation. Although POC and PON analyses were performed simultaneously using an elemental analyser, N was often close to the detection limit, in which case, the values were discarded, thus yielding more results for C than for N. The POC/PON measurements of Collodaria were rejected for the same reason.

2.3. Assessment of bSi production rates (ρ_P)

For the measurements of bSi production rates (ρ_P), we used the radioisotope of silicon (^{32}Si) (Leynaert et al., 1996; Tréguer et al., 1991). Immediately after isolation, glass vials containing between 1 and 50 cells of the same taxonomic group were incubated on deck with 800 becquerel (Bq) of high specific activity ^{32}Si, for 24 h in a flowing-seawater incubator to maintain constant water temperature. The light in the incubation baths was attenuated by

means of neutral screen to 50% of the incident light. The ^{32}Si additions increased silicic acid concentrations in the incubation bottles by less than 10 nM, a negligible value compared to the dissolved silica (DSi) concentration in seawater. A split of the seawater sample used for the incubation was stored for subsequent analyses of silicic acid concentration using the automated method of Aminot & Kérouel (2007).

After incubation, samples were filtered by gentle (<150 mmHg) vacuum filtration onto 47mm diameter, 0.6 µm pore-size polycarbonate membrane filters (Nuclepore), and rinsed twice with filtered seawater to wash away non-particulate ^{32}Si. Each filter was then placed in a clean 20 ml polypropylene liquid scintillation vial and the vial was capped loosely to allow the sample to dry at room temperature for 48 h. The vials were then capped tightly and returned to the laboratory for counting.

The activity of ^{32}Si in the samples from the incubation experiments was determined using the Cerenkov counting method (Leynaert, 1993) three months after the samples were filtered, allowing ^{32}Si and its daughter isotope ^{32}P to return to secular equilibrium. Although this method is less sensitive than some others (Brzezinski and Phillips, 1997), it was chosen because it allows using the materials for further bSi analyses. Twenty-four hours before assessing the activity on the filter, HF (2.0 ml of 2.5N) was added to each sample to dissolve all bSi. Samples were assayed using a Wallac Model 1414 scintillation counter. Because ^{32}Si does not produce Cerenkov emissions, the procedure allowed quantifying the amount of ^{32}P only. However, as ^{32}Si and ^{32}P are in secular equilibrium the activities of the two isotopes are equal, and the ^{32}Si activity can be deduced from that of ^{32}P (Leynaert, 1993). Triplicate 40 min counts were performed on each sample. Counting precision (95% Confidence Interval) was < ± 1%, except for a few very low-activity samples yielding < 250 CPM (counts per minute), for which counting precision was ± 2-5%. Counts yielding less than three times the background (8 CPM) were discarded. Collodarians without siliceous spicules or shells (*e.g*. *Collozoum spp*.) were incubated in parallel to obtain a production blank, which yielded production rates close to the detection limit, *i.e*., below 0.02 nmol Si $cell^{-1}$ day^{-1} in all cases.

2.4. Extrapolation of siliceous rhizarians to the global ocean: bSi stocks and production rates

We performed an estimate of rhizarian abundances based on the compilation of worldwide data of Boltovskoy et al. (2010), supplemented with more recent studies (see Supplementary material). Our database contained 1191 data points of Polycystina and Phaeodaria densities

(cells m^{-3}) in plankton samples collated from 22 publications. Most of the studies used plankton nets to collect rhizarians, including vertical and horizontal tows. Other studies sieved Niskin bottle samples to quantify abundances of these organisms (See details in Supplementary material).

These data were averaged over two bins: tropical-subtropical (40°N to 40°S), and colder waters (>40°N or S), each in turn was subdivided into two depth layers: 0-200 m, and below 200 m depth (Table 2). For the Phaeodaria, where the literature information is scarcer, all species were pooled in a single group (Phaeodaria). For the Polycystina, densities of Spumellaria and Nassellaria were estimated separately (and also used separately in subsequent calculations).

Table 2. Mean abundances in cells m-2 and [cells m-2] of Polycystina and Phaeodaria, as reported in 22 publications based on plankton materials. Note: values include all cells recorded (*i.e.*, living and dead shells).

	40°N-40°S				>40°N/S			
	0 - 200 m		200 -1000 m		0 - 200 m		200 - 1000 m	
N° of datapoints	523		91		383		194	
N° of sources	14		7		12		9	
Polycystina								
Collodaria	52	[10439]	10	[7756]	0	[1]	0	[13]
Spumellaria	235	[46993]	72	[57223]	79	[15876]	37	[29588]
Nassellaria	892	[178316]	105	[83742]	103	[20645]	69	[55288]
Phaeodaria								
Phaeodaria	20	[3940]	4	[3217]	5	[957]	1	[478]

To convert abundance values reported in literature into bSi stocks (nmol Si m^{-2}) and production rates (ρ_P µmol Si m^{-2} day^{-1}), we used the estimates obtained in our cruises. For each taxonomic group, we established ranges based on the minimum and maximum values for both bSi stock and ρ_P (Table 1). To obtain global estimates, we considered an area of 2.68E^{14} m^2 (40°N to 40°S) for the warm waters and an area of 9.3E^{13} m^2 (>40°N or S) for the cold waters.

3. Results

3.1. Elemental composition: bSi, POC and PON

bSi content

Overall, bSi per cell varied over one order of magnitude, from 1.24 ± 0.79 nmol Si $cell^{-1}$ (mean ± standard deviation [SD]) for Collodaria to 26.09 ± 11.80 nmol Si $cell^{-1}$ for *Aulacantha*. The bSi

content differed significantly between *Aulacantha* (Kruskal-Wallis, $P < 0.05$) and the other groups (Figure 2).

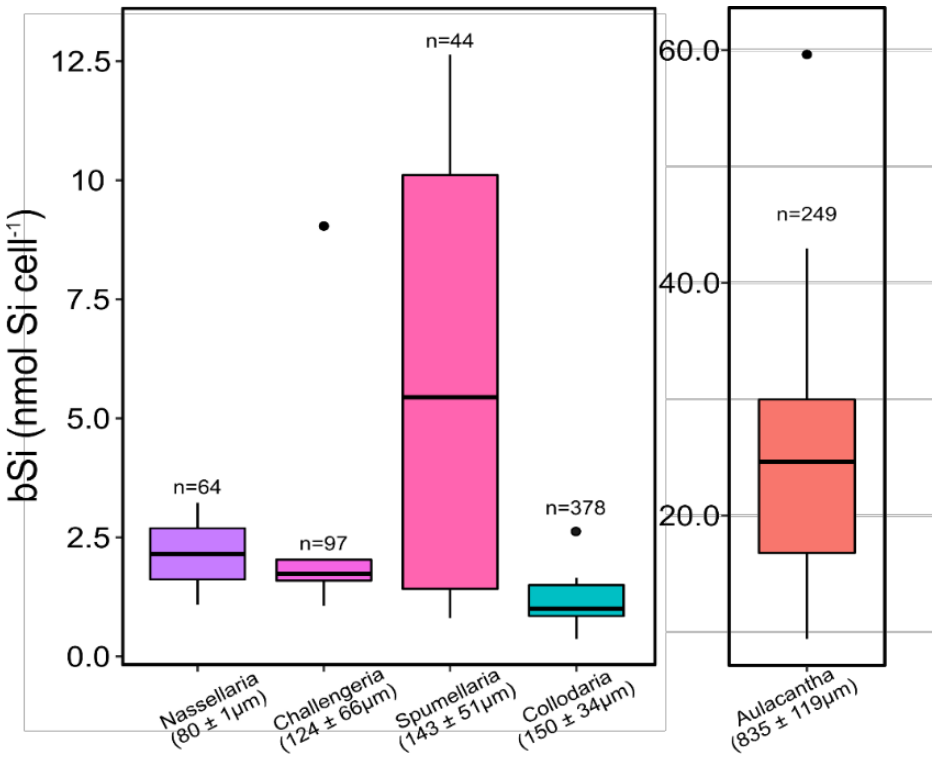

Figure 1. bSi content and size of the taxa studied. *n* denotes the number of specimens (or individual cells, for the Collodaria *n**) analysed. Colours correspond to the taxonomic groups identified in Figure 3.

The largest cells (*i.e.*, genus *Aulacantha*) have the highest Si content. In order for our data to be comparable with the units reported in the literature, Si concentrations were converted from nmol Si cell^{-1} to µg Si cell^{-1} assuming a molecular weight of 67 g mol^{-1} for hydrated amorphous silica (Mortlock and Froelich, 1989).

We evaluated the log-log relationship between the Si content and cell size of the rhizarians surveyed. Based on the Si contents of 3 samples of Nassellaria (64 individuals), 4 samples of Spumellaria (65 individuals), 6 samples of Collodaria (378 individuals), 5 samples of *Challengeria* (97 individuals) and 17 samples of *Aulacantha* (249 individuals), Si content (Q_{bSi}) was significantly associated with the cell's equivalent spherical diameter (ESD) (R^2 = 0.8, F(1, 33)=129, $P < 0.001$) according to the following equation:

$$log_{10}(Q_{bSi}) = [-3.61 \pm 0.29] + [1.30 \pm 0.11] \cdot log_{10}(ESD) \qquad (1)$$

Where Q_{bSi} is in µg Si cell^{-1} ± standard error (SE) and ESD in µm ± SE.

POC/PON content and C/N ratios

The POC and PON content of the rhizarians analysed differed significantly between taxa (ANOVA, P<0.001; excluding the Nassellaria, for which no data were available). Nitrogen measurements were obtained for 24 samples including a total of 507 siliceous rhizarians cells. Overall, PON concentrations ranged between 0.001 and 0.02 µmol N cell^{-1}.

In these 24 samples, the POC content (Q_C) varied between 0.09 ± 0.05 and 0.26 ± 0.13 µmol C cell^{-1}. The highest Q_C was found for *Aulacantha* cells. However, the relationship between Q_C and ESD was not significant. The average C/N ratio was 12.

3.2. Rhizarian bSi production rates

We successfully measured, for the first time, the silicic acid uptake (ρ_P) rates of 31 rhizarian samples (781 individuals). Rates of bSi production ranged from 0.17 ± 0.05 nmol Si cell^{-1} day^{-1} for Nassellaria to 1.78 ± 3.10 nmol Si cell^{-1} day^{-1} for *Aulacantha* (Table 1). Production rates seem to be related to cell size.

In order to estimate specific uptake rate (V_P, in day^{-1}), ρ_P were normalized to the concentration of bSi (ρ_P/bSi) (Tables 1 and 3). The largest cells (*Aulacantha*) present the lower V_P, while Nassellaria, the smallest cells found in this study, had the highest V_P.

Table 3. Specific uptake rates for Polycystina, Phaeodaria and diatoms. Note: values for diatoms are from Claquin et al. (2006) and references therein.

Groups	V_P (d^{-1})	Reference	Area of study
Polycystina			
Collodaria (individual)	0.48	This study	Mediterranean Sea
Nassellaria	0.26	This study	Mediterranean Sea
Spumellaria	0.08	This study	Mediterranean Sea
Phaeodaria			
Aulacantha	0.07	This study	Mediterranean Sea
Challengeria	0.11	This study	Mediterranean Sea
Diatoms			
	0.96	Leynaert et al. (2001)	Equatorial Pacific
	0.40	Nelson and Brzenzinski (1990), Brzezinski and Nelson (1996)	Sargasso Sea
	0.62	Nelson and Dortch (1996)	Mississipi
	0.06	Nelson and Tréguer (1992)	Ross Sea
	1.80	Goering et al. (1973)	Peru upwelling
	0.19	Leblanc et al. (2003)	Northwest Mediterranean Sea
	0.38	Kristiansen et al. (2000)	Southern Norway
	1.02	White and Dugdale (1997)	California
	1.06	Bonnet (2001)	Bay of Brest
	0.21	Brzezinski et al. (1998)	Central North Pacific
	0.31	Nelson et al. (2001)	Southern Ocean

3.3. Worldwide Si standing stocks and production rates (ρ_P)

According to the literature data collated, densities of Polycystina and Phaeodaria peak in the upper layers where their abundances (*i.e.*, cells L^{-1}) are ~1.5-8.5 times higher than below 200 m depth, with higher contrasts in the warm waters. Nevertheless, low densities integrated

throughout large depth intervals often yield larger standing stocks below 200 m than in the 0-200 m layer, especially at low latitudes (Table 2). Our estimates suggest that polycystine and phaeodarian bSi standing stocks in the water column range from 0.3 to 2.2 mmol of bSi m^{-2} (Table 4). For ρ_P, we obtained a tentative range of 5 to 58 Tmol yr^{-1} (Table 4). The ρ_P are of more consequence in temperate waters than in cold waters, which reflects differences in abundances. Production rates throughout the water column are similar in the two oceanic zones considered.

4. Discussion

4.1. Filling the gaps in size-Si relationship. From small to giant protists.

Our work on the assessment of the elemental composition of siliceous rhizarians included several small-sized Polycystina (Collodaria, Nassellaria and Spumellaria), as well as the larger Phaeodaria, encompassing a wider size spectrum than that covered by previous studies. Takahashi (1981) was the first to report the Si content, weight, length, width, projected area, and biovolume of polycystines and phaeodarians. However, his studies were based on dead cells recovered from sediment traps. Using these data and specimens collected off the coast of California, Biard et al. (2018) established an allometric relationship that shows that the Si content of phaeodarians is closely associated with cell length and cell biovolume. These relationships were chiefly based on large specimens (0.6 to >10 mm, average: 2 mm), and have not hitherto been validated for the smaller rhizarians.

In order to investigate whether their Si content is associated with biovolume and cell size (expressed as ESD) throughout a wider size-range, we combined our measurements and Si content values with the log-log linear relationship shown by Biard et al. (2018). The result of this exercise showed that over a range of 103 to 3920 µm, rhizarian Si content is significantly associated with biovolume (R^2 = 0.86, F(1, 93)=593, P<0.001):

$$log_{10}(Q_{bSi}) = [-4.05 \pm 0.18] + [0.52 \pm 0.02] \cdot log_{10}(biovolume) \qquad (2)$$

Where Q_{bSi} is in µg Si $cell^{-1}$ ± SE and biovolume in μm^3 ± SE.

Si content is also correlated with the ESD (Figure 3; R^2 = 0.86, F(1, 93)=593, P<0.001):

$$log_{10}(Q_{bSi}) = [-4.20 \pm 0.18] + [1.56 \pm 0.06] \cdot log_{10}(ESD) \qquad (3)$$

Where Q_{bSi} is in µg Si cell^{-1} ± SE and ESD in µm ± SE. Biard's length data were converted to ESD for this analysis.

The slope of equation 3 is similar to those of Biard et al. (2018) for ESD (ANCOVA, P=0.41), confirming its validity for a wide spectrum of rhizarians sizes.

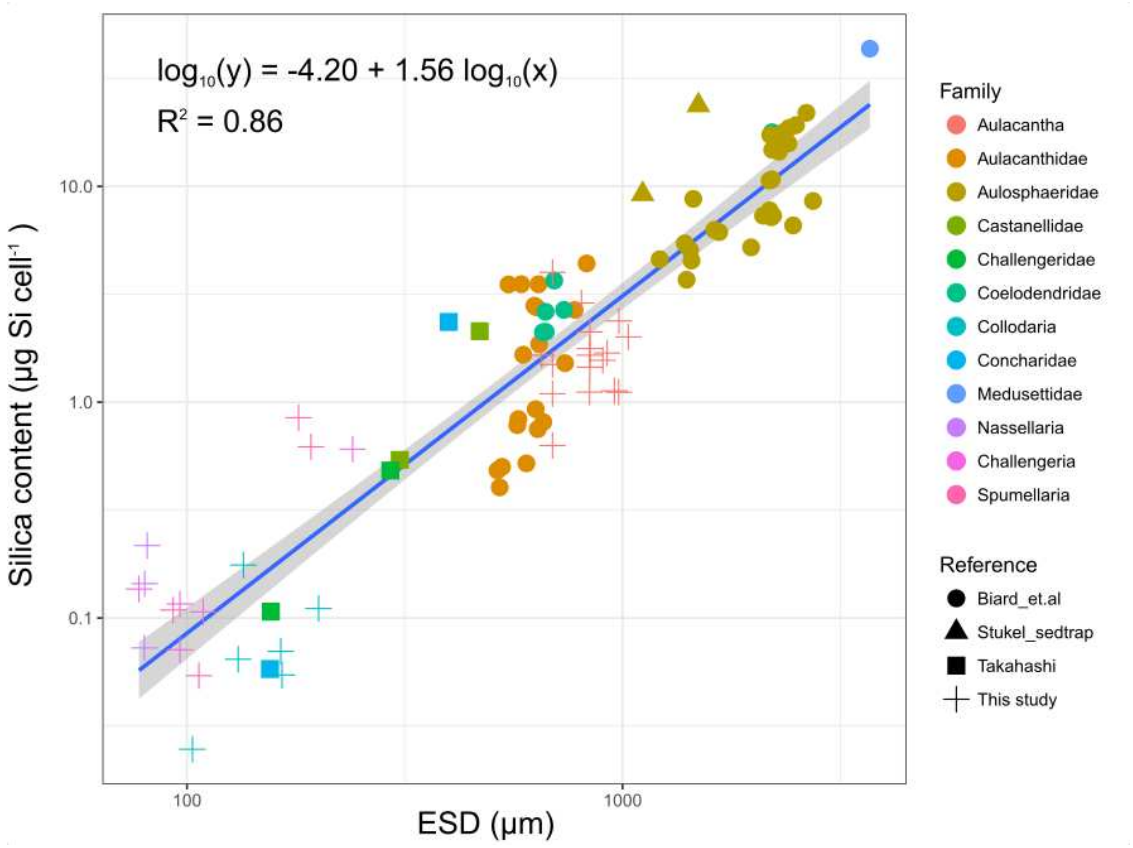

Figure 3. Relationship between the Si content of Polycystina and Phaeodaria and their ESD (µm) across all the specimens assessed. Regression (blue line) and 95% confidence interval (gray shading). Combined data from Biard et al. (2018) and this study.

Silica content has previously been shown to be related to cell size in other siliceous organisms, such as diatoms. Conley et al. (1989) observed that the Si content of diatoms varies over five orders of magnitude depending on cell size and found a significant log-log linear relationship between Si content and biovolume. However, the relationship for diatoms gives much lower cellular bSi concentrations (100 times lower on average) than for rhizarians of comparable size. Thus, among the siliceous planktonic organisms in the ocean, rhizarians appear to be the most silicified.

Although the largest cells contain more Si, they are not necessarily the densest according to our conversion from Si biomass to density. Nassellarians, which are the smallest cells in our

study, had 530 µg bSi mm^{-3}, while *Aulacantha*, the largest cells analysed (measurements based on the solid skeleton), barely reached 10 µg bSi mm^{-3}. As reported recently, the structure of Polycystina and Phaeodaria differs considerably. Polycystine skeletons are solid, whereas phaeodarian skeletons are porous and in some species, including *Aulacantha* they are composed of loose spines protruding from the cell (Nakamura et al., 2018) (Figure 4). Sedimentation rates in the water column are likely to be affected by differences in density of these structures, as observed by Baines et al. (2010) for diatoms.

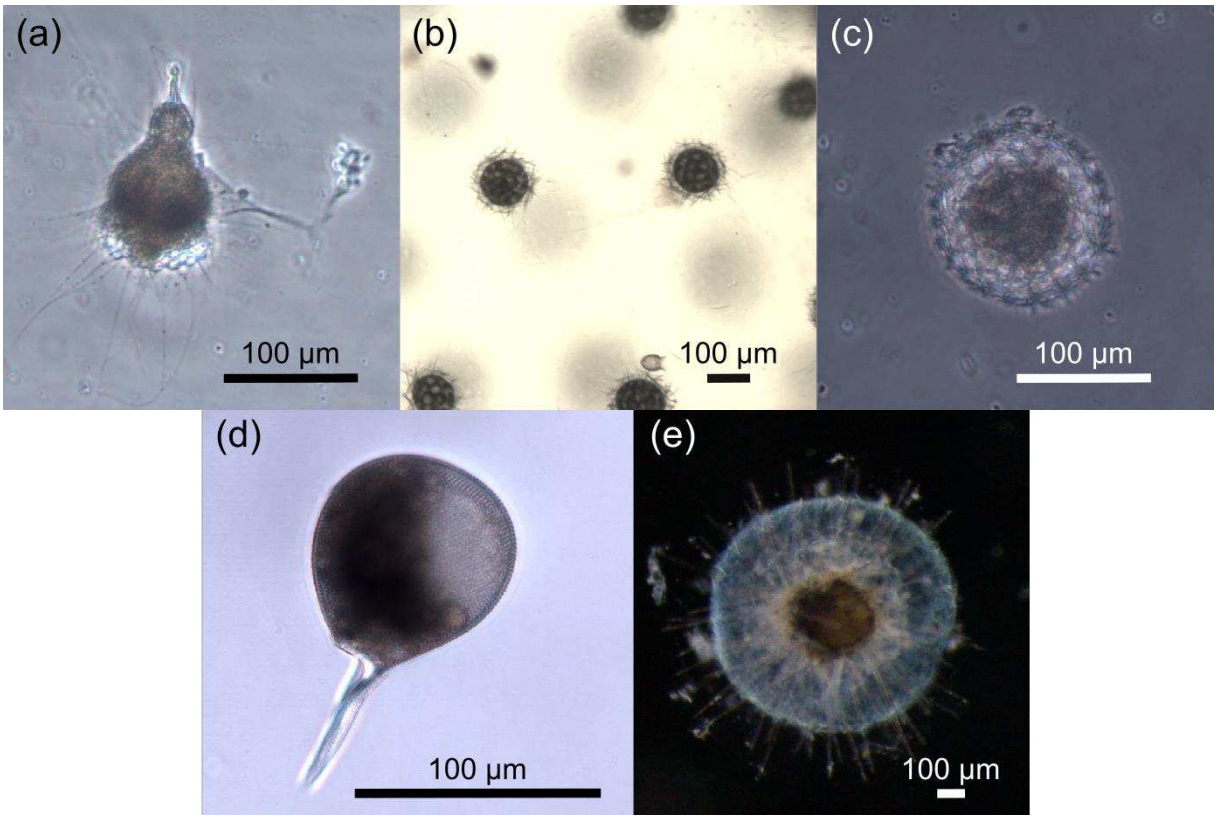

Figure 4. Images of the most abundant morphotypes surveyed in this work, including Polycystina (a-c), and Phaeodaria (d-e). (a) Nassellaria - Pterocorythidae (b) Collodaria-Sphaerozoidae (c) Spumellaria - Hexastyloidea (d) Challengeridae - *Challengeria xiphodon* (e) Aulacanthidae - *Aulacantha scolymantha.*

As opposed to Si, we were not able to find any relationship between POC and PON and cell size, therefore an average was calculated per taxon (Table 1). Data on rhizarian Q_C are scarce. To our knowledge, the first Q_C published are those of Michaels et al. (1995) where they reported extremely variable Q_C values for solitary collodarians, ranging from 0.009 to 0.28 mg C mm^{-3}. Stukel et al. (2018) estimated a Q_C for Aulosphaeridae of 0.011 mg C mm^{-3} based on a downward revision of Biard et al. (2016) measurements. Our data, are high when compared to those in these two studies. Polycystina and Phaeodaria Si:C molar ratios (0.03 to 0.1) are

lower than those of diatoms (0.13 ± 0.04), according to data reported by Brzezinski (1985) for twenty-seven diatom species. On the other hand, our mean C/N ratio (~12) is higher than that reported by Michaels et al., (1995) for colonial collodarians (8.2), and much higher than the Redfield ratio (6.6). Higher molar ratios for the colonial radiolarians could be due to the presence of mucopolysaccharide material surrounding the colonies (Michaels et al., 1995).

4.2. The silicic acid uptake rates of rhizarians ($\boldsymbol{\rho_P}$)

In this study, ρ_P were measured using the radioisotope ^{32}Si, quantifying, for the first time the ability of these protists to consume dissolved Si from seawater. Our results show consumption rates ranging from 0.17 nmol Si cell^{-1} day^{-1} (for Collodaria) to up to 1.78 nmol Si cell^{-1} day^{-1} (*Aulacantha*).

Comparison of these results with the ρ_P of other plankton, in particular diatoms, is complicated by the fact that the rates measured for diatoms in the field are expressed in terms of volume (*i.e*. per liter), rather than "per cell". For diatoms, ρ_P per cell were only assessed in culture experiments in laboratory controlled conditions (Del Amo and Brzezinski, 1999; Riedel and Nelson, 1985) yielding values around 0.001-21 pmol Si cell^{-1} day^{-1}. In contrast, the consumption rates of silicic acid uptake by the rhizarians assessed in this work ranged from 200 to 2000 pmol Si cell^{-1} day^{-1}, which is around 100 times higher relative to diatoms, and consistent with what was observed for the Si content, also 100 times higher in rhizarians.

To gain insight into the role of rhizarians in the Si cycle we assessed the V_P of these organisms by normalizing the silicic acid uptake rates to the bSi concentration (Table 3). Our V_P ranged from 0.07 to 0.48 day^{-1}, for *Aulacantha* and Collodaria, respectively. Despite differences in the methods used, these values are generally, in line with results previously found for "larger rhizarians", whose average V_P was ~0.1-0.2 day^{-1} (Stukel et al., 2018). Our values also agree with those found for diatoms worldwide (0.06-1.80 d^{-1}) for a large temperature range (Table 4).

Based on these results, we evaluated the turnover rates of these protists ($t = ln2/V_P$) assuming that the rhizarians analysed in this study reproduce by binary cell division, which might not always be the case, as sexual reproduction may also occur (Boltovskoy et al., 2017). Turnover rates range between 3 and 10 days (for *Aulacantha* and Spumellaria, respectively), which are comparatively low when compared to phytoplankton which usually span from several hours to a few days ((Flynn et al., 2018; Krause et al., 2017).

Table 4. Estimated values of bSi stock and production as derived from our experimental data using the minimum and the maximum values for each group and the information detailed in Table 2. Note: we estimated for each toceanic area a value of production in Tmol Si yr^{-1}.

	Stock (µmol Si m^{-2})			
	0-40°N-40°S		>40°N/S	
	0-200 m min-max	>200 m min-max	0-200 m min-max	>200 m min-max
Collodaria	3.9 - 27.5	2.9-20.4	0.0-0.0	0.0-0.0
Spumellaria	38.1 - 594.0	46.4 - 723.3	12.9 - 200.7	24.0 - 374.0
Nassellaria	192.6 - 576.0	90.44 - 270.49	22.3 - 66.7	59.7 - 178.4
Phaeodaria	4.2 - 234.9	3.4 - 191.8	1.0 - 57.1	0.51- 28.5
Total	238.7 - 1432.3	143.1 - 1206.0	36.2 - 324.4	84.12- 580.9
	Production (µmol Si m^{-2} d^{-1})			
	0-40°N-40°S		>40°N/S	
	0-200 m min-max	>200 m min-max	0-200 m min-max	>200 m min-max
Collodaria	0.6 - 20.6	0.5 - 15.3	0.0-0.0	0.0 - 0.0
Spumellaria	5.6 - 159.3	6.9 - 194.0	1.9 - 53.8	3.6 - 100.3
Nassellaria	19.6 - 35.7	9.2 - 16.8	2.3 - 4.1	6.1 - 11.1
Phaeodaria	0.4 - 46.7	0.4 - 38.1	0.1 - 11.3	0.1 - 5.7
Extrapolation (Tmol Si yr^{-1})	2.6 - 25.7	1.7 - 25.8	0.1 - 2.4	0.3 - 4.0

4.3. Potential impact of siliceous rhizarians on the Si cycle of the World Ocean

Since the 1970s, silicified rhizarians (formerly collectively designated as Radiolaria) have drawn attention for their role in the marine Si cycle (Heath, 1974). Takahashi (1983) suggested that, in some oceanic areas, the daily flux of rhizarian bSi ranges around 20% to 30% of the overall bSi. Biard et al. (2016, 2018) found that the biomass of large Rhizaria, the so-called "giant protists", could constitute a substantial fraction of the >600-µm plankton biomass representing more than a third of the bSi standing stocks in oligotrophic and high nutrient-low chlorophyll regions of the ocean. These data conflict with the fact that in most global oceanic silicon budget estimates, only diatoms (Nelson et al., 1995; Tréguer et al., 1995) and more recently sponges (Maldonado et al., 2019; Tréguer & De La Rocha, 2013), are taken into account. This standpoint, however is gradually changing. For example, Tréguer and De La Rocha (2013) suggested that up to 23% of the bSi standing stocks in the upper 120 m of the

ocean could be associated with rhizarians. However, due to the lack of information at that time, estimating the contribution of these organisms to the marine Si cycle was overly speculative.

Diatoms' bSi production is restricted to the photic layer. In contrast, rhizarians inhabit (and produce bSi) throughout the entire water column. Although their concentrations decrease sharply with depth,

depth-integrated values (*i.e.*, individuals per m^{-2}) can be as high, or even higher, at depth than in the surface (0–100 m) layers (Boltovskoy, 2017a, 2017b; Kling & Boltovskoy, 1995).

According to our results, the water column bSi standing stock due to small-sized rhizarians (average ESD ~0.1 mm for Polycystina and Challengeria and 0.8 mm for Aulacantha) ranges from 0.5 to 3.5 mmol Si m^{-2}. Although small in size, these protists would increase by up to 35% the biomass of the giant protists (Aulosphaeridae, average size ~2 mm), estimated by Biard et al. (2018) and ranging between 0.01 and 10 mmol Si m^{-2}. In order to obtain a global ocean scale estimate of biomass in the water column, we combined the two size-classes yielding a pool of bSi of 0.5 to 13.5 mmol Si m^{-2}.

With regard to global rhizarian production rates, our assessment suggests a tentative range of 5 to 58 Tmol Si yr^{-1} for the whole water column. Tréguer and De La Rocha (2013) estimated that in the photic layer of the World Ocean, the production of bSi is 240 Tmol Si yr^{-1} (mainly by diatoms; Nelson et al., 1995). According to these figures, our estimates indicate that in a steady state ocean (*i.e.*, where inputs and losses of Si are balanced), the rhizarians analyzed (<1 mm) account for 2% to 19% of these 240 Tmol Si yr^{-1}. This suggests that the contribution of these rhizarians to the production of bSi in the euphotic layer should not be neglected even though they are orders of magnitude less abundant than diatoms. If we take into account the average bSi standing stock (5 mmol Si m^{-2}) estimated by Biard et al. (2018) for the family Aulosphaeridae ("large rhizarians") and assuming a VP of 0.1 day^{-1} (from our measurements), giant rhizarians could produce 65 Tmol of bSi yr^{-1}, which would have to be added to the production of the smaller rhizarians.

This estimate is based on data from the Mediterranean western basin and the California current, two oceanic zones with significant hydrographic differences. Extrapolating standing stocks and production values from specific oceanic areas to the global ocean has obviously important caveats. Contrasts in Polycystina and Phaeodaria standing stocks in warm versus cold waters have been accounted for in our estimates. Abundances of these protists tend to

be much lower in northern latitudes. However, physiological processes (including production and doubling rates) and seasonality, which likely depend on water temperature, have not been considered. In the contemporary global ocean, the factors controlling the distribution, abundances, and silica production of rhizarians are poorly constrained. Although in our estimates efforts were made to consider living cells only, an important limitation of the extrapolations performed is the distinction between living and dead cells, in particular concerning production estimates, for which only physiologically active cells are relevant. Researchers have tried to circumvent this problem by discriminating cells with cytoplasm attached to the skeleton, either in unstained (Boltovskoy et al., 1993; Nimmergut & Abelmann, 2002) or in stained samples (Ikenoue et al., 2015; Matsuzaki et al., 2016). However, undecayed cytoplasm can take from weeks to months to disappear completely, which renders these techniques unreliable (Grego et al., 2013). In contrast, nuclear stains yield more realistic estimates of the proportions of living rhizarians (Boltovskoy, 2017a, 2017b), but they are seldom used (Gowing, 1986; Gowing & Coale, 1989; Nöthig & Gowing, 1991).

In attempting to overcome this potential bias, we estimated the proportions of living cells as a function of depth and latitude using data from studies that used the more reliable technique (nuclear stains) only (Gowing, 1986; Gowing & Coale, 1989; Klaas, 2001; Nöthig & Gowing, 1991). Using this information, we performed empirical best fit analyses of samples based on location and taxonomic group, obtaining a linear and an exponential regression. The results of this exercise suggest that in warm and temperate waters (40°N to 40°S), above 200 m, 61% of all Polycystina (*i.e*., all individuals retrieved in the sample, including *in situ* living and dead cells sinking from above) are represented by living cells, whereas below 200 m, 11% are alive. For Phaeodaria, the figures are 96% and 83%, respectively. In cold water areas (>40°N or S), above 200 m, living Polycystina are ~90% and ~75% below 200 m; for Phaeodaria, the values are 97% and 73%, respectively (See supporting information). Therefore, our estimate of 2% to 19% (5 to 58 Tmol Si yr^{-1}) of the global oceanic bSi production is indicative of maximum values; excluding purportedly dead cells from the overall polycystine and phaeodarian standing stocks decreases these figures to 1–10% (2 to 30 Tmol Si yr^{-1}).

On the other hand, there also are potential biases which may involve underestimations in our bSi production. Our data on subsurface depth-integrated abundances are based on a conservative approach, using the 200- to 1,000-m layer only, but many radiolarians are known to dwell and often reach highest abundances below 1,000 m (Kling & Boltovskoy, 1995; Suzuki

& Not, 2015), which might render our integrated subsurface abundance figures too low. In addition, spicule-bearing Collodaria are not included in our abundance estimates. Collodaria include colonies composed by tens to thousands of cells, either naked (*e.g.*, Collozoum sp.) or provided with siliceous spines embedded in the cytoplasm (*e.g.*, *Sphaerozoum* sp.).

There also are solitary species (single cells with or without siliceous spicules). In this study, abundance data for this group are based on shelled organisms only (*e.g.*, Collosphaeridae), because information on densities of species with siliceous spicules scattered around the central capsule (without a solid shell; *e.g.*, genera *Sphaerozoum, Rhaphidozoum*) is virtually null. However, the very few surveys that made rough estimates of the densities of shelled and spicule-bearing Collodaria suggest that, in warm waters, the latter are at least as abundant as the former (Swanberg, 1979). Some other rhizarians with siliceous spines, like *Sticholonche zanclea* (Taxopodia, sensu Adl et al., 2018), are not included in our abundance estimates due to the lack of information which is certainly associated to their delicate skeletons disintegrating rapidly after death (Takahashi & Ling, 1980).

Further, our experiments were carried out with a limited set of radiolarian species pooled into high taxonomic levels, which might represent a potential source of bias when extrapolating these results to global ocean scales. However, our measurements always included several different species (of the same higher level taxon), which presumably takes this variability into account, at least as far as tropical/subtropical waters are concerned. Their representativeness for cold water areas is conceivably lower. Nonetheless, for the Polycystina, size does not seem to be affected by temperature. Indeed, the weight of the skeleton of 48 polycystine species estimated by Jacot Des Combes and Abelmann (2009) is unrelated to their preferred sea surface temperatures (*i.e.*, the sea surface temperatures where they peak in abundance, as estimated from worldwide distribution data by Boltovskoy & Correa, 2016). However, Lomas et al. (2019) found that Si: biovolume ratio increased in diatoms that had adapted to cold water. Whether this effect also impacts Rhizaria is still a research focus. Thus, although these results are preliminary, we contend that the potential bias involved is marginal.

This study highlights the significant contribution of rhizarians to the standing stock and production of bSi on a global scale and challenges the current assumption that diatoms alone control the Si cycle in marine surface waters. Further studies are required on the ecology and physiology of rhizarians and the factors controlling their growth and skeleton's dissolution rate before we can fully elucidate rhizarians' role in the Si and other marine biogeochemical cycles.

Acknowledgements

The authors are grateful to the MOOSE observation national network (funded by CNRS-INSU and Research Infrastructure ILICO), which sustains the annual ship-based hydrographic sections in the northwestern Mediterranean Sea (MOOSE-GE). We also thank the science team and crew of the RSS James Clark Ross and the RV Atalante and Pierre Testor (CNRS, LOCEAN) as head of the MOOSE GE-2017 mission cruise. We are grateful to D. Gonzalez Santana, H. Whitby, and N. van Horsten for English proofreading and comments. We also want to thank S. l'Hélguen and J. F Maguer for the organic component analysis.

Data used in this manuscript are publicly available on the SEANOE website (see https://www.seanoe.org/data/00594/70596/). This work was funded by the "Agence Nationale de la Recherche" grants ISblue (ANR-17-EURE-0015 and ANR IMPEKAB) and LabexMER (ANR-10-LABX-19). This study is a contribution to the international IMBER project and was supported by the UK Natural Environment Research Council National Capability funding.

Chapter 2 – Biogenic silica production of Rhizaria in contrasting environments

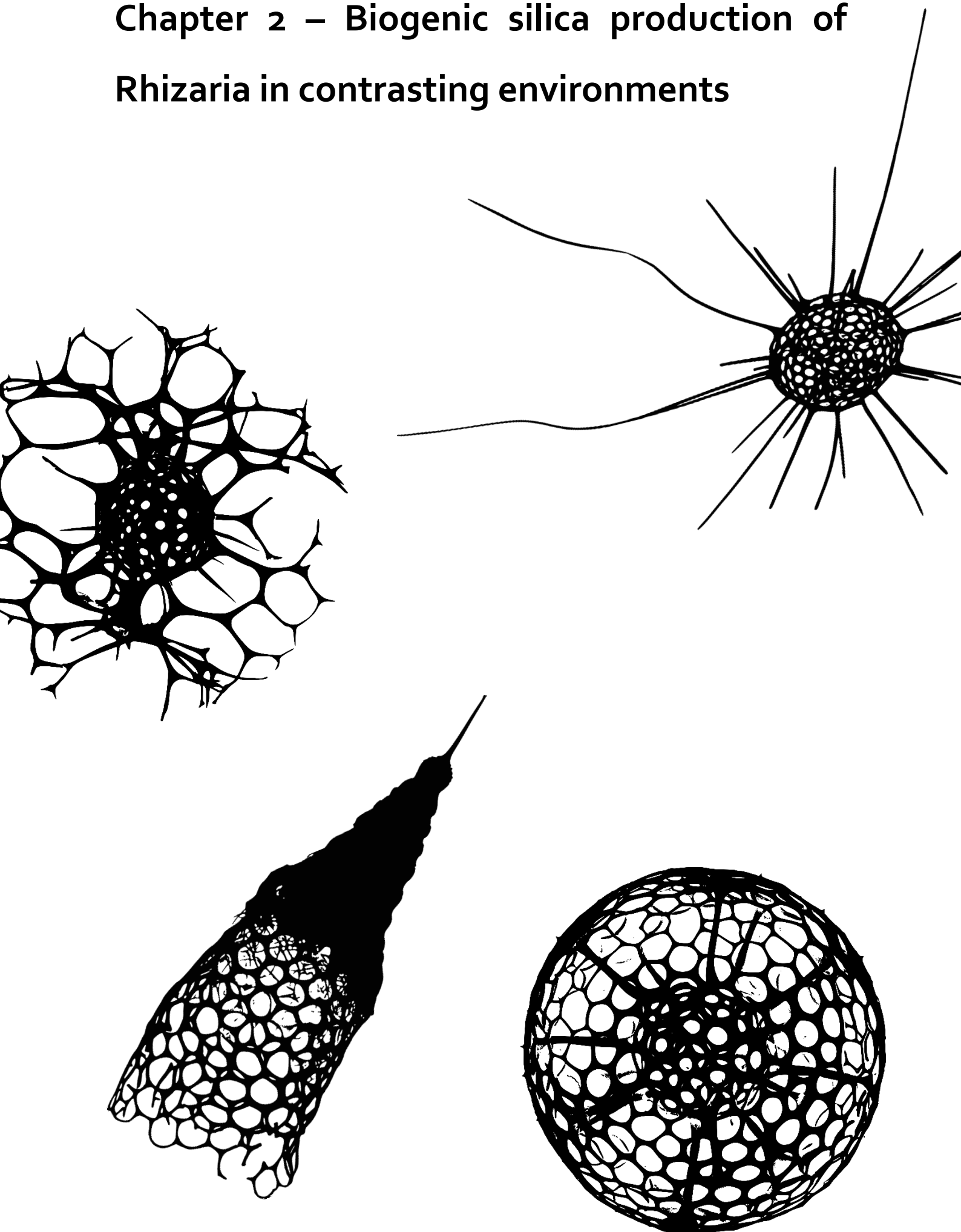

Drawings of Nassellaria and Spumellaria specimens from Miguel Méndez-Sandin pictures.

Context of the work

Considering the initial global estimate based on specimens collected in the Mediterranean Sea, we wanted to investigate whether there are variations in cellular biogenic silica content and bSi uptake rates in contrasting ocean regions.

This second chapter presents the results obtained from the analysis of the samples collected during the Ross Sea Environment and Ecosystem Voyage 2019, TAN1901 cruise in the SW Pacific Sector of the Southern Ocean (SO) (Chapter 2.1). The TAN1901 was the second of two research voyages to the Ross Sea region funded by the New Zealand Ministry of Business, Innovation, and Employment (MBIE) for the 2018 and 2019 austral summer seasons. We collaborated with Andrés Gutiérrez-Rodríguez and Karl Safi (NIWA) during the cruise, where they conducted production experiments with ^{14}C. The Southern Ocean (SO), also called the "Silica Ocean", is a paradise for silicifiers. Concentrations of silicic acid are the highest in the world, silicifiers abound and great amounts of biogenic silica accumulate. Diatoms, rhizarians and sponges cohabit, interact and compete for silica.

This chapter also contains information about the sampling strategy adopted during the Atlantic Meridional Transect (AMT28) cruise (Chapter 2.2), a north-south transect in the Atlantic Ocean, which crosses a wide variety of marine ecosystems and biogeographic provinces for Radiolaria, as defined by Boltovskoy and Correa (2016) (Figure 5 of the Introduction). Preliminary results for this research cruise are reported in Annex 1.

During the TAN1901 and AMT28 expeditions, we incubated both phytoplankton communities and isolated Rhizaria specimens simultaneously, to assess the relative contribution of each group to the biomass and production of biogenic silica in the water masses sampled. In addition, we also studied the elementary composition of a variety of Rhizaria specimen in carbon and nitrogen content.

Chapter 2.1. – Rhizaria in the Southern Ocean

Biogenic silica production by Rhizaria and Diatoms in the Southern Ocean

Natalia Llopis Monferrer[1,5], Aude Leynaert[1], Paul Tréguer[1], Andrés Gutiérrez-Rodríguez[2], Brivaela Moriceau[1], Morgane Gallinari[1], Mikel Latasa[3], Stéphane L'Helguen[1], Jean-François Maguer[1], Karl Safi[4], Matthew H. Pinkerton[2], Fabrice Not[5]

[1]Univ Brest, CNRS, IRD, Ifremer, LEMAR, F-29280 Plouzane, France

[2]National Institute of Water and Atmospheric Research, Wellington, New Zealand

[3]Centro Oceanográfico de Gijón/Xixón, Instituto Español de Oceanografía (IEO), Gijón/Xixón, Asturias, Spain

[4]National Institute of Water and Atmospheric Research, Hamilton, New Zealand

[5]Sorbonne University, CNRS, UMR7144, Ecology of Marine Plankton Team, Station Biologique de Roscoff, Roscoff, France

Under review at Limnology and Oceanography

Abstract

We examined in parallel biogenic silica production and elementary composition (biogenic silica-bSi, particulate organic carbon and particulate organic nitrogen) of Rhizaria and diatoms in the Pacific sector of the Southern Ocean (SO) during austral summer (January-February 2019). From incubations using the ^{32}Si radioisotope, silicic acid uptake rates were measured at 15 stations distributed in the Polar Front Zone, the southern Antarctic Circumpolar Current and the Ross Sea Gyre. Diatoms largely dominated the biogenic silica standing stock and production of the euphotic layer. Rhizaria cells were far more silicified (up to 5.83 nmol-Si $cell^{-1}$) and their individual silicic acid uptake rates were up to 3 orders of magnitude higher than diatoms. However, the average Si/C ratio of Rhizaria (0.05 ± 0.03) was much lower than the Si/C ratio of the phytoplankton community (0.21 ± 0.13). Since SO represents approximately 20% of the global surface of the oceans and Rhizaria contributed to Si production of the upper 200 m ranging from 0.3 to 36.8 µmol-Si $m^{-2}d^{-1}$ in this area, we hypothesize that their contribution to global Si production is lower at high latitudes than in the rest of the ocean (*i.e.*,

maximum of 5% of global bSi production). The Antarctic paradox of Rhizaria (non-negligible contribution to Antarctic siliceous sediments but low abundances in surface waters) is discussed.

Key words: silica cycle, silicic acid uptake, Rhizaria, diatoms, Southern Ocean

1. Introduction

Up to 23.5% of the overall biogenic silica (bSi) production occurs within polar regions (Tréguer and De La Rocha, 2013; Tréguer, 2014), most of it in the Southern Ocean (SO). The SO, sometimes referred to as the "silica ocean" (Honjo et al., 2008), has among the highest dissolved silicic acid (dSi) concentrations of the world ocean. The SO is typified by a prominent siliceous-rich deposit on the seabed, the Antarctic opal-belt (Tréguer et al., 1995) which is mainly composed of diatomaceous oozes (Dutkiewicz et al., 2015). Diatoms are indeed the major contributors of the bSi production in the surface SO (*e.g*. Nelson and Gordon, 1982), from which they are exported to the sea floor (Tréguer, 2014). This siliceous phytoplankton taxa often dominate microalgae assemblages, particularly in highly productive zones such as coastal embayment (Smith and Kaufman, 2018) and in the Antarctic Circumpolar Current (ACC), and south of the Polar Front (PF), where they can account for up to one third of the southern marine Si production (Pondaven et al., 2000).

Patches of radiolarian oozes are also common in the Antarctic opal belt (Dutkiewicz et al., 2015), which suggests that the contribution of siliceous rhizarians to the bSi production of the SO is non negligible. However, while there have been many studies on bSi production by diatoms in the SO, very little is known of the contribution of other pelagic silicifiers. At world ocean scale, silicified Polycystine Radiolaria (*e.g*., Nassellaria, Spumellaria) and Phaeodaria can contribute substantially to global marine bSi production (Llopis Monferrer et al., 2020). Silicified Polycystine Radiolaria and Phaeodaria, all belonging to the Rhizaria lineage, are heterotrophic marine planktonic single-celled eukaryotic organisms. These protists are ubiquitous across the global ocean, throughout the entire water column (Suzuki and Not, 2015). In the dSi-rich SO, numerous studies have reported the presence of several species of Rhizaria from water column to surface sediments (Abelmann and Gersonde, 1991; Maldonado et al., 2019). Despite the evidences of the presence of these organisms in the SO and the

biogeographical importance of this region to the Si cycle (Tréguer, 2014), to our knowledge the Si uptake by Rhizaria in the SO has never been assessed.

Most of these protists form siliceous skeletons but have previously been disregarded in the marine Si cycle, mainly due to the lack of information about their physiology, ecology and biogeochemistry. Additionally, these organisms are difficult to sample using conventional plankton nets because of their delicate structures (Nakamura et al., 2018).

In order to contribute to the understanding of the link between the C and Si biogeochemical cycles and constrain the contribution of Rhizaria to the Si cycle in the SO, this regional study specifically aims at: (i) determining the abundance, biomass and elemental composition of siliceous Rhizaria in the upper water column (0-200 m) of the western Pacific sector of the SO and the Ross Sea region, and (ii) measuring the Si uptake rates for Rhizaria and the phytoplanktonic community.

2. Material and methods

2.1. Study area

The *Ross Sea Marine Environment & Ecosystem Voyage 2019* (TAN1901) was conducted during austral summer (January and February 2019) on board of the R/V Tangaroa, sailing from New Zealand to the Ross Sea. The survey covered mainly oceanic and shelf-slope waters of the Ross Sea region with a focus on the eastern flank of the Iselin Bank and the Ross Gyre. Historically, the Ross Sea Gyre had received considerably less attention than the western continental shelf of the Ross Sea region (*e.g*. Nelson et al., 1994). This study presents results from a subset of 15 stations where CTD casts and net tows were combined to assess water column biogeochemistry and where Si uptake was measured using incubation-based experiments.

The area studied was divided into three hydrographically and ecologically distinct sub-regions arranged as zonal bands delimited by fronts (Figure 1).

1. The Polar Front Zone (PFZ). This zone is delimited by the sub-Antarctic front (SAF) and the Polar Front (PF). Only station 3 was located in this sub-region.

2. The southern Antarctic Circumpolar Current (sACC). This zone is located between the PF (~61.5°S) in the north and the southern boundary of the ACC (sbACC) in the south (~65°S). stations 5 and 32 were located within this sub-region.
3. The Ross Sea Region (RSR). This zone lies south of the sbACC. Most of the stations were located in this zone (stations 7, 9, 11, 13, 15, 17, 20, 22, 24, 26 and 29).

No plankton net tow was performed at station 2. Therefore, this station was not included for the Rhizaria-phytoplankton comparison.

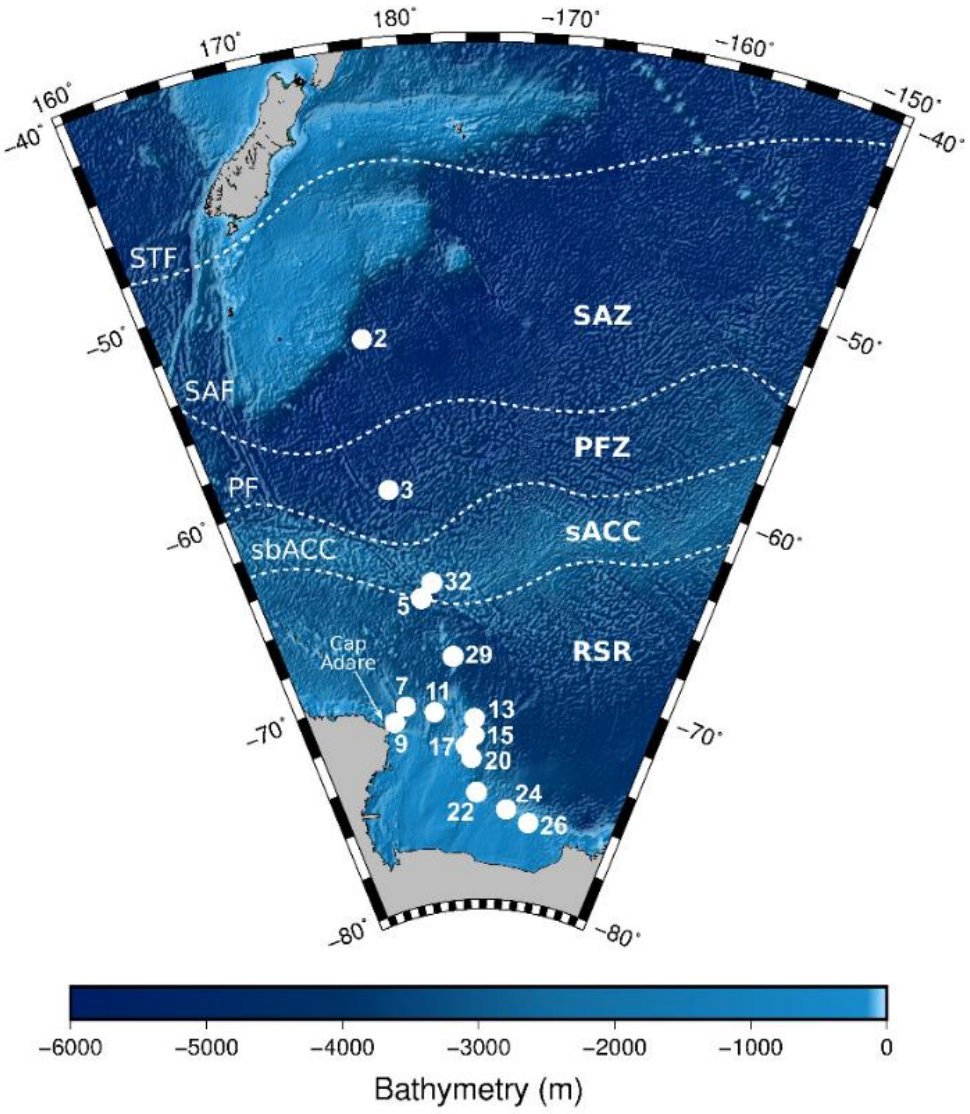

Figure 1. Map of the Pacific sector of the Southern Ocean with station locations (white dots) and approximate location of the Sub-tropical front (STF), Sub-Antarctic zone (SAZ), Sub-Antarctic front (SAF), Polar Front (PF), Polar Front Zone (PFZ), southern Antarctica Circumpolar Current (sACC), southern boundary of the ACC (sbACC) and Ross Sea Region (RSR).

2.2. Sample collection and analyses

2.2.1. Water column – Niskin bottle samples

Dissolved material

A Seabird system was deployed to perform CTD profiles coupled with a 10L Niskin bottles for collection of water samples from 3 to 8 discrete depths. Seawater was sampled at each station to determine nutrients concentrations (NO_3^-, NO_2^-, NH_4^+, $Si(OH)_4$, PO_4^{3-}). Seawater was filtered into a 50 mL falcon tube using a 0.2µm Supor filter cartridge (Acropak, Pall-Gelman) connected directly to the Niskin bottle. Samples were capped with parafilm and frozen at -20°C until analysis in the laboratory. Nutrients concentrations were measured using an Astoria Pacific API 300 micro-segmented flow analyzer (Astoria-Pacific, Clackamas, OR, United States).

Particulate organic material

For the determination of particulate organic matter in the water column, seawater samples were collected in 15 stations at 6 depths between 0 and 100 m. To measure biogenic silica (bSi) and lithogenic silica (lSi) concentrations, 1 L of seawater was filtered onto 0.6 µm, 47 mm Isopore polycarbonate filters (GE Healthcare Whatman). In the seawater filtered from the Niskin bottle, we assume that mainly diatoms contribute to the bSi biomass, with the contribution of rhizarians being negligible. After filtration, filters were kept in petri dishes and stored at room temperature. Analyses were performed using the double digestion method according to (Brzezinski and Nelson, 1989). After NaOH extraction, filters were assayed for lSi by HF digestion during 48 h using the same filter.

For particulate organic carbon (POC) and particulate organic nitrogen (PON) measurements, 1 L of seawater was filtered onto 25 mm GF/F pre-combusted filters (at 450°C during 4 h). Filters were then dried in the oven at 60°C and kept at room temperature. POC and PON concentrations were measured using a C/N analyser (Flash EA, ThermoFisher Scientifc).

Pigments

For High-performance liquid chromatography (HPLC) analysis, 2.2 L of seawater were filtered onto 25-mm GF/F (Whatman) filters. Filters were folded and dry-blotted before storing them at -80°C until laboratory analysis. For station 24, only 1.58 L were filtered before the filter clogged.

Pigments were extracted with 2.5 mL of 90% acetone spiked with 8'-apo-carotenal as internal standard. Filters in acetone were sonicated for 30 s in a tube inside a beaker with ice and stored at -20°C for 24 h. Samples were filtered prior to injection onto a 1100 Agilent HPLC system. The chromatographic conditions for the analysis are described in Latasa (2014). Standards from VKI and Sigma were used to identify and quantify pigment concentrations. We used the coefficients of Uitz et al. (2006) to make a rough estimation of the contribution of different phytoplankton groups to the total Chlorophyll *a* (Chl *a*).

Silicic acid uptake rate

Biogenic silica production was determined as silicic acid uptake rates (ρ_P) at 3 depths for 15 stations using the radioactive isotope labeling ^{32}Si method (Leynaert et al., 1996). Polycarbonate bottles filled with 160 mL seawater were spiked with 800 Bq of radio-labeled ^{32}Si silicic acid solution (Los Alamos Laboratory, specific activity of 18.5 kBq µg-Si^{-1}). Samples were immediately placed in temperature-controlled (ir33+, CAREL) deck-board incubators fitted with neutral density filters to simulate several light levels corresponding to different percentages of incident irradiance (%E_0 = 70, 40, 28, 16, 4, 1%). Flow-through incubators were placed in three HDPE insulated water baths (1000 LT series), each connected independently to a closed system that regulated the temperature of the large water and the flow-through incubators inside. Bottles for ρ_P measurements were incubated for 24 h. At the end of the incubation period, samples were filtered by gentle (<150 mmHg) vacuum filtration onto 47 mm diameter, 0.6 µm pore-size polycarbonate membrane filters (Nucleopore) and rinsed twice with filtered seawater to wash away non-particulate ^{32}Si. Filters for Si uptake rates determination were placed in a 20 mL polypropylene liquid scintillation vial that was capped loosely to allow the sample to dry at room temperature for 48 h. The vials were then capped tightly and stored until analysis. ^{32}Si activity was measured after 3 months on a scintillation counter (Tri-Carb 4910TR, Perkin Elmer) by Cerenkov method (Leynaert, 1993). The background for the ^{32}Si radioactive activity counting was 8 cpm. Samples for which the measured activity was less than 3 times the background were considered to lack Si uptake activity and therefore not considered in further calculations.

Phytoplankton determination

At each station, 500 mL samples were collected from the Niskin bottles, and preserved in Lugol's iodine solution (1% final concentration) for enumeration and taxonomic identification

of phytoplankton by inverted light microscopy according to the method of (Utermohl, 1958) and procedures described in Safi et al. (2007). Briefly, 150 mL subsamples were settled for 24 h before being examined in Utermohl chambers on an inverted microscope (Leitz). When possible, organisms were identified to genus or species level. Biovolume was then calculated by optical microscopy for each species, by measuring between 30 and 50 cells and using formulae representing the geometrical solids that approximated cell shape and adjusted for cell shrinkage. Phytoplankton biovolume was calculated from the dimensions of each taxon (silicoflagellates, Haptophyceae, Raphidophyceae, Cryptophyceae, Chrysophyceae, euglenoids, and monads which were largely small flagellates) and approximated geometric shapes (spheres, cones, ellipsoids) following Sun and Liu (2003) and Olenina et al. (2006).

2.2.2. Net tow samples

Vertical plankton tow samples were carried out with a Bongo net (64 and 200 µm mesh size, mouth diameter: 50 cm) from 200 m to the surface every other day during the TAN1901 cruise. The volume of seawater filtered through the net was estimated using a digital flowmeter (Model 23.090-23.091 – KC Denmark A/S) mounted in the mouth of the net.

Cell counting

The net tow samples were split using the Motoda box. A subsample was fixed with lugol's iodine solution (2% final concentration). Rhizaria abundances were determined in triplicate 3 mL subsamples using an inverted light microscope (Zeiss Axio Vert. A1) back in the laboratory. Concentrations were estimated taking into account the volume of seawater filtrated by the net. The remaining sample was immediately diluted in filtered seawater (0.2 µm) and screened under the microscope to isolate single cells of siliceous Rhizaria. Isolation process could take several hours. During this time, the samples were kept in a light and temperature controlled incubator (MIR-254 Cooled Incubator, Sanyo) to minimize stress to the organisms.

Single cell organisms were isolated using a Pasteur pipette and sorted according to two taxonomic groups, Nassellaria and Phaeodaria. Among the Phaeodaria, we were able to confidently differentiate two species, *Protocystis tridens* and *Protocystis harstoni*. Every specimen collected was imaged and analysed using the ImageJ software to determine morphometric dimensions.

Particulate organic material

For POC and PON cells content, from 1 to 50 individuals of the same taxonomic group and similar size were rinsed in filtered seawater (FSW) and filtered onto 25 mm GF/F pre-combusted filters (at 450°C for 4 h). Filters were then dried in the oven at 60°C and then kept at room temperature. POC and PON concentrations were measured back in the laboratory using a C/N analyser (Flash EA, ThermoFisher Scientific).

Silicic acid uptake rate

For ^{32}Si incubations, 1 to 50 individual cells of the same taxonomic group and similar size were transferred to 20 mL glass vials filled with FSW of 200 m depth. Samples were then spiked with 800 Bq of the radio-labeled ^{32}Si silicic acid solution (Los Alamos Laboratory, specific activity of 18.5 kBq µg-Si^{-1}). Immediately after the addition of the isotope, Rhizaria samples were placed in the deck incubators together with the water column samples. Following the 24 h incubation, the bottles' content was filtered and processed following the same protocol as for the water column samples.

The radioactivity was measured by the Cerenkov effect on the filters without addition of any scintillation cocktail. The Cerenkov method is less sensitive than some others (Brzezinski and Phillips, 1997), however, it allows to use the materials for further biomass analyses. Results were normalized by cell abundance for cell specific silica production. After measuring the uptake rates, the filter was analysed to obtain the bSi of Rhizaria. A single digestion in hydrofluoric acid (HF) was performed, since the samples only contained isolated rhizarians there was no possible interference with lithogenic Si as there might have been when filtering raw seawater (see Ragueneau et al., 2005) . We added 0.2 mL of HF 2.5N to the polymethylpentene (PMP) tubes containing the filters. The filter was then compressed and submerged in HF until air bubbles were removed. The tube was tightly capped and kept under a fume hood, at room temperature for 48 h to complete the digestion of the bSi of the Rhizaria specimens. After complete digestion, 9.8 mL of saturated boric acid solution (H_3BO_3) were added and dSi was measured by colorimetric method on a AA3 HR Auto-Analyzer SEAL-BRAN+LUEBBE (Brzezinski and Nelson, 1989). Standards used for calibration were prepared with the same matrix as for the samples (HF/ H_3BO_3).

3. Results

3.1. Physical and chemical parameters distribution

Sea surface water temperature (SST) varied from about 8°C in the SAZ to -1.5°C in the RSR during the expedition (Figure 2). Overall, the dSi concentration at 10 m depth increased along a north-to-south gradient. Surface dSi concentrations were lower than 1 µM-Si in the PFZ and the sACC (stations 3 and 5). South of the Antarctic Circumpolar Current (ACC), concentrations of dSi raised above 40 µM-Si (stations 5 and 32), reaching ~80 µM-Si (station 29) within the Ross Sea Region (RSR). In contrast, NO_3^- surface concentrations varied only slightly compared to those of the dSi (mean 27.8 ± 4.8 µM-N; range = 15.8 - 32.14 µM-N). This distribution of surface nutrient concentrations shows a transition from NO_3^- rich but $Si(OH)_4^-$ depleted waters in the north to waters enriched with both $Si(OH)_4^-$ and NO_3^- at higher latitude (> 65°S), and corresponds to a sharp increase in the Si/N ratio (mol/mol) southward (Figure 2).

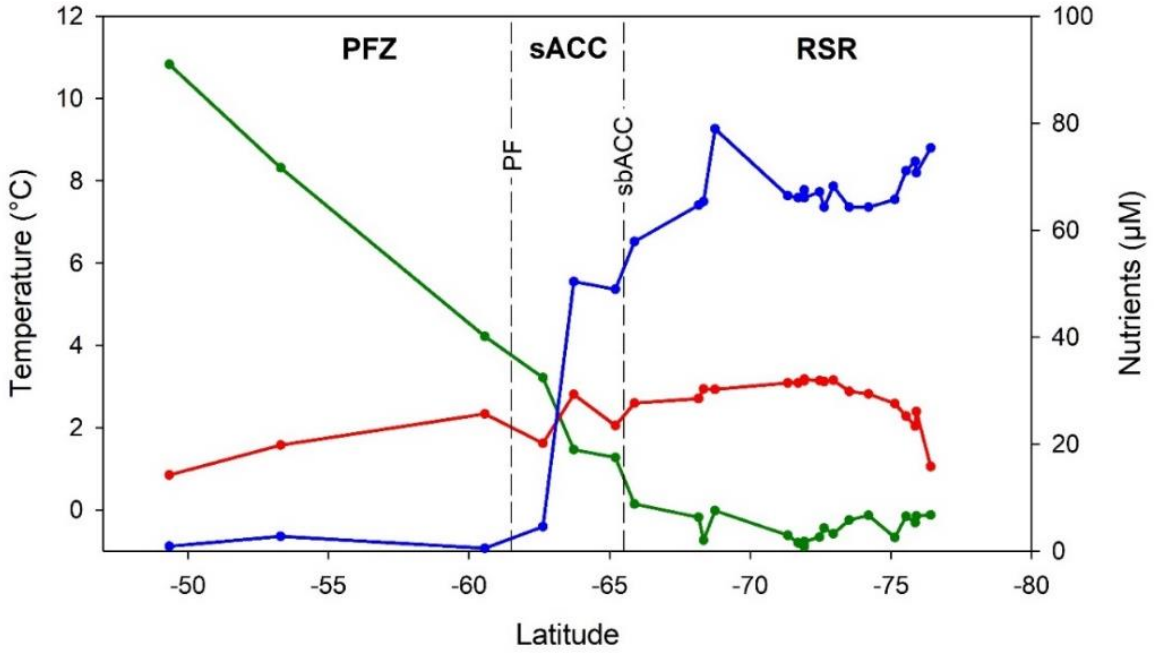

Figure 2. Distribution of temperature (green), nitrates (red) and silicates (blue) at 10 m depth along the cruise track from North (SW Pacific sector) to South (Ross sea region). Dots represent stations location. Vertical dashed lines represent the Polar Front (PF) and the southern boundary of the ACC (sbACC) delineating the three sub-regions considered for the study: Polar Front Zone (PFZ), southern ACC (sACC) and the Ross Sea Region (RSR).

Biogenic silica concentrations at 10 m depth in the water column, ranged between 0.18 µmol-Si L^{-1} and 6.36 µmol-Si L^{-1} (Table 1). With the exception of station 9, (5.47 µmol-Si L^{-1}), bSi

concentrations in the RSR (1.42 ± 1.43 µmol-Si L^{-1}, n = 11) were on average lower than in the sACC (5.6 (± 1.1) µmol-Si L^{-1}, n = 2).

Table 1. Particulate organic carbon (POC) and particulate organic nitrogen (PON) content, C/N and Si/C ratios and biogenic silica stocks (bSi), Si uptake rates (ρ_P) and specific uptake rates (V_P) of the phytoplankton community at 10 m depth. Sub-antarctic Zone (SAZ), Polar Front Zone (PFZ), southern Antarctic Circumpolar Current (sACC). NA means that no values were available.

Station #	Sub-region	Latitude	Longitude	POC µmol L^{-1}	PON µmol L^{-1}	bSi µmol L^{-1}	C/N	Si/C	ρ_P µmol Si d^{-1}	V_P d^{-1}	Diatoms cell L^{-1}
2	SAZ	-53.300	175.483	6.58	0.95	0.66	6.95	0.10	0.02	0.03	NA
3	PFZ	-60.578	175.865	7.64	1.12	1.67	6.83	0.22	0.02	0.01	NA
5	sACC	-65.857	177.938	15.39	2.46	4.77	6.26	0.31	0.25	0.05	262544
32	sACC	-65.207	179.242	13.40	2.20	6.36	6.09	0.48	0.03	0.00	NA
Mean sACC				*14.39*	*2.33*	*5.57*	*6.18*	*0.39*	*0.14*	*0.03*	
7	RSR	-70.838	173.891	6.68	1.02	1.53	6.57	0.23	0.10	0.06	26015
9	RSR	-71.500	171.953	12.08	1.92	5.47	6.28	0.45	0.34	0.06	22079
11	RSR	-71.295	177.933	5.43	0.83	1.59	6.51	0.29	0.08	0.05	16484
13	RSR	-71.687	-176.206	3.95	0.62	0.72	6.34	0.18	0.04	0.05	1920
15	RSR	-72.464	-176.322	6.11	1.07	0.98	5.70	0.16	0.07	0.08	30113
17	RSR	-72.951	-177.653	6.95	1.15	0.97	6.03	0.14	0.09	0.09	103300
20	RSR	-73.517	-176.877	5.28	0.88	0.85	6.01	0.16	0.04	0.04	9501
22	RSR	-75.133	-176.040	9.00	1.42	1.81	6.34	0.20	0.19	0.10	NA
24	RSR	-75.901	-170.564	5.65	0.92	1.07	6.14	0.19	0.10	0.09	5621
26	RSR	-76.414	-166.120	8.82	1.56	0.18	5.65	0.02	0.02	0.12	NA
29	RSR	-68.748	-178.849	6.24	1.07	0.43	5.86	0.07	0.05	0.11	NA
Mean RSR				*6.93*	*1.13*	*1.42*	*6.13*	*0.19*	*0.10*	*0.08*	

Concentrations of POC varied from 4.0 to 15.4 µmol-C L^{-1} along the cruise track. Maximum concentrations were observed in the sACC, 15.4 µmol-C L^{-1} at station 5 and 13.4 µmol-C L^{-1} at station 32 (Table 1). Secondary peaks of POC were observed at the southernmost station in the RSR (station 26, with 8.8 µmol-C L^{-1}) and at the westernmost station (station 9, with 12.1 µmol-C L^{-1}), the latter being the closest to the continental shelf. The highest concentrations of PON (2.5 µmol-N L^{-1} at station 5 and 2.2 µmol-N L^{-1} at station 32) were observed in the sACC (~65°S), being on average 2-fold higher than the concentration measured in the RSR (1.1 ± 0.4 µmol-N L^{-1}, Table 1).

This trend was confirmed by the evolution of the Si/C ratios (mol/mol) which varied from 0.39 on average in the sACC to 0.19 in the RSR (Table 1). C/N molar ratios at 10 m did not vary substantially along the transect (6.24 ± 0.4), with a minimum of 5.65 at station 26 located near a polynya, and a maximum of 6.95 at station 2, located in sub-Antarctic waters (Table 1). When integrated in the upper 100 m of the water column, bSi and POC concentrations did not follow the same pattern along the transect (Figure 3). Although for both communities (Rhizaria and

diatoms), highest depth-integrated concentrations were found in the sACC at stations 5 and 32 with 348.3 mmol-Si m^{-2} and 1309.9 mmol-C m^{-2}, respectively. The decrease in concentration within the RSR was much sharper for bSi than for POC, suggesting a lower contribution of diatoms to the overall phytoplankton community in this area.

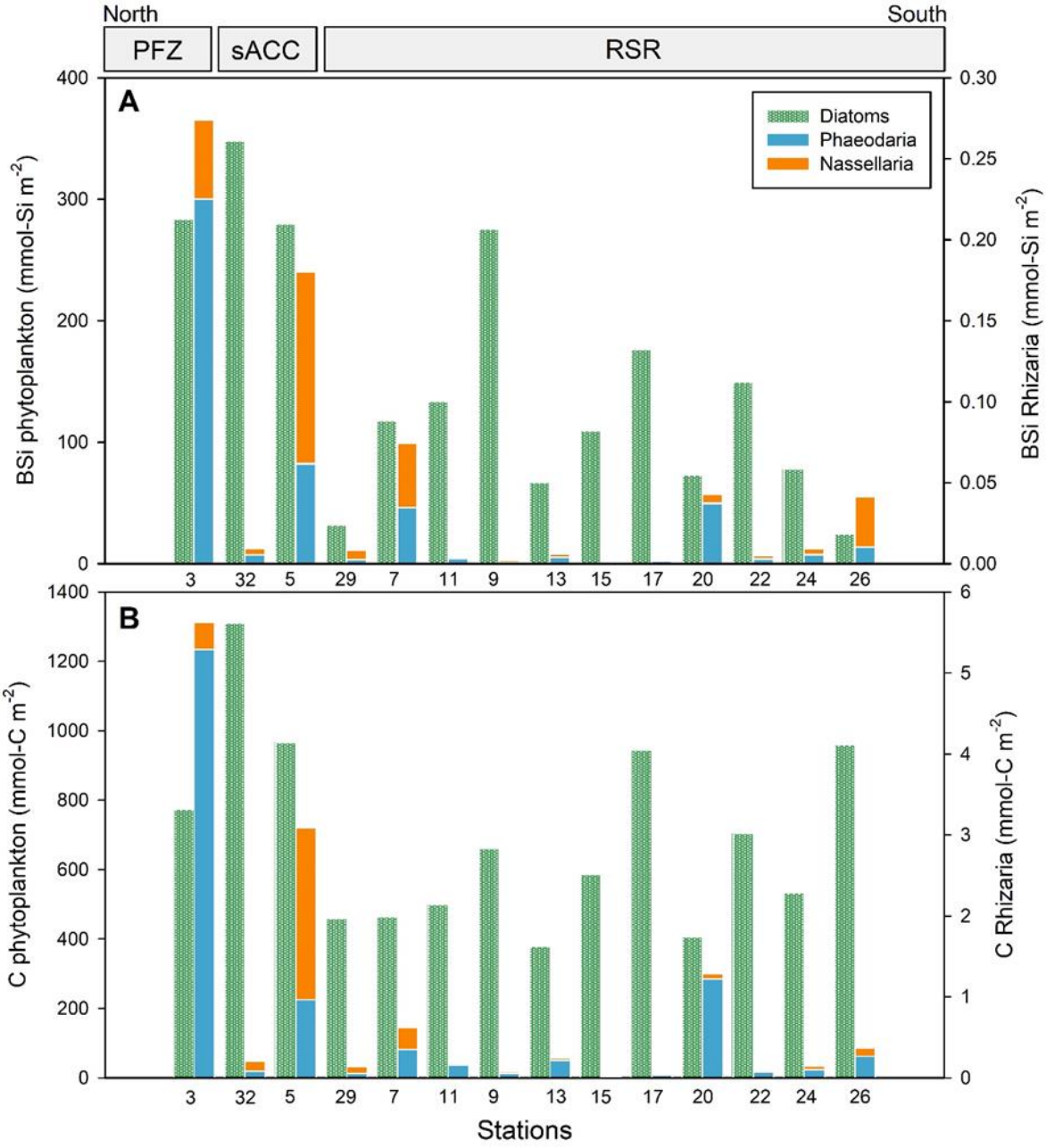

Figure 3. Contribution of siliceous phytoplankton community (diatoms) and Rhizaria to the (A) biogenic silica (bSi) biomass in mmol-Si m^{-2} and to the (B) Carbon biomass in mmol-C m^{-2} integrated from the upper 100 m and 200 m of the water column for the phytoplankton community and Rhizaria, respectively. Note: Y axis for diatoms and Rhizaria vary of several orders of magnitude.

3.2. Chlorophyll concentrations and phytoplankton community composition

Surface Chl *a* concentration averaged 340.2 ± 242.0 ng Chl *a* L^{-1}, ranging from 101.1 to 924.3 ng Chl *a* L^{-1} (Figure 4). The highest values observed were associated to the ACC (station 32) and coastal waters close to Cape Adare (station 9). Diatoms dominated the phytoplankton community in the surface waters, accounting on average for 50% of the total Chl *a* biomass, except at stations 26 and 3 (Figure 4). Analyses of phytoplankton composition indicated that station 17 located within the RSR was dominated (>50% of abundance) by *Chaetoceros* sp. stations 11 and 13 were dominated by *Corethron* sp. In the southernmost stations we observed a dominance of the *Nitzschia* sp.

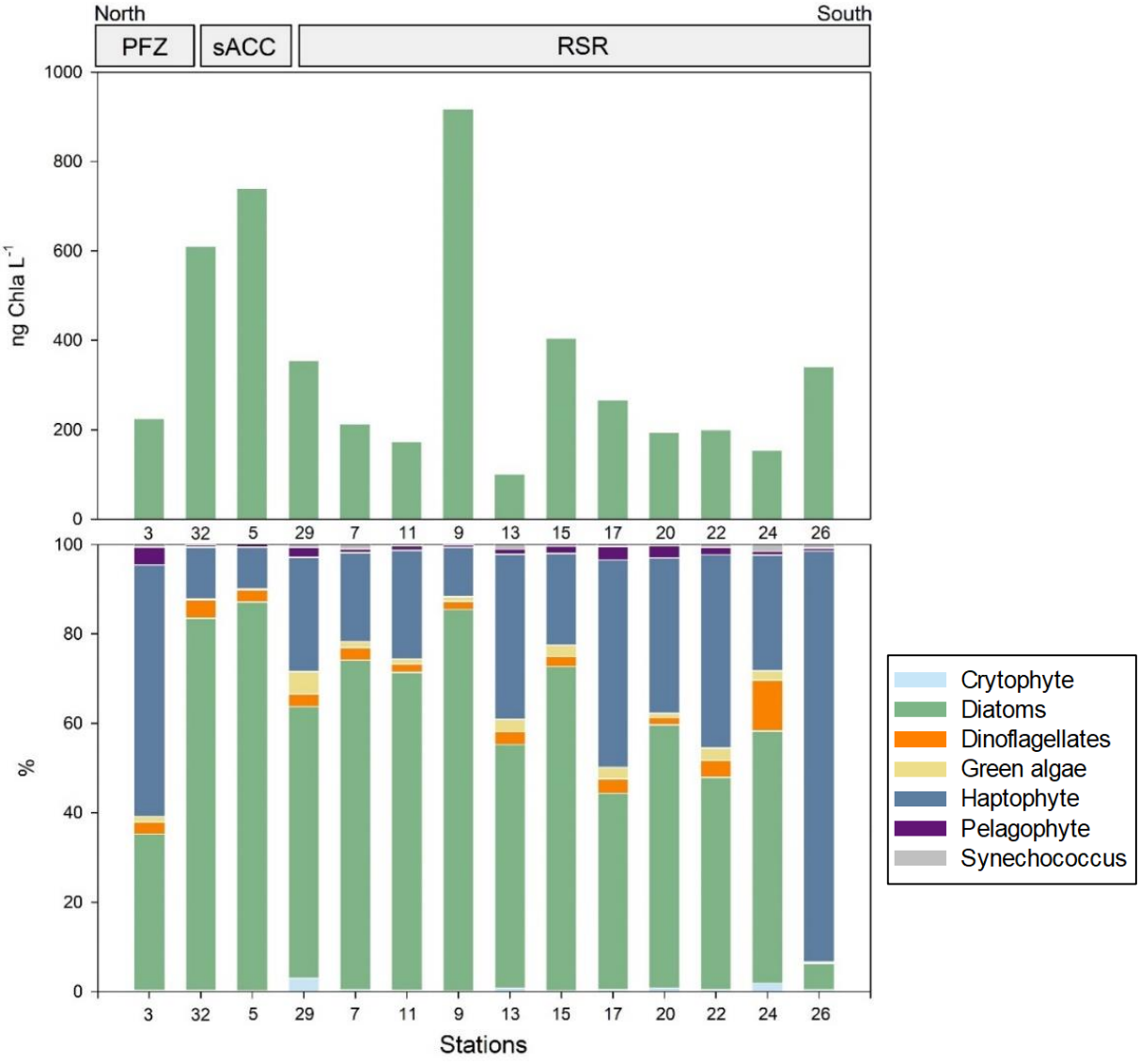

Figure 4. Phytoplankton Chl *a* concentration from North to South at the different stations (A) contribution of the entire phytoplankton community in ng Chl *a* L^{-1}. (B) Relative contribution of the different phytoplanktonic groups.

Haptophytes were the second most important taxonomic group, contributing ~30% of the total Chl *a* biomass, except for station 26 where they accounted for > 90% of total Chl *a* (Figure 4). Other phytoplankton groups such as dinoflagellates and green algae made up < 5% of the total Chl *a*, while the contribution of cryptophytes, pelagophytes and Synechococcus was relatively minor (<1% of the total Chl *a*).

3.3. Rhizaria cell abundances

In the first 200 m of the water column, the highest abundances of Rhizaria (> 200 cells m^{-3}) were located at stations north of the RSR (stations 3 and 5). However, station 32, which was located near station 5, sampled about a month later, yielded less than 30 cells m^{-3} (Table 2). The lowest abundances (less than 50 cells m^{-3}) were observed within the RSR, except at station 20 where rhizarians cells abundances reached a maximum of 111 cells m^{-3}.

Table 2. Biogenic silica stocks, POC and PON content including C/N and Si/C ratios of the Rhizaria and Si uptake rates and specific uptake rates. Cells' abundances and cell size are also included. For abundances estimates, the mean coefficient of variation (CV) of the triplicates was of 36%, 28% and 22% for *Protocystis tridens*, *Protocystis harstoni* (Phaeodaria) and Nassellaria respectively. n denotes the number of specimen analysed. * The values of organic content are averages.

Station	Sub-region	Latitude	Longitude	Species	n cells	Abundance cell m^{-3}	Major axis µm	PON nmol N cell^{-1}	POC nmol C cell^{-1}	bSi nmol Si cell^{-1}	C/N	Si/C	ρ_P nmol Si cell^{-1} d^{-1}	V_P d^{-1}
3	PFZ	-60.564	175.845	*P. tridens*	27	453	101±15	NA	NA	2.33	NA	NA	0.13	0.06
3	PFZ	-60.564	175.845	*P. harstoni*	NA	NA	NA	NA	NA	NA	NA	NA	NA	NA
3	PFZ	-60.564	175.845	Nassellaria	9	51	80±12	NA	NA	4.75	NA	NA	0.56	0.12
5	sACC	-65.877	177.928	*P. tridens*	NA	NA	NA	NA	NA	NA	NA	NA	NA	NA
5	sACC	-65.877	177.928	*P. harstoni*	12	40	101±18	NA	NA	5.83	NA	NA	0.77	0.13
5	sACC	-65.877	177.928	Nassellaria	60	212	74±12	5.69	49.27	2.80	8.66	0.06	0.66	0.24
32	sACC	-65.206	179.247	*P. tridens*	NA	NA	NA	NA	NA	NA	NA	NA	NA	NA
32	sACC	-65.206	179.247	*P. harstoni*	80	8	85±3	3.80	34.66	2.93	9.12	0.08	0.33	0.11
32	sACC	-65.206	179.247	Nassellaria	80	21	101±44	4.11	34.18	1.00	8.32	0.03	0.06	0.06
Mean sACC				*P. tridens*	*27*	*453*		*NA*	*NA*	*2.33*	*NA*	*NA*	*0.13*	*0.06*
				P. harstoni	*46*	*24*		*3.80*	*34.66*	*4.38*	*9.12*	*0.08*	*0.55*	*0.12*
				Nassellaria	*50*	*95*		*4.90*	*41.73*	*2.85*	*8.49*	*0.04*	*0.43*	*0.14*
7	RSR	-70.847	173.924	*P. tridens*	17	16	no picture	NA	NA	4.53	NA	NA	0.97	0.21
7	RSR	-70.847	173.924	*P. harstoni*	17	10	116	NA	NA	7.57	NA	NA	1.32	0.17
7	RSR	-70.847	173.924	Nassellaria	12	41	no picture	NA	NA	4.81	NA	NA	1.00	0.21
9	RSR	-71.499	171.963	*P. tridens*	68	4	96±2	9.40	66.47	0.63	7.07	0.01	0.26	0.42
9	RSR	-71.499	171.963	*P. harstoni*	5	<1	120	NA	NA	4.70	NA	NA	1.60	0.34
9	RSR	-71.499	171.963	Nassellaria	11	3	81±12	NA	NA	3.57	NA	NA	0.94	0.26
11	RSR	-71.296	177.896	*P. tridens*	58	6	100	7.79	100.19	1.75	12.86	0.02	0.31	0.18
11	RSR	-71.296	177.896	*P. harstoni*	21	2	109±9	8.31	106.30	NA	12.79	NA	NA	NA
11	RSR	-71.296	177.896	Nassellaria	27	1	83±18	NA	NA	3.05	NA	NA	0.80	0.26
13	RSR	-71.694	-176.216	*P. tridens*	51	6	99±12	7.86	70.00	3.01	8.91	0.04	0.82	0.27
13	RSR	-71.694	-176.216	*P. harstoni*	36	5	115±4	11.29	139.06	2.54	12.32	0.02	0.73	0.29
13	RSR	-71.694	-176.216	Nassellaria	75	4	66±5	3.64	36.24	2.77	9.96	0.08	0.58	0.21
15*	RSR	-72.465	-176.333	*P. tridens*	160	2	93±9	4.49	42.14	1.82	9.39	0.04	0.98	0.54
15	RSR	-72.465	-176.333	*P. harstoni*	NA	NA	NA	NA	NA	NA	NA	NA	NA	NA
15	RSR	-72.465	-176.333	Nassellaria	NA	NA	NA	NA	NA	NA	NA	NA	NA	NA
17	RSR	-72.951	-177.655	*P. tridens*	80	3	96±2	2.31	23.49	1.79	10.17	0.08	2.65	1.48
17	RSR	-72.951	-177.655	*P. harstoni*	NA	NA	NA	NA	NA	NA	NA	NA	NA	NA
17	RSR	-72.951	-177.655	Nassellaria	NA	NA	NA	NA	NA	NA	NA	NA	NA	NA
20*	RSR	-73.518	-176.869	*P. tridens*	120	111	93±4	NA	NA	1.68	NA	NA	0.47	0.28
20	RSR	-73.518	-176.869	*P. harstoni*	NA	NA	NA	NA	NA	NA	NA	NA	NA	NA
20	RSR	-73.518	-176.869	Nassellaria	NA	NA	NA	NA	NA	NA	NA	NA	NA	NA
24	RSR	-75.903	-170.558	*P. tridens*	80	11	97±2	4.49	33.77	1.86	7.52	0.06	0.14	0.08
24	RSR	-75.903	-170.558	*P. harstoni*	29	2	111	NA	NA	3.56	NA	NA	1.48	0.41
24	RSR	-75.903	-170.558	Nassellaria	50	6	62±9	NA	NA	3.12	NA	NA	0.19	0.06
26	RSR	-76.415	-166.134	*P. tridens*	NA	NA	NA	NA	NA	NA	NA	NA	NA	NA
26	RSR	-76.415	-166.134	*P. harstoni*	NA	NA	NA	NA	NA	NA	NA	NA	NA	NA
26	RSR	-76.415	-166.134	Nassellaria	46	50	76±8	1.60	14.85	NA	9.28	NA	NA	NA
29	RSR	-68.747	-178.849	*P. tridens*	38	5	89±11	NA	NA	2.26	NA	NA	0.14	0.06
29*	RSR	-68.747	-178.849	*P. harstoni*	42	<1	111±10	NA	NA	2.93	NA	NA	1.59	0.54
29	RSR	-68.747	-178.849	Nassellaria	40	13	92±32	NA	NA	2.28	NA	NA	0.41	0.18
Mean RSR				*P. tridens*	*75*	*18*		*6.06*	*56.01*	*2.15*	*9.32*	*0.04*	*0.75*	*0.39*
				P. harstoni	*25*	*5*		*9.80*	*122.68*	*4.26*	*12.55*	*0.02*	*1.34*	*0.35*
				Nassellaria	*37*	*17*		*2.62*	*25.55*	*3.27*	*9.62*	*0.08*	*0.65*	*0.20*

Rhizaria specific composition changed with latitude: in the northern sector (PFZ, station 3) phaeodarians of the genus *Protocystis* dominated, whereas Nassellaria was the most abundant group in the sbACC. Among the genus *Protocystis*, *P. tridens* and *P. harstoni* were the most common species. Other species such as *P. swirei*, *P. balfouri* and *P. micropelecus* were also recorded occasionally, but they were not abundant enough (less than 10 specimens per sample) to be included in our experiments. Nassellaria were largely dominated by the genus *Antarctissa* spp. (family Plagoniidae). As for Phaeodaria, the diversity of Nassellaria was noticeably higher at the northern stations, where representatives of the families Artrostrobiidae, Spyridae and Theopteridae were common. Only taxa with sufficiently high abundance (> 30 specimens per sample) were used for the experiments.

Regardless of the taxonomic groups, cell size of the collected specimens varied slightly, ranging from 62 µm for the smallest Nassellaria to a maximum of 115 µm for the largest Phaeodaria (Table 2).

For the estimation of the elemental cell content, a total of 1351 cells were analysed, with 816 cells for bSi analyses and 535 cells for POC and PON (Table 2).

Overall, bSi per cell varied from 0.6 to 7.6 nmol Si $cell^{-1}$ (Table 2). The POC cellular content varied between 14.9 and 139.1 nmol C $cell^{-1}$, with *P. harstoni* being the group with the highest POC content (139.1 nmol C $cell^{-1}$). The PON cellular content varied between 1.6 and 11.3 nmol N $cell^{-1}$.

Regarding the molar ratios, Nassellaria had the lowest C/N ratio (9.1 ± 0.7), while Phaeodaria exhibited similar average but more variable C/N ratios (10.0 ± 2.2). The Si/C ratios of Nassellaria (0.05 ± 0.02), and Phaeodaria (0.04 ± 0.03) were similar on average and not significantly different among taxonomic groups (ANOVA, P = 0.8).

Using cell abundances in the water column and cellular bSi and POC content, we calculated the bSi and POC concentrations of Rhizaria (bSi_{Rhiz} and POC_{Rhiz}) integrated in the upper 200 m of the water column, corresponding to the maximum depth at which the plankton net was deployed (Figure 3). Along the latitudinal transect, bSi_{Rhiz} (Figure 3A) followed the same pattern as cell abundances, with higher values at stations located north of 67°S, in the PFZ and in the sACC (0.3 and 0.2 mmol-Si m^{-2} at stations 3 and 5 respectively) although values at station 32 (0.01 mmol-Si m^{-2}), located very close to the station 5 were an order of magnitude lower. In the RSR, bSi_{Rhiz} concentrations were lower, average 0.02 ± 0.02 mmol-Si m^{-2}.

In contrast to the spatial distribution of bSi_{Rhiz}, POC_{Rhiz} concentrations did not show a clear pattern. POC_{Rhiz} concentrations varied from 0.01 mmol-C m^{-2} to 5.62 mmol-C m^{-2} (Figure 3B). Across the study area, the maximum value of POC_{Rhiz} concentration was observed at station 3, in the PFZ. In the RSR, maximum POC_{Rhiz} concentration (1.28 mmol-C m^{-2}) was determined at station 20.

3.4. Rhizaria and diatoms silicic acid uptake rate

Rates of dSi uptake (ρ_P) integrated in the upper water column ranged from 1263.9 to 17474.2 µmol-Si m^{-2} d^{-1} for diatoms and from 0.48 to 37.97 µmol-Si m^{-2} d^{-1} for Rhizaria, respectively (Figure 5). Phytoplankton community ρ_P was always 2 or 3 orders of magnitude higher than Rhizaria ρ_P. At station 5, located in the sACC, we observed the highest productivity values in terms of both, diatoms (12541.4 µmol-Si m^{-2} d^{-1}) and Rhizaria (38.0 µmol-Si m^{-2} d^{-1}). In the northern stations, Rhizaria ρ_P values were below 10 µmol-Si m^{-2} d^{-1} although some stations

displayed higher values (station 3, 5 and 7 with 21.2, 38.0 and 14.9 µmol-Si m^{-2} d^{-1}, respectively). Rates of dSi uptake become lower consistently starting at station 11.

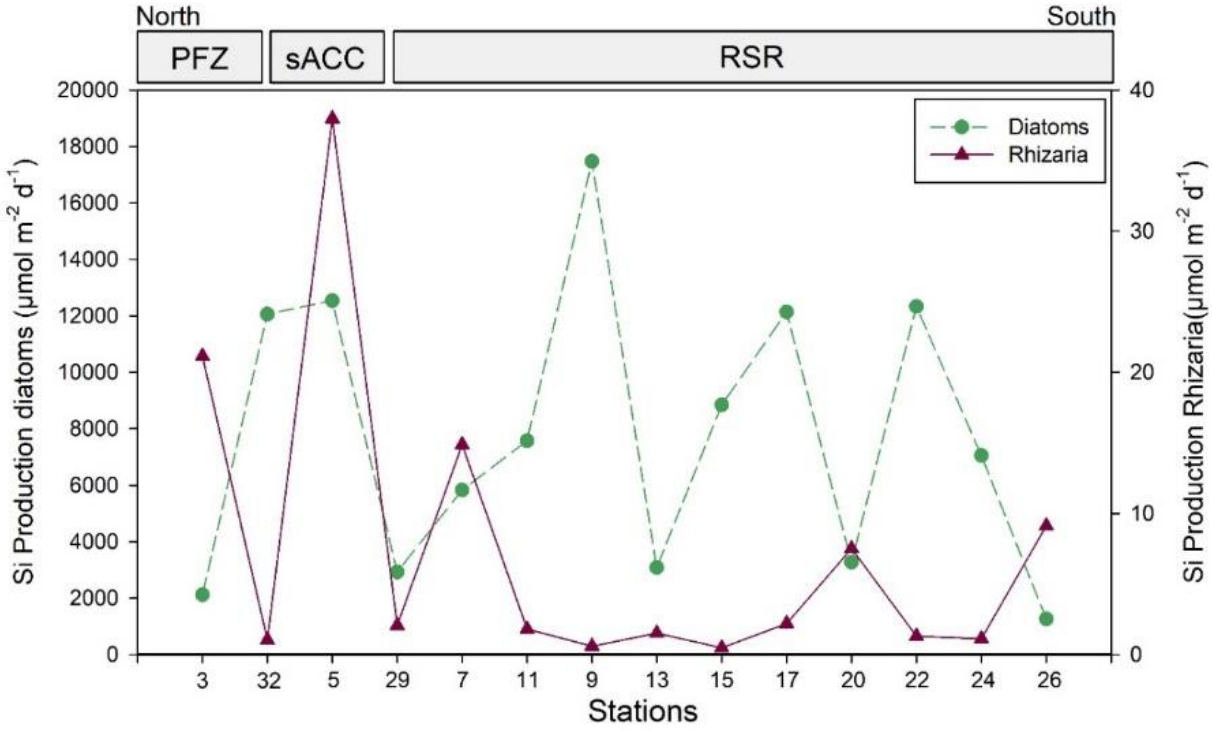

Figure 5. Silica production integrated from the upper 100 m and 200 m of the water column for the phytoplankton community (diatoms) and Rhizaria, respectively. Note: Y axis for diatoms and Rhizaria vary of several orders of magnitude.

In the RSR, we found the highest values of ρ_P for phytoplankton community (17474.2 µmol-Si m^{-2} d^{-1}) at station 9, located close to the coast off Cape Adare.

Specific Si uptake rates (V_P – dSi uptake rates normalized to bSi concentration) of the phytoplankton community were on average 0.06 d^{-1} (range <0.01-0.12) at 10 m depth (Table 1). These rates tended to be higher in the RSR (average 0.08 d^{-1}) compared to those measured in the sACC (average 0.03 d^{-1}) and PFZ (average 0.01 d^{-1}). Specific Si uptake rates for Rhizaria were higher than those found for the phytoplankton community, averaging 0.18, 0.36 and 0.29 d^{-1} for Nassellaria, *P. tridens* and *P. harstoni* respectively (Table 2).

4. Discussion

4.1. Abundance of Rhizaria in the SO compared to other regions of the global ocean

Abundances found during the TAN1901. In the 0-200 m layer, the Rhizaria abundances ranged from <1 cell m^{-3} to 505 cells m^{-3}, with the highest values measured in the PFZ and the sACC**.** We observed a sharp variation in cell abundances within the sbACC, between station 5 and 32. The large difference observed may be explained by the presence of the AAC, which is a known area of high kinetic energy that can generate a large spatial heterogeneity at sub-mesoscale and affect plankton distribution (Carrasco et al., 2003). It could also be explained by the delay of the sampling date as station 5 was sampled on the outward journey, 25 days before station 32 which was sampled on the return leg, corresponding potentially to a different period of the development of Rhizaria communities.

Abundances in the SO. Our results are in the range of abundances reported to date in other sectors of the SO (Abelmann and Gowing, 1997), with higher values as we go northward (Table 3). However, linking the variability observed between abundances data to the seasonal dynamic of these protists or to rapid changes in environmental conditions is still a challenge. While the overall pattern of phytoplankton evolution is well studied in this area, with a spring bloom of haptophyte that accumulates until late December, followed by a diatoms bloom (Smith and Kaufman, 2018), little information is available about rhizarians growth patterns. Scarcity of Rhizaria abundance data in the SO limits the comparison between our data and previous studies. In particular, there are not enough data and temporal coverage to assess seasonal evolution in this complex and dynamic Antarctic region.

Table 3. Mean abundances or ranges (in parentheses) of polycystine and Phaeodaria in polar waters found in this study and reported in previous surveys. Note that in this study we only studied of the polycystine, the Nassellaria order because we did not collect enough spumellarians to conduct experiments, but other studies may also include specimens of the Spumellaria order.

Reference	Area	Season	Year	Depth interval (m)	Polycystine (cells m^{-3})	Phaeodaria (cells m^{-3})	Comment
This study	PFZ	Jan-Feb	2019	0-200	51	453	
This study	sbACC	Jan-Feb	2019	0-200	(21 - 212)	(8 - 40)	
This study	RSR	Jan-Feb	2019	0-200	(1 - 41)	(<1 - 111)	
Llopis Monferrer et al. (2020)	>40°N-S	NA	2020	0-200	183	5	review
Abelmann & Gowing (1997)	>45°S (Atlantic sector)	April	1991	0-200	(325 - 408)	NA	
Alder & Boltovskoy (1993)	Weddell Sea	March	1991	0-200	NA	700	
Alder & Boltovskoy (1993)	Weddell Sea	Nov-Jan	1986	0-200	1441	534	
Morley & Stepien (1985)	Weddell Sea	Oct-Nov	1981	0-200	(8 - 154)	(4 - 132)	
Tanaka et al. (2008)	Subartic Pacific	June	2006	0-250	NA	6	

Rhizaria abundances worldwide. Our data fit with the worldwide Rhizaria data compilation reported by Llopis Monferrer et al. (2020), where estimated abundances of these protists ranged from 5 to 183 cells m^{-3} for high latitude oceans (>40°N-S). In fact, estimates of concentrations of living Rhizaria in polar seas are scarce and very variable (Table 3). For the central subarctic Pacific Tanaka et al. (2008) reported Phaeodaria abundances of 6 cells m^{-3} in the first 250 m of the water column, while 4 to 132 phaeodarian cells m^{-3} and 8 to 154 cells m^{-3} polycystine radiolarians were reported for the Weddell Sea by Morley and Stepien (1985). In the present study, reported Rhizaria cells abundance were lower (1 to 212 cells m^{-3} for polycystine and 1 to 111 cells m^{-3} for phaeodarians) than the living cell concentrations reported in the Atlantic sector of the Southern Ocean (325 to 408 cells m^{-3}) (Abelmann and Gowing, 1997) which tended to decrease towards lower latitudes (northern of the PFZ). The different species collected could explain part of the opposite trend observed. It should be noted that the siliceous Rhizaria abundance assessed here only includes the most representative species of small Rhizaria (< 300 µm). Larger cells were often recorded in the samples (including Spumellaria and Phaeodaria of the family Aulacanthidae) albeit in low numbers and were therefore not included in our estimates. Besides, the fragile skeleton of larger Rhizaria probably broke due to entanglement with other cells during sampling using plankton nets.

4.2. Elemental composition of Rhizaria and diatoms in the SO compared with other regions of the global ocean

***Allometric relationship for Rhizaria*.** The bSi content of siliceous Rhizaria has been investigated using different approaches, from living cells collected using net-tows (Biard et al., 2018; Llopis Monferrer et al., 2020), settling cells recovered from sediment traps (Takahashi, 1981), to fossil assemblages from the sediments (Lazarus et al., 2009). An

allometric relationship was established by Biard et al. (2018) showing that Si content of large Rhizaria (Phaeodaria; > 600 µm) is closely associated with cell length and biovolume. This relationship was expanded by Llopis Monferrer et al. (2020) over a wider size range. When adding the information on silica content (Q_{bSi}) of the 32 samples collected in the present survey, including Nassellaria and Phaeodaria, to the data of Llopis Monferrer et al., (2020) (Figure 6) we conclude that the Q_{bSi} was significantly correlated with the cell's equivalent diameter (ESD) (R^2 = 0.85, p < 0.001, n=126) according to the following equation;

$\log_{10}(Q_{bSi}) = [-3.47 \pm 0.13] + [1.32 \pm 0.05] \log_{10}(ESD)$

Despite the global trend of increasing Q_{bSi} with cell size, we observed light variations at a local scale (Ross Sea). Indeed, if we plot Q_{bSi} versus ESD for our data set alone, the slope is significantly different (ANCOVA, p < 0.01) from the one calculated by Llopis Monferrer et al. (2020). Specimens analysed for the present study display higher Q_{bSi} than those found in other areas of the global ocean (Figure 6), suggesting a higher degree of silicification of individuals in the dSi-rich SO.

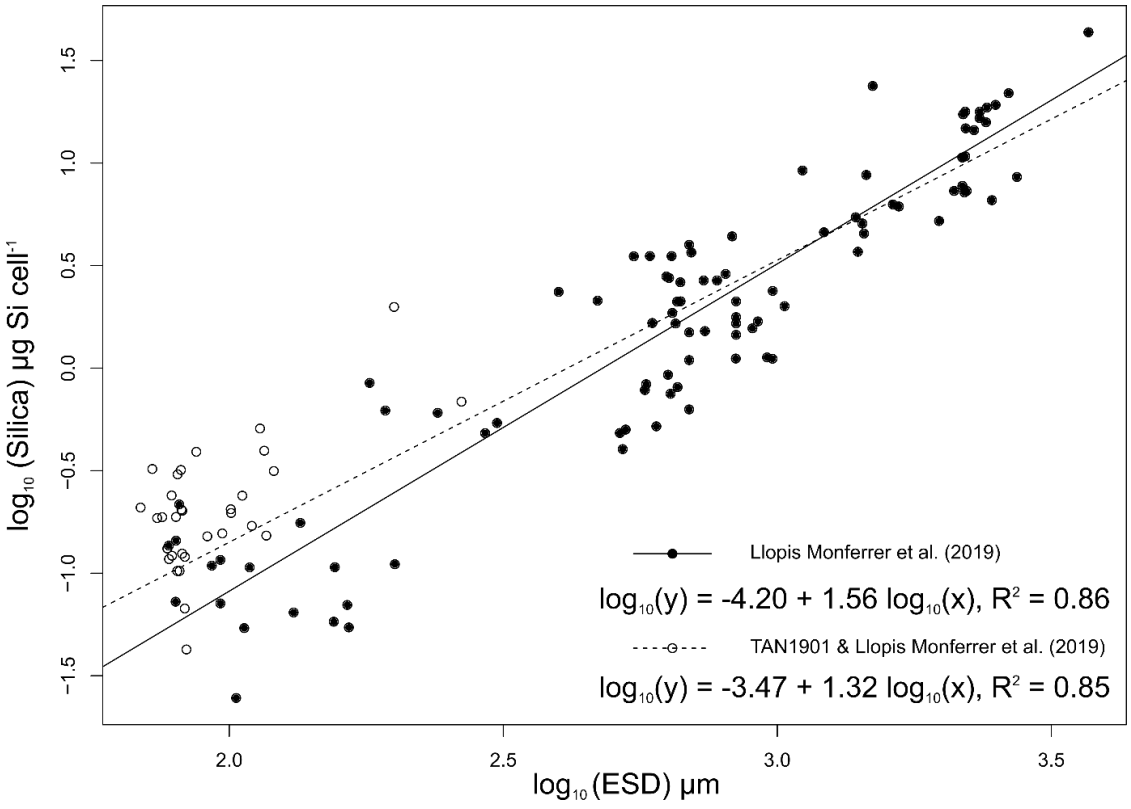

Figure 6. Relationship between the Si content of Polycystina and Phaeodaria and their ESD (µm) across all the specimens assessed Previous data comes from Biard et al. (2018), Llopis Monferrer et al. (2020) and this study.

***Si/C and C/N molar ratios in Rhizaria and diatoms*.** Rhizaria Si/C ratios (0.05 ± 0.03) were much lower to those found for diatoms (0.21 ± 0.13). These molar ratios for Rhizaria are consistent with the Si/C ratios of 0.03 found for Nassellaria and *Challengeria* sp. (a genus morphologically similar to *Protocystis* sp.) in the upper 500 m of the Mediterranean Sea (Llopis Monferrer et al., 2020). Despite having higher Q_{bSi}, Si/C did not differ when compared to individuals from other oceanic regions (Llopis Monferrer et al., 2020), suggesting an increase in C when Si increases. Our estimates for the phytoplankton assemblage (diatoms) are typical of Antarctic ecosystems (Smith and Kaufman, 2018) and higher than the average value 0.13 for diatoms growing in replete nutrients conditions (Brzezinski, 1985). It is a known fact that such higher Si/C ratios can be due to micronutrient limitation, particularly iron, characteristic of the SO (Claquin et al., 2006; Leynaert et al., 2004). While the mechanisms behind the increase of Si/C molar ratios in diatoms have been studied (*e.g.*, Claquin et al., 2006), it is difficult to apply these processes to Rhizaria, which are heterotrophs.

Previous data of C/N molar ratios for Rhizaria are scarce. In the samples collected during the TAN1901 expedition, the C/N ratio was 6.2 on average (5.7 to 7.0), remarkably similar to the Redfield ratio (6.6), but much lower than those found by Michaels et al. (1995) for colonial radiolarians (8.2) and by Llopis Monferrer et al. (2020) for several rhizarian groups including Nassellaria, Spumellaria, Collodaria and Phaeodaria (average 12). The C/N ratios of the phytoplankton of the TAN1901 expedition were within the range observed for actively growing phytoplankton assemblages and cultures (6.3 ± 1.4) (Garcia et al., 2018).

On the one hand, our SO values of Si/C for Rhizaria are consistent with recent observations in the Mediterranean Sea, despite the very different oceanographic and biogeochemical settings compared to those of TAN1901 (Llopis Monferrer et al., 2020). On the other hand, the C/N ratios observed in the present study were highly variable in comparison with previous studies (Llopis Monferrer et al., 2020; Michaels et al., 1995), which conflicts with the assumption that Rhizaria from different regions possess similar elementary compositions. This suggests that variations in the C/N ratios seem to be affected by species compositions and/or environmental conditions. A substantial fraction of Polycystine radiolarians harbour symbionts (Decelle et al., 2015), which may influence the molar ratios. Further investigations should be made to explore to which extent this association may affect molar ratios.

4.3. Comparative Si uptake rates of Rhizaria and diatoms in the SO vs. other regions of the global ocean

To our knowledge, this is the first time that dSi uptake by Rhizaria is assessed in the SO. The rates measured (from 0.58 ± 0.32 nmol Si cell^{-1} d^{-1} for Nassellaria up to 1.12 ± 0.50 nmol Si cell^{-1} d^{-1} for *P. harstoni* (Phaeodaria)) are in the higher range when compared to those found for the Mediterranean Sea, which ranged from 0.17 (± 0.05) nmol Si cell^{-1} d^{-1} (Nassellaria) to up to 0.34 ± (0.23) nmol Si cell^{-1} d^{-1} (*Challengeria* spp. – a phaeodarian genus similar to *Protocystis* sp.) (Llopis Monferrer et al., 2020).

After cells counting by microscopy, we also estimated individual rates of dSi uptake for diatoms in the upper 10 m of the water column (Table 1). For diatoms collected within the RSR (Figure 1), these rates ranged from 0.9 to 18.5 pmol-Si cell^{-1} d^{-1} with an average of 8.4 (± 6.9) pmol-Si cell^{-1} d^{-1}. These values show that the average cellular dSi uptake of diatoms is up to 3 orders of magnitude lower than that found for Rhizaria. This comparison may be misleading because sizes involved are very different, with rhizarians being at least one order of magnitude larger than diatoms.

The specific Si uptake rates (V_P) of Rhizaria from the 0-200 m layer of the SO (from 0.1 to 0.4 d^{-1}, Table 2) agree with values measured in the Mediterranean Sea (0.07 to 0.48 d^{-1}) (Llopis Monferrer et al., 2020). Stukel et al. (2018) discussed specific growth rates of the Aulosphaeridae (large Phaeodaria) estimated from theoretical values. Aulosphaeridae growth rates were in the range of 0.05 and 0.5 d^{-1}. According to their results, populations living deeper in the water column had lower growth rates than those living in the uppermost 100 m of the water column. Diatom V_P rates in the RSR (Figure 1) were, on average, 0.08 ± 0.03 d^{-1}, in accordance to what has been previously found in this region (0.06 d^{-1}) by Nelson and Tréguer (1992). Specific Si uptake rates for Rhizaria exhibit values close to Antarctic diatoms (0.31 d^{-1}) (Nelson et al., 2001), and also from other warmer oceanic regions (0.19 d^{-1}) (Leblanc et al., 2003). However, values reported for diatoms in the present study are much lower than values found in other more productive oceanic regions such as the Peru upwelling (1.8 d^{-1}, Goering et al., 1973) or California (1.02 d^{-1}, White and Dugdale, 1997).

Due to low abundances of Rhizaria during the TAN1901 expedition, the impact of these protists integrated over the upper 200 m, was modest (from 0.1 to 13.4 mmol m^{-2} y^{-1}), compared to diatoms which contribute to >95 % of the total silicic acid uptake. However, our

data confirms those of Llopis Monferrer et al. (2020), which showed that about 10% of the Rhizaria's silica production takes place in cold waters (>40°N/S). This is not the case for diatom bSi production that ranges from 460 to 6380 mmol-Si m^{-2} y^{-1} for stations located at the continental shelf break of the Ross Sea, much lower than those reported previously for the inner Ross Sea (800 to 3000 mmol-Si m^{-2} y^{-1}, Nelson et al. (2002)), and in the same range as those of productive coastal temperate ecosystems (Shipe and Brzezinski, 2001).

4.4. An Antarctic paradox for siliceous Rhizaria?

Given the high dSi concentration of its surface and deep waters, the Antarctic ocean is expected to favour the production of benthic and pelagic silicifiers, including Rhizaria. Our integrated values of dSi uptake by Rhizaria in the upper 200 m of the SO (Table 4) match those estimated by Llopis Monferrer et al. (2020) for the same layer (0-200 m) of worldwide cold-waters (>40°N-S) (0.1 to 53.8 µmol-Si m^{-2} d^{-1}). To obtain the latter values, Llopis Monferrer et al. (2020) converted global Rhizaria abundances into dSi uptake using cell specific rates from the Mediterranean Sea concluding that Rhizaria may contribute 2-19% of the total bSi production, thus playing a potentially important role in the world ocean silica cycle.

Table 4. Biogenic silica stocks (bSi) and Si uptake rates (ρ_P) integrated in the upper 100 m and 200 m for diatoms and Rhizaria, respectively.

Station	Sub-region	bSi (mmol-Si m^{-2})		ρ_P (µmol-Si m^{-2} d^{-1})	
		Rhizaria	diatoms	Rhizaria	diatoms
3	PFZ	0.27	283.6	21.1	2119.3
32	sACC	0.01	348.3	1.2	12061.8
5	sACC	0.17	279.7	36.8	12541.4
Mean sACC		*0.09*	*314.00*	*19.00*	*12301.61*
29	RSR	0.01	31.9	1.7	2927.3
7	RSR	0.07	118.0	13.6	5827.7
11	RSR	0.00	133.7	2.2	7572.5
9	RSR	0.00	275.8	0.8	17474.2
13	RSR	0.01	67.1	2.1	3084.5
15	RSR	0.00	109.7	0.3	8842.0
17	RSR	0.00	176.6	2.4	12138.7
20	RSR	0.04	73.2	7.5	3268.6
22	RSR	0.00	149.8	1.3	12329.8
24	RSR	0.01	78.0	1.1	7055.7
26	RSR	0.04	24.3	9.2	1264.0
Mean RSR		*0.02*	*112.55*	*3.85*	*7435.01*

Indeed, it has been reported that radiolarian ooze can predominate in the sediments of some areas around Antarctica (Dutkiewicz et al., 2015). Coincidentally, Maldonado et al. (2019),

analysing a sediment core in the Pacific region of the SO, showed that if most of the sedimentary bSi is represented by diatoms, radiolarians can contribute up to 5.7% of the total bSi, which suggests a substantial contribution of Rhizaria to the production of bSi and to its export to the deep ocean. In contrast, the contribution of Rhizaria to the total integrated bSi in the 0-200 m layer of our study area is only less than 0.1%.

Diatoms, which are photosynthetic organisms and therefore only thrive in the photic zone, Rhizaria are known to inhabit in the entire water column (Biard and Ohman, 2020), with specific communities and highest abundances occurring at depth (peak at 200-400 m in these cold southern waters; Suzuki and Not, 2015). Although present low cell densities, deep-living species usually inhabit much larger depth intervals, and cell abundance integration results in comparatively high standing stocks compare to surface communities (Kling and Boltovskoy, 1995). Other studies highlight the importance of Rhizaria under the twilight zone, with approximately 50% of the phaeodarians inhabiting between 250 and 3000 m depth (Tanaka and Takahashi, 2008). Since our plankton tows did not extend below 200 m, it is very likely that several groups of Rhizaria were under-represented and would be missing for a global budget in the Si cycle. According to Llopis Monferrer et al. (2020), between 62 and 75% of the biomass and Si production of the Rhizaria occurring at high latitudes (> 40°N-S) would take place in the twilight zone, below 200 m depth.

In addition, plankton-tow samples provide limited coverage in space and time for estimating standing stocks, while sediment traps and sediments samples integrate the signal over longer time scales (Abelmann and Gersonde, 1991). Cell densities observed in this study could be biased by the seasonality patterns in rhizarians communities as very few is known about the ecology of these organisms. Boltovskoy et al. (1993) found that radiolarians abundances (as recorded in sediment trap samples) can vary throughout the year over one order of magnitude, which poses the possibility that our samples underestimated their longer-term densities.

Another potential explanation for the paradoxically low abundance of Rhizaria we found in the water column compared to their observed contribution to bSi accumulation in Antarctic sediments, may be a different balance of remineralization and sinking. Rhizaria dissolution occurs mostly on the sea-floor (Takahashi, 1981), while diatoms dissolution occurs both in the water column and in the sediments (Tréguer and De La Rocha, 2013). Thermodynamically, the

coldest the marine waters, the lowest the dissolution of bSi. In addition, Rhizaria may dissolve a lot more slowly than diatoms (Maldonado et al., 2019), and/or can sink a lot faster.

When analysing our community composition data, it appears that abundances of diatoms and those of Rhizaria in surface water occur opposite at most stations (higher densities of diatoms correspond to lower densities of Rhizaria). Worldwide, silicified Rhizaria (Polycystines and Phaeodaria) and diatoms occur in highly variable proportions, with diatoms always dominating the cold high-latitude regions. From data acquired during the *Tara* Ocean expedition, Hendry et al. (2018) suggested that diatoms might exclude Rhizaria because they display a strong affinity for dSi and thus outcompete Rhizaria especially at intermediate and shallow depths where dSi is often scarce. However, there are reports of high abundances of Phaeodaria associated with high primary production and diatom blooms, although some of them are from high-latitude areas where Si is rarely limiting (Nimmergut and Abelmann, 2002).

Despite the lower abundance of Rhizaria relative to diatoms in the euphotic layer of the SO, their higher resistance to dissolution (Takahashi, 1981), and high individual Si uptake rates confers them a potentially important role on the Si cycling and export to the deep ocean.

Acknowledgments

The authors would like to thank the captain and crew of RV Tangaroa for their efforts in facilitating the sampling during TAN1901, as well as other participants for their help. We thank H. Whitby, N. van Horsten, M. López-Acosta and Wen-Hsuan Liao for their valuable help. We are particularly grateful to D. Boltovskoy and E. Thiébaut for their helpful comments and fruitful discussions. We also would like to thank M. Legoff for the silicates analysis. This work was funded in New Zealand by MBIE Endeavour Fund programme Ross-RAMP (C01X1710) with assistance from NIWA Strategic Science Investment Fund (SIFF) Coasts and Oceans, Programme 4. This work was supported by the French National program LEFE (Les Enveloppes Fluides et l'Environnement) and ANR RadiCal (ANR-18-CE01-0011)

Chapter 2.2 – Rhizaria in the Atlantic Ocean

Biogenic silica content and silicic acid uptake rates of Rhizaria along a latitudinal transect in the Atlantic Ocean

The AMT-28 research cruise (JR18-001) left the 23rd of September from Harwich (England), 2018 aboard the RSS James Clark Ross, and arrived in Mare Harbour, Falkland Islands on the 29th of October 2018, crossing the northern Atlantic in boreal autumn and the southern Atlantic in austral spring.

The Atlantic Meridional Transect crosses a wide range of ecosystems (Figure 1), from subpolar to tropical regions, therefore covering strong environmental gradients and biological diversity (Smyth et al., 2017).

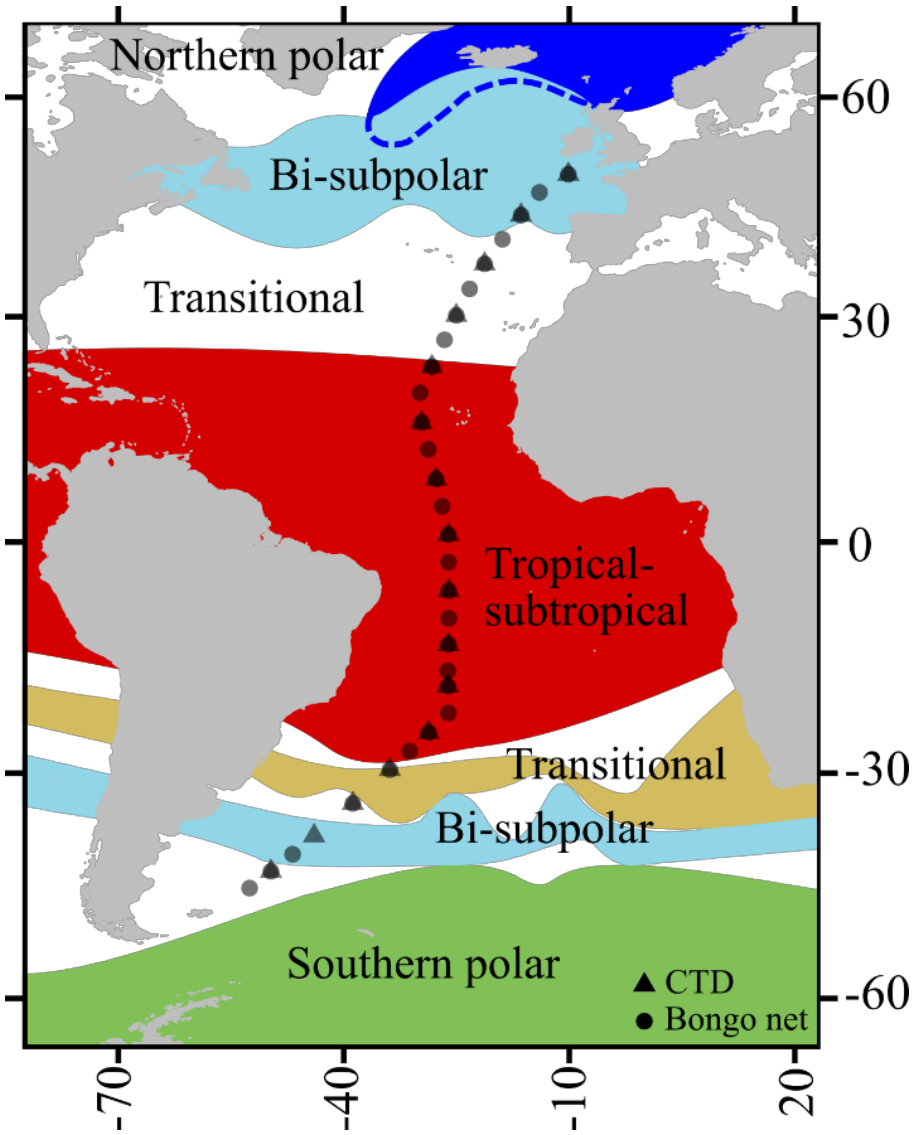

Figure 1. AMT-28 cruise track overlies the province boundaries established by Boltovskoy and Correa, (2016).

The transect provides an ideal setting to study variations in silicic acid uptake and biogenic silica content of Rhizaria as it crosses 5 of the 7 bioregions identified worldwide. based on the distribution and relative abundance of 307 radiolarian species from plankton, sediment trap and surface sediments of the global ocean (Boltovskoy and Correa, 2016). With data obtained from this cruise, we want (1) to assess species distributions, abundances and biomass of Rhizaria and diatoms along the transect, and (2) to establish a relationship between production and abiotic parameters in biogeochemical areas (as defined in Boltovskoy and Correa, 2016).

1. Sampling

Hydrographic parameters. Temperature, salinity, dissolved oxygen, and fluorescence data were obtained by a CTD survey at each sampling station. The criterion to estimate the mixed layer depth (MLD) was based on the method defined by de Boyer Montégut et al. (2004). Silicic acid concentration in sea water was analyzed at each station and for each sampling depth using the automated method of Aminot and Kérouel (2007).

1.1. Biogeochemical parameters. Seawater samples were collected every other day at six different depths using Niskin bottles. Samples for silicic acid (dSi), particulate organic carbon (POC), nitrogen (PON) and biogenic silica (bSi) concentrations were collected for all depths, while only 3 depths were used for silicic acid uptake experiments. At each sampling station water was filtered onto a 0.4 µm GF/F filter for POC and PON analyses or onto a 0.8 µm polycarbonate (PC) membrane filter for bSi determination. GF/F filters were frozen at -20°C and PC membranes were stored at room temperature in petri dishes until off site analysis.

1.2. Zooplankton samples. Plankton samples were collected daily at predawn at similar locations as the CTD casts using a WP-2 bongo (57 cm diameter of the mouth - 120 µm mesh size/ 63 µm cod-end) vertical haul from 200 m or 250 m to the surface at 0.21 m s^{-1}. The sample was divided into 2 subsamples of 2 L by the beaker technique. A subsample of 750 mL was concentrated using a 50 µm mesh sieve and preserved with acidic lugol's solution (2% final concentration) in a 250 mL dark plastic bottle to avoid light and stored at 4°C for later cell counts. For genomics analyses, 500 ml were filtered through 10 µm polycarbonate filter. Filters were flash-frozen in liquid nitrogen and stored independently at -80°C until DNA

extraction. The remaining sample was immediately diluted in filtered seawater (0.2 µm) and screened under the microscope to isolate single cells of siliceous Rhizaria. Single cell organisms were isolated using a Pasteur pipette and sorted according several taxonomic groups.

2. Elementary composition and assessment of silicic acid uptake rates

Elementary composition and silicic acid uptake experiments were conducted following the protocol in (Llopis Monferrer et al., 2020).

During this cruise, biogeochemical and physical characteristics changed rapidly. Preliminary results revealed a great diversity of Rhizaria species and highly variable bSi cell content and silica production.

Samples are still under analysis, which has been delayed due to the lockdown situation. Interpretation is premature and will be developed in the coming months. Preliminary results are reported in Annex 1.

Chapter 3 – Merging imaging technologies and metabarcoding to characterize the Rhizaria community

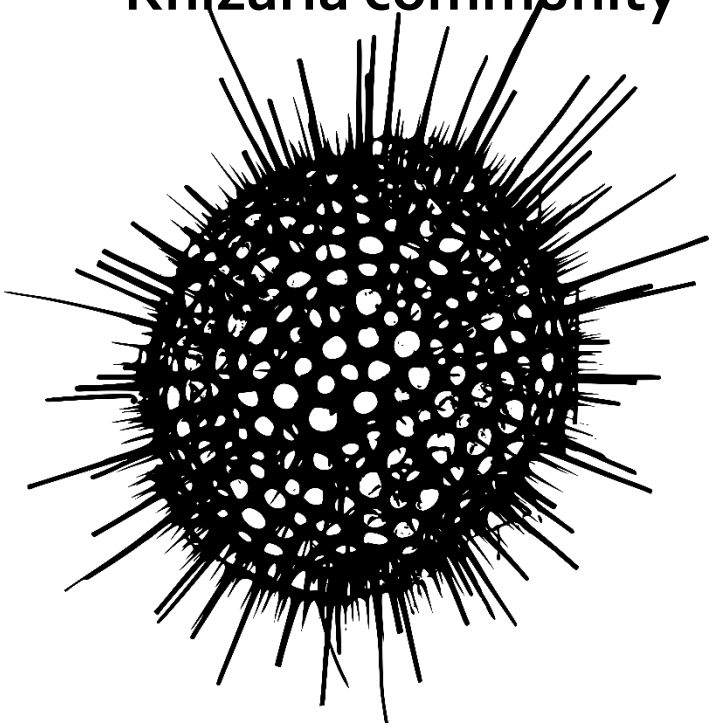

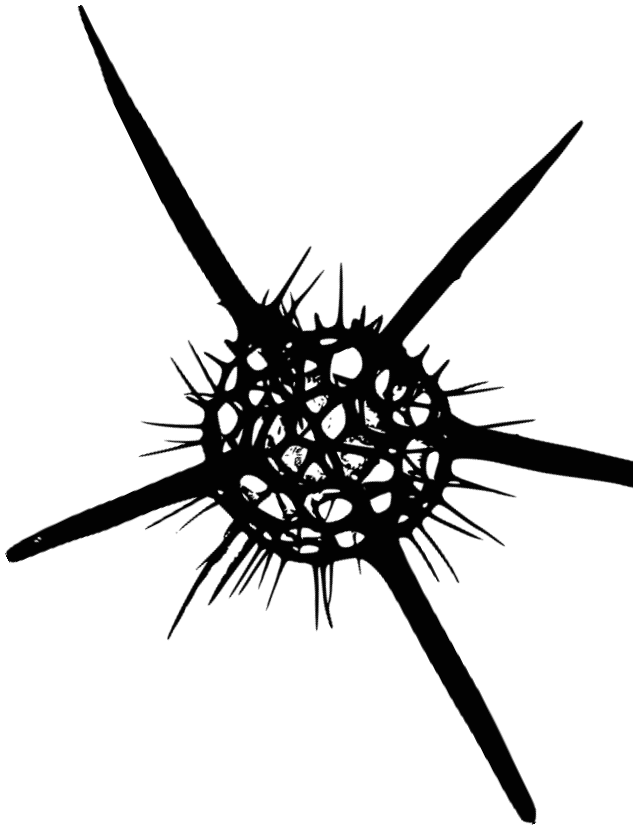

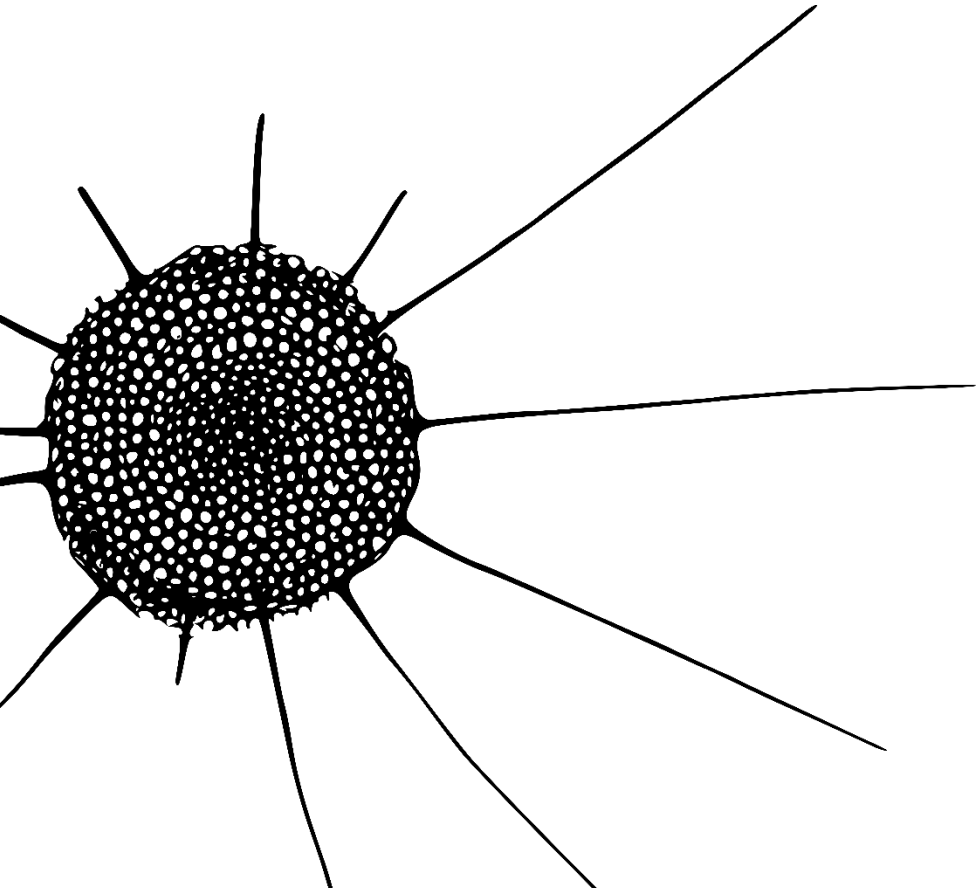

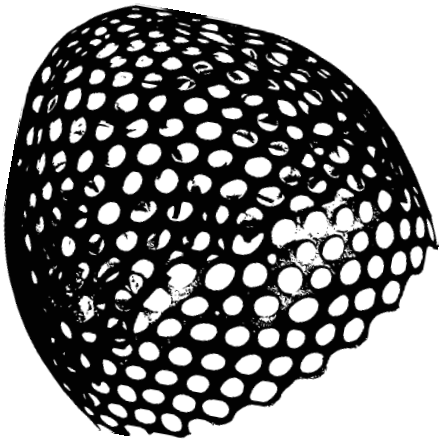

Drawings of Nassellaria and Spumellaria specimens from Miguel Méndez-Sandin pictures.

Context of the work

The first two chapters of this thesis were mainly focused on small rhizarians (<600 µm) due to the sampling strategy employed. However, the size of these protists covers a much wider spectrum, from few micrometres to several millimetres.

This chapter is dedicated to the exploration of the entire size spectrum of Rhizaria. I took a paired approach, using imaging and molecular tools to study Rhizaria diversity, size and abundances. Data were obtained in the North-Western Mediterranean Sea in autumn 2017 during the MOOSE-GE 17 cruise. Using the individual size obtained with the imaging tools and the allometric relationship previously established (Chapter 1), which links cell size to silica content, I estimated the contribution of the different size class and taxonomic groups of Rhizaria to the biogenic silica standing stock in the upper 500 m of this area.

With this chapter I intend, on the one hand, confirm the global estimates presented in the first chapter of this thesis, as well as to disclose the potential role of these organisms as a whole.

Merging imaging technologies and metabarcoding to assess Rhizaria abundances, diversity and contribution to the silicon cycle in the Mediterranean Sea

Natalia Llopis Monferrer[1,2], Tristan Biard[3], Miguel Méndez-Sandin[2], Fabien Lombard[4], Aude Leynaert[1], Paul Tréguer[1], Fabrice Not[2]

[1]Univ Brest, CNRS, IRD, Ifremer, LEMAR, F-29280 Plouzane, France

[2] Sorbonne University, CNRS, UMR7144 Adaptation and Diversity in Marine Environment (AD2M) laboratory, Ecology of Marine Plankton team, Station Biologique de Roscoff, Place Georges Teissier, 29680 Roscoff, France

[3]LOG, Laboratoire d'Océanologie et de Géosciences, Univ. Littoral Côte d'Opale, Univ. Lille, CNRS, UMR 8187, Wimereux,France

[4]Sorbonne Université, CNRS, Laboratoire d'Océanographie de Villefranche, Villefranche-sur-Mer, France

In preparation

Abstract

Siliceous Rhizaria (polycystine radiolarians and phaeodarians) are important contributors to carbon and silica cycles. Considering their broad diversity of species and their wide size range (from a few micrometres up to several millimetres), assessing the entire community is challenging. Here, imaging and DNA-metabarcoding tools were used to investigate the diversity and abundance of the entire size spectrum of silicified Rhizaria in the oligotrophic North-Western Mediterranean Sea. The diversity and relative contribution of the different taxonomic groups differed considerably among the methods used. Based on quantitative abundances and cell biovolume information estimated with imaging tools along with an allometric relationship linking biogenic silica content (bSi) to cell size, we were able to assess the contribution of Rhizaria to the global bSi standing stocks in the upper 500 m of the water column. Rhizaria accounted for up to 6% of the total bSi biomass of the planktonic community, with a respective contribution of 25%, 20% and 55% for each of the size fractions considered (64-200 µm, 200-1000 µm and >1000 µm). We discuss the limits of each method and suggest strategies to improve the quantitative characterization of the entire Rhizaria community.

1. Introduction

The marine environment represents the largest ecosystem on Earth, housing a broad variety of planktonic organisms, from viruses and bacteria to unicellular and small multicellular eukaryotes. These organisms, which span more than six orders of magnitude in size, form complex ecological networks that sustain major biogeochemical cycles (Edwards et al., 2013).

While phytoplankton forms the base of marine food webs, zooplankton can occupy numerous trophic levels and can contribute to carbon (C) export through mechanisms such as vertical migration and fecal pellets (Toullec et al., 2019). So far, studies of plankton assemblages have focused either mostly on diatoms, dinoflagellates and cyanobacteria to characterize phytoplankton assemblages, or on copepods and euphausiids to assess the role of zooplankton in the ocean (Buitenhuis et al., 2006), mainly because of their high abundances. These are however few and very specific compartments, only representing limited aspects of the functional diversity of plankton (Le Queré et al., 2005), thus neglecting the potential role of other organisms when developing biogeochemical models (Lombard et al., 2019).

In recent years, automated sampling devices, image analysis technologies and machine learning algorithms have been developed to quantify abundances of marine organisms (Lombard et al., 2019) and to accelerate the analysis of planktonic samples which are generally time-consuming (Benfield et al., 2007). In addition to image processing, DNA-metabarcoding, with its broad taxonomic coverage, has become an exciting alternative to morphological observation, being largely used to explore the diversity of microbial communities (de Vargas et al., 2015; Faure et al., 2019). There are uncertainties associated with each method. Imaging tools do not cover all the size spectra and several methods need to be used simultaneously (Lombard et al., 2019). Molecular tools produce compositional data, abundances of specific groups are inherently influenced by abundances of other groups (Gloor et al., 2017). To better understand the global significance of these organisms and to be able to include them in the biogeochemical models, the full extent of siliceous rhizarians should be investigated combining both methods.

Recent studies highlighted the importance of Rhizaria in the modern oceanic ecosystems (Biard et al., 2016; Llopis Monferrer et al., 2020). Rhizaria are a group of unicellular eukaryotic organisms that span a wide range of sizes, from tens to hundreds of micrometers with some

capable of forming colonies up to over 1 m in length. While some rhizarians build their skeletons of calcium carbonate (*e.g.*, Foraminifera) or strontium sulfate (*e.g.*, Acantharia), numerous marine rhizarians form siliceous skeletons (*e.g.*, Nassellaria, Spumellaria and Phaeodaria) (Takahashi et al., 1983). Considering their large diversity of species, broad size spectrum and extended range of vertical niches (Biard and Ohman, 2020) as well as various trophic modes, Rhizaria lack a full characterisation and quantification of their significance in biogeochemical cycles.

Small siliceous Rhizaria (< 600 µm, mainly radiolarians) have been identified as being responsible for up to 19% of the bSi production in the global ocean (Llopis Monferrer et al., 2020), while large specimens (> 600 µm), in terms of abundances, represented approximately 33% of the large zooplankton in the upper water column (Biard et al., 2016).

Historically, living Rhizaria, have been collected using conventional plankton nets, closing plankton nets and Niskin bottles (*eg.*, Boltovskoy, 2003; Boltovskoy et al., 1993; Ishitani and Takahashi, 2007). These conventional sampling methods collect more efficiently smaller specimens, which are also more abundant (*e.g.*, Boltovskoy et al., 2010). So far, large individuals have seldom been taken into account, mainly due to the fragility of their skeletons and only fragments are generally found in the nets. The development of *in situ* imaging techniques has enabled the first characterizations and estimates of these organisms (Biard et al., 2016). Since then, only a handful of studies have attempted to evaluate their role in the biological carbon pump and the silicon cycle (*e.g.*, Biard et al., 2016; Guidi et al., 2016). Knowledge about the distribution and abundances of living Rhizaria is still highly fragmented due to the scarcity of the data and heterogeneity between collection methods and sample analyses. Therefore, these protists have been patchily sampled and neither their distribution nor their role in the biogeochemical cycles, particularly in the Si cycle, are well understood.

We participated in the Mediterranean Ocean Observing System for the Environment – Grande Echelle (MOOSE-GE) cruise in September 2017. This cruise is one of the few in the world, during which FlowCam, ZooScan and UVP imaging technologies were deployed simultaneously and merged with DNA metabarcoding. We used this integrative approach to characterize the entire Rhizaria community, its abundance and diversity. Our overarching objective was to assess the contribution of rhizarian biogenic silica (bSi) standing stock and potential taxa specific contribution to the Si cycle on a regional scale.

2. Material and Methods

2.1. Study Area

Sampling was conducted at 16 sites during the MOOSE-GE 2017 expedition (September 2017) on board R/V Atalante in the North-Western basin of the Mediterranean Sea (NWMS) (Figure 1). The NWMS is characterized by oligotrophic conditions with regions of intermittent fluorescence (Mayot et al., 2017). The Gulf of Lion is an important area of deep water formation (Donoso et al., 2017). This system is very dynamic, with intense mesoscale activity along the coastal current and mid-sea eddies present along the basin (Robinson et al., 2001), which certainly influence changes in planktonic communities.

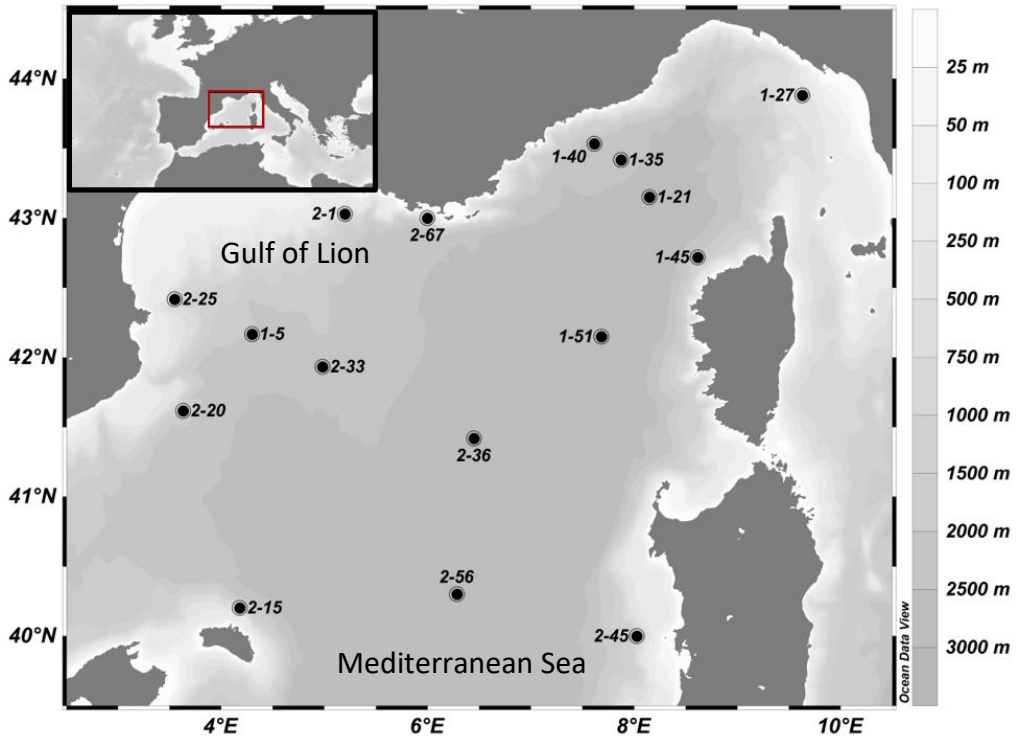

Figure 1. Map of the study area (North Western Mediterranean basin) of the MOOSE-GE expedition with positions of the sampling stations (LEG-Station) that were analysed in this study.

2.2. Environmental and biogeochemical data

At every station, physical and biogeochemical parameters were sampled using a rosette carrying 12 Niskin bottles (12 L) and equipped with a CTD (Seabird Electronics) to measure temperature and salinity. Nutrients (nitrate, phosphate and silicic acid) were analysed following the method of Aminot and Kérouel (2007). To measure biogenic silica (bSi) concentrations, 1 L of seawater sampled at 1 to 3 depths distributed between the surface and

the deep chlorophyll maximum (DCM), was filtered onto 0.6 µm, 47 mm isopore polycarbonate filters (GE Healthcare Whatman). After filtration, filters were kept in petri dishes and stored at room temperature. Analyses were performed using the double digestion method according to Brzezinski and Nelson (1989).

2.3. Plankton collection

A triple net, with 64, 200 and 500 µm mesh sizes was deployed at the constant speed rate of 0.8 m s^{-1} for vertical tows down to 500 m depth. A flowmeter was attached to the mouth of the net to quantify the amount of water passing through the net. Once the net was on board the ship, samples concentrated in each cod-end were diluted in 4 L of 0.2-µm filtered seawater and divided into several subsamples.

For the 64 µm cod-end, a subsample of 1.5 L was concentrated on a 50 µm mesh sieve and preserved with acidic lugol's solution (2% final concentration) in a 250 mL dark plastic bottle to avoid light and stored at 4°C for later analysis with the FlowCAM.

For the 200 µm cod-end, a subsample of 1.5 L was concentrated using a 180 µm sieve. The content of the sieve was poured into a 250-mL plastic bottle with 25 – 30 mL tetraborax buffered formaldehyde (4%v/v) and stored at room temperature for later analysis with the Zooscan imaging system (Gorsky et al., 2010).

For genomics analyses, 1 L of each cod-end (64, 200 and 500 µm), was filtered through 10 µm polycarbonate filter. Filters from the different size fractions were flash-frozen in liquid nitrogen and stored independently at -80°C until DNA extraction.

2.4. Image acquisition and processing

2.4.1. FlowCAM analyses

The FlowCAM (Fluid Imaging Inc.) is an imaging system for measuring and classifying organisms and particles (3 to 5000 µm, depending on the objective chosen) present in a liquid medium. Samples fixed with lugol's solution were analysed using a FlowCAM at the Villefranche Platform for Quantitative imaging ("PIQv," n.d.). Prior to the analysis, samples were filtered using a 200 µm sieve to remove large particles and avoid clogging of the FlowCAM chamber. Plankton organisms were counted using the "auto-trigger mode" of the

FlowCAM. Samples were examined under a 4x objective lens, and pumped through a 3mm x 0.3mm chamber for 45min or until reaching 30000 images. Raw images were saved in order to analyse them using the Zooprocess software (Gorsky et al., 2010).

2.4.2. Zooscan analyses

The Zooscan (Hydroptic) is a plankton scanner which takes high resolution image of planktonic samples (Gorsky et al., 2010). Samples in tetraborax-formaldehyde 4%v/v were digitized at 4800 dpi using the Zooscan at the Villefranche-sur-mer Platform for Quantitative imaging. Each of the samples collected were first divided into two size fractions using 1000 µm sieves: d1 for the organisms larger than 1 mm and d2 for the organisms smaller than 1 mm. Each of the two size fractions (d1, d2) was subsampled using a Motoda splitter to reach aliquots containing nearly 500 to 1000 objects, and imaged with the Zooscan at 2400 dpi resolution (Gorsky et al., 2010). Each image contained ~500-1000 objects.

2.4.3. In Situ Imaging – UVP analyses

The Underwater Vision Profiler UVP5 (Hydroptic) was integrated on the CTD-rosette. The UVP5 allows the acquisition of particles and zooplankton images larger than >600 µm and to quantify them in a known volume of water. The UVP operates a 4 MPix camera imaging a field of view of approximately 180 x 180 mm^2 about 200mm in front of the camera. Vertical profiles exceeded 500 m except Station 27 (Leg1). Only data from the upper 500 m of the water column was used in this study in order to compare with the results from the plankton nets, which were deployed up to 500 m deep.

2.4.4. Metabarcoding sequencing

DNA was extracted using the MasterPure Complete DNA and RNA Purification Kit (Epicentre) following manufacturer's instructions. Polymerase chain reaction (PCR) amplification was performed with the general eukaryotic primer pair TAReuk454FWD1 (5'-CCAGCASCYGCGGTAATTCC-3') and TAReukREV3 (5'-ACTTTCGTTCTTGATYRA-3') targeting the V4 hypervariable region of the 18S rDNA (Stoeck et al., 2010). Sequencing was performed using the Illumina MiSeq platform (2x250 bp).

2.5. Data analysis

2.5.1. Imaging

All raw images generated by FlowCAM, Zooscan and UVP were analysed and processed using the Zooprocess software (Gorsky et al., 2010). Extracted images were uploaded to Ecotaxa, an online collaborative software dedicated to visual exploration and taxonomic annotations of planktonic images (Picheral et al., 2017). The Random Forest algorithm (Breiman, 2001) was used to classify all objects into major plankton categories. Automatic classification was visually inspected to ensure the quality of the sorting. Only images corresponding to siliceous Rhizaria were picked out for subsequent analyses. Images (Rhizaria and non-Rhizaria) generated for this study will enrich the Ecotaxa database and can be used to improve automatic classification (Picheral et al., 2017). For each instrument, abundances (ind m^{-3}) of each rhizarian category were calculated at every station and morphological measurements associated to each vignette, such as body length and width, were used to obtain biovolumes.

2.5.2. Metabarcoding data curation and analysis

Raw reads obtained from sequencing were processed and clustered following DADA2 (Callahan et al., 2016). Resulted amplicons sequence variants (ASVs) were taxonomically assigned using global search implemented in Vsearch (Rognes et al., 2016) against PR2 v4.11.0 database updated with Radiolaria sequences from (Méndez-Sandín, 2019). ASVs were considered for further analyses if they were present in at least 2 samples and if they had more than 10 total reads. The final dataset was composed of a total of 271 ASVs, normalized by sample to relative abundance.

2.6. Rhizaria biovolume and biogenic silica content

To estimate the area of the imaged specimen, only pixels having values above a certain grey level were considered (Picheral et al., 2017). From the area we calculated the equivalent spherical diameter (ESD) (Equation1) to prevent overestimation of the individual's biovolume, since in some cases, the skeleton can have complex shapes, including long and irregular spines.

$$ESD = 2\,x\,\sqrt{\frac{Area}{\pi}} \qquad (1)$$

where *ESD* (in µm) is the equivalent spherical diameter and *Area* is the pixel area of the imaged organism.

Then, we calculated the biovolume (µm^3) using the following equation:

$$Volume = \frac{4}{3} x\ \pi\ x\ \left(\frac{ESD}{2}\right)^3 \qquad (2)$$

where ESD is the spherical diameter calculated with equation 1.

After calculating the biovolume (equation 2), we calculated individual Si content of Rhizaria by using the log-linear relationship established by Llopis Monferrer et al. (2020), which relates Si content to biovolume (R^2 = 0.86):

$$log_{10}(Q_{bSi}) = [-4.05 \pm 0.18] + [0.52 \pm 0.02] log_{10}(biovolume) \qquad (3)$$

where Q_{bSi} is the biogenic silica content of the specimen (µg-Si cell^{-1}).

3. Results

3.1. Environmental data

Surface temperature in autumn ranged from 16.0°C to 22.2°C. Integrated Chlorophyll *a* (Chl *a*) values over the 0-150 m layer, varied between 2 and 45 mg m^{-2}. Mean sea surface temperature was 21.9 ± 2.6 °C, and the depth of deep chlorophyll maximum (DCM) varied from 42 to 95 m, with integrated values of Chl *a* over the 0 – DCM layer ranging from 2 to 45 mg m^{-2}.

Nutrients were integrated over the 0-500 layer (Table 1). Stations were characterised by a broad range of nutrient concentrations. Nitrate concentrations ranged from 1971 to 4060 mmol m^{-2}. Phosphate concentrations ranged from 78 to 157 mmol m^{-2}. Silicic acid integrated concentrations varied from 1363 to 3003 mmol m^{-2}.

Biogenic silica concentrations, integrated over the 0-DCM layer ranged from 1.7 to 6.8 mmol-Si m^{-2}.

Table 1. Study sites location and collection date. Distance to the coast, deep Chlorophyll maximum (DCM), bottom depth, air and sea temperature for each station. Nutrient values were integrated over the 0-500 m layer. Chlorophyll a (Chl *a*) and biogenic silica (bSi) values were integrated over the 0-DCM layer. NA means that no values were available.

Station #	Date YYYYMMDD	Latitude (°N)	Longitude (°E)	Distance to the coast km	DCM m	Chl *a* mg m^{-2}	Bottom depth m	Sea Temp. °C	bSi mM m^{-2}	$\sum NO_3$ mM m^{-2}	$\sum PO_4$ mM m^{-2}	$\sum Si(OH)_4$ mM m^{-2}
leg1-005	20170901	42.17	4.30	96	57	45	1909	21.8	1.7	2625	115	2024
leg1-021	20170905	43.15	8.15	78	71	17	2582	22.4	2.0	3216	142	2376
leg1-027	20170906	43.88	9.63	23	84	16	405	24.5	2.4	1917	78	1363
leg1-035	20170907	43.42	7.88	49	80	31	2330	23.0	2.3	3729	152	2616
leg1-040	20170908	43.53	7.62	28	70	22	2237	23.3	2.0	3589	153	2693
leg1-045	20170909	42.72	8.62	19	83	16	1558	23.8	3.5	4060	157	3003
leg1-051	20170910	42.15	7.68	76	83	11	2768	21.5	2.3	3333	132	2251
leg2-001	20170912	43.03	5.20	36	48	2	1109	16.1	1.7	3106	119	1845
leg2-015	20170914	40.20	4.18	14	95	20	839	25.4	2.7	2392	96	2032
leg2-020	20170915	41.62	3.63	50	86	29	954	23.8	2.8	3182	94	2304
leg2-025	20170916	42.42	3.55	33	68	30	897	18.3	6.8	3126	128	2245
leg2-033	20170917	41.93	4.98	146	68	22.3	2352	19.3	5.5	3660	154	2658
leg2-036	20170918	41.42	6.45	189	76	20	2690	21.6	4.3	3212	134	2190
leg2-045	20170919	40.00	8.03	29	90	20	1153	23.6	5.5	2184	86	1735
leg2-056	20170920	40.30	6.28	179	80	15.5	2828	23.1	5.6	2940	120	2117
leg2-067	20170921	43.00	6.00	13	42	NA	1005	18.7	2.2	NA	NA	NA

3.2. Rhizaria size spectra

A total of 753 Rhizaria specimens were imaged using the three imaging devices (FlowCAM, Zooscan and UVP). The overall size of the analysed organisms ranges from 45 to 3663 µm in equivalent spherical diameter (ESD) (Figure 2). The FlowCAM records the smallest individuals, with an ESD ranging from 45 to 176 µm (mean ± standard deviation; 103 ± 26 µm), of the three instruments, the FlowCAM is the only one capable of imaging some of the polycystine radiolarians (i.e., Spumellaria and Nassellaria) and phaeodarians of the genus *Challengeria*. The Zooscan only captured individuals with ESD ranging from 365 to 1244 µm (799 ± 146), which all belonged to the family Aulacanthidae (Phaeodaria) in this study. The UVP imaged the largest individuals, starting with an ESD of 945 µm up to 3662 µm (1279 ± 429 µm), with smallest individuals belonging to the family Aulacanthidae and the largest cells to the Coelodendridae family (both Phaeodaria).

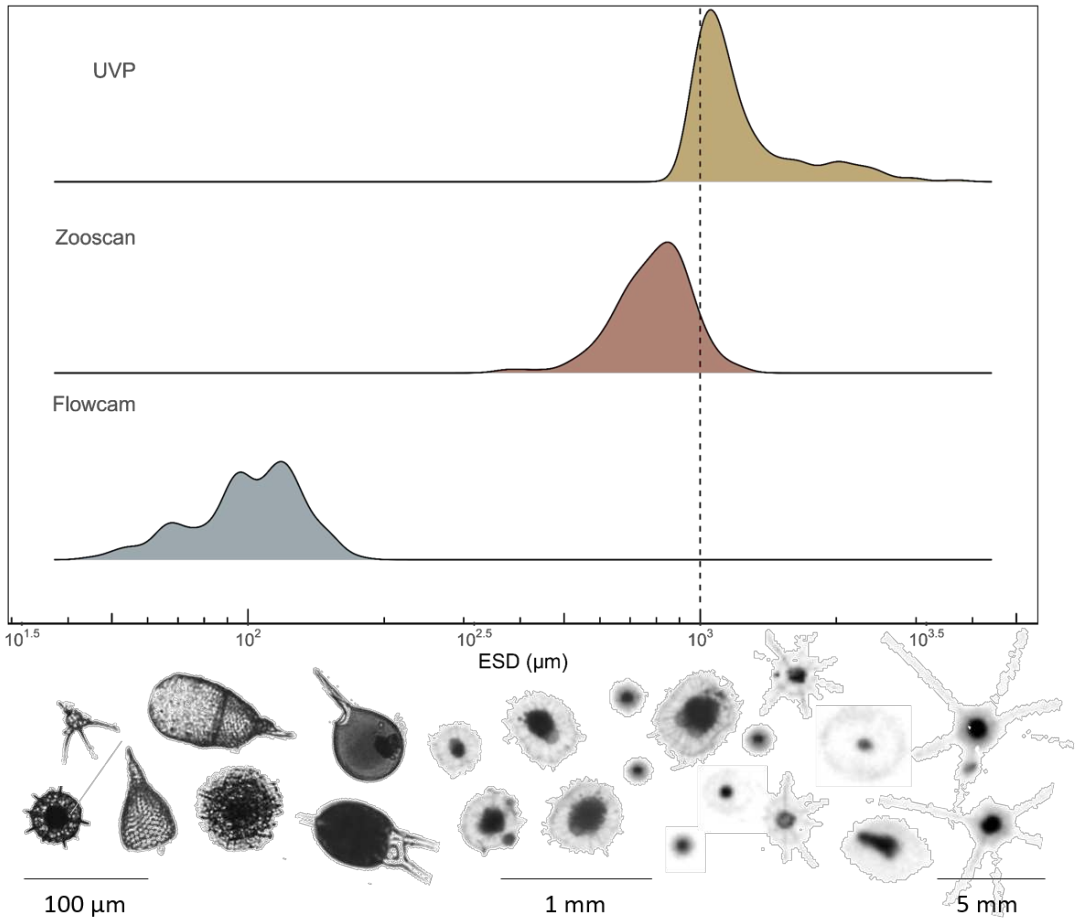

Figure 2. Comparison of the total size range of Rhizaria (in equivalent spherical diameter; ESD) that imaging tools used in this study can sample. Rhizaria imaged in this study using the three imaging tools: FlowCAM, Zooscan and UVP. Dashed line represents the upper limit of the Zooscan data considered and the lower limit of the UVP data, which was established to avoid overlap between these two instruments.

We observed a discontinuity between the size class captured by the FlowCAM and the Zooscan. From 176 µm (largest individual imaged by the FlowCAM) and 365 µm (smallest individual imaged by the Zooscan), no specimen was observed. However, there was a size (ESD) overlap between Aulacanthidae individuals captured by the Zooscan and the UVP. In order not to overestimate Rhizaria abundances (*i.e.*, counting twice the same size fraction), we excluded the specimens with an ESD larger than 1000 µm from the Zooscan data, and specimens with an ESD equal or smaller than 1000 µm from the UVP data.

3.3. Rhizaria diversity and abundance

From imaging data, the quantitatively most abundant taxonomic groups were the smallest ones (Nassellaria, Spumellaria and phaeodarians of the genera Challengeria). Conversely, in

the metabarcoding data, organisms belonging to the largest families (*i.e.*, Coelodendridae and Aulacanthidae) contributed most to the relative abundance (Figure 3).

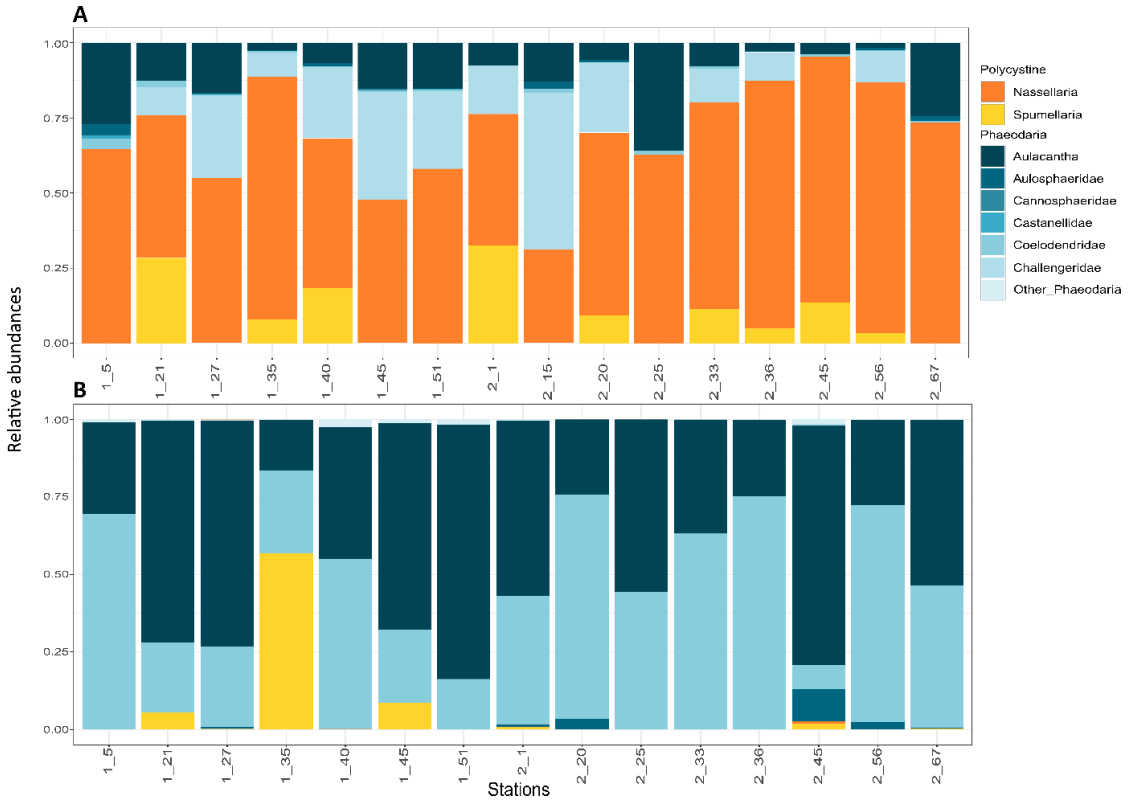

Figure 3. (A) Imaging technologies data. Bar chart showing the diversity and relative abundance of main taxonomic groups of Rhizaria cumulated from the different size fractions (>64 µm, 200-1000 µm, >1000 µm), from data obtained using the FlowCAM, Zooscan and UVP. (B) Molecular metabarcoding data. Bar chart showing the diversity and relative abundance of main taxonomic groups of Rhizaria in the different size fractions cumulated (>64 µm, >200µm, >500µm) of the V4 rDNA from vertical tow nets. No metabarcoding data was available for stations leg2-05.

Rhizaria belonging to the >64 µm size class represented a total of 4.53 % (± 3.49) of the eukaryotic community reads. Rhizaria of the > 200 µm size fraction represented a 11.3 % (± 7.80), and the largest fraction, > 500 µm represented the highest percentage, 15.8 % (± 13.90). When comparing the relative abundances obtained by both methods (imaging and molecular), on the same size fraction sampled, we observed that the taxonomic groups determined by each method were not the same. Consequently, the computed relative abundances differed for the different methods (Table 2, Figure 3).

Table 2. Presence and absence of the different taxonomic groups for the entire size spectra studied using imaging and metabarcoding (Metabar.) methods. No metabarcoding data was available for stations leg2-05. * For the

imaging methods, we grouped Castanellidae and Cannosphaeridae, for metabarcoding it comprises other non-identified groups.

Groups	Nassellaria		Spumellaria		Challengeridae		Aulacanthidae		Coelodendridae		Aulosphaeridae		Other Phaeo.*	
Method	Imaging	Metabar.	Imaging	Metabar.	Imaging	Metabar.	Imaging	Metabar.	Imaging	Metabar.	Imaging	Metabar.	Imaging	Metabar.
Leg-Stn														
leg1-005	x					x	x	x	x	x	x		x	x
leg1-021	x		x	x	x	x	x	x	x	x				x
leg1-027	x	x		x	x	x	x	x		x		x	x	x
leg1-035	x		x	x	x		x	x	x	x	x			
leg1-040	x	x	x		x		x	x	x	x	x			x
leg1-045	x			x	x		x	x	x	x			x	x
leg1-051	x				x		x	x	x	x			x	x
leg2-001	x		x	x	x		x	x		x		x		x
leg2-015	x				x		x		x		x			
leg2-020	x		x	x	x		x	x	x	x	x			x
leg2-025	x						x	x	x	x				
leg2-033	x		x		x		x	x	x	x				x
leg2-036	x		x		x		x	x	x	x	x			x
leg2-045	x	x	x	x		x	x	x	x	x				x
leg2-056	x		x	x	x	x	x	x	x	x	x	x		x
leg2-067	x			x		x	x	x	x	x	x	x		x

Abundances of specimen (*i.e.*, cells m^{-3}) were established based on quantitative methods (imaging tools). The smallest size range investigated in this study, the 64-200 µm (FlowCAM) showed the highest abundance values at all stations, ranging from 5.0 to 61.1 cell m^{-3} (Table 2). The small size fraction was dominated in all stations by Nassellaria, except Station leg2-015, which was dominated by spumellarians. Phaeodaria of the genus *Challengeria* were observed in lower proportions but often (in 12 of the 16 stations studied) (Figure 3).

Overall, using imaging techniques, which allowed us to quantify abundances, smaller specimens were more abundant at all stations, with abundances of larger specimens relatively similar when using the Zooscan or the UVP, although they do not analyse the same taxonomic groups (Figure 4).

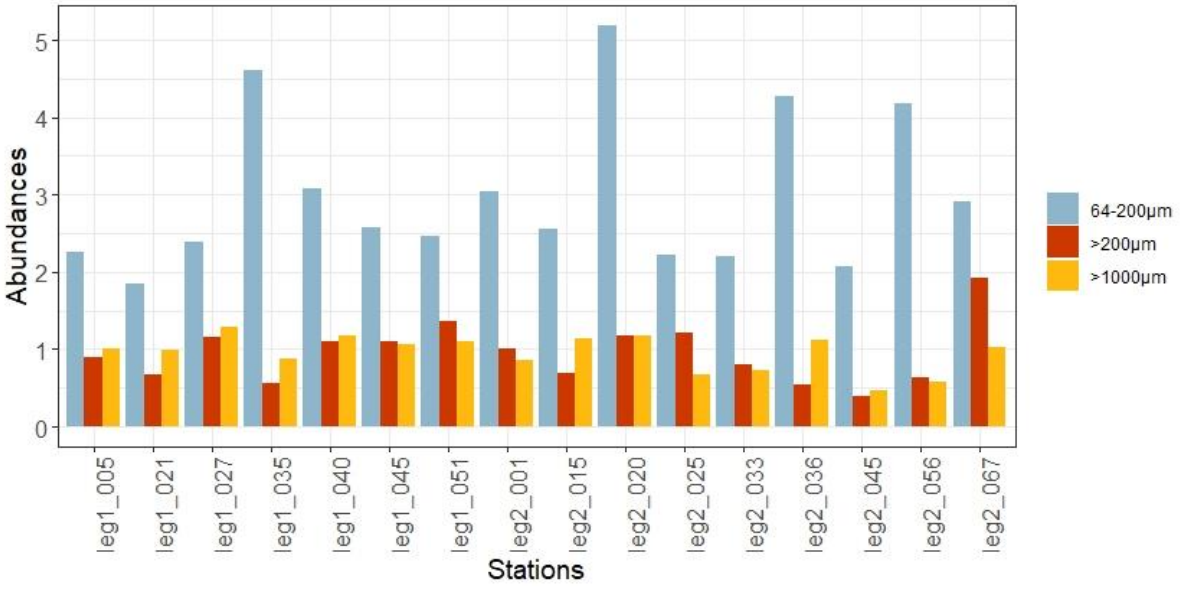

Figure 4. Abundances in cells m^{-3} of the Rhizaria observed using the FlowCAM (64-200 µm), Zooscan (>200 µm) and UVP (>1000 µm) devices during the MOOSE-GE (2017) cruise.

Regarding the 200-1000 µm size fraction, which corresponded to data obtained with the Zooscan, abundances of specimens identified as Aulacanthidae, the only category imaged with this instrument, varied from 0.2 to 4.6 cells m^{-3}. Rhizarian abundances in the largest size fraction (>1000 µm), imaged by the UVP were generally slightly lower than those found for the >200 µm size fraction, with the exception of some stations (Table 3). The Phaeodaria groups found during this cruise belong to the families Aulacanthidae, Castanellidae, Coelodendridae, Aulosphaeridae and Cannosphaeridae (Figure 3).

Table 3. Abundance of siliceous Rhizaria collected using three different devices corresponding a different size ranges. FlowCAM corresponds to 64-200 µm, Zooscan to >200 µm and UVP to individuals >1000 µm.

Station	**Size sampled**		
Leg-Stn	**64-200 µm**	**>200 µm**	**>1000 µm**
	Rhizaria concentration (cell m^{-3})		
leg1-005	5.1	1.1	1.7
leg1-021	10.2	0.5	1.3
leg1-027	17.2	1.9	1.8
leg1-035	42.5	0.4	1.0
leg1-040	41.7	1.7	1.9
leg1-045	15.5	1.7	1.3
leg1-051	19.8	2.4	1.4
leg2-001	26.2	1.4	0.7
leg2-015	13.0	0.7	1.9
leg2-020	53.9	1.9	1.9
leg2-025	5.0	2.4	0.6

leg2-033	19.4	1.2	0.7
leg2-036	61.1	0.5	1.4
leg2-045	10.1	0.2	0.3
leg2-056	40.8	0.5	0.7
leg2-067	16.9	4.6	1.5

3.4. Contribution of Rhizaria to bSi standing stock

When converted to biomass using the allometric relationship (Equation 3), we found that the largest individuals (>1000 µm) contributed the most to the total Si stock in the water column, from 0.5 to 70.3 µmol-Si m^{-2}. Overall, the small and medium sized individuals (> 64 – 1000 µm) contributed equally to the largest individuals at all stations, except at offshore stations leg2-36, leg2-56, where small sized individuals dominated. These stations presented the deepest bottom depths (Figure 5). Small Rhizaria (< 200 µm) contributed to the bSi standing stock from 2 to 50% depending on the sampling stations, contributing from 1.1 to 39.9 µmol-Si m^{-2} (Table 4).

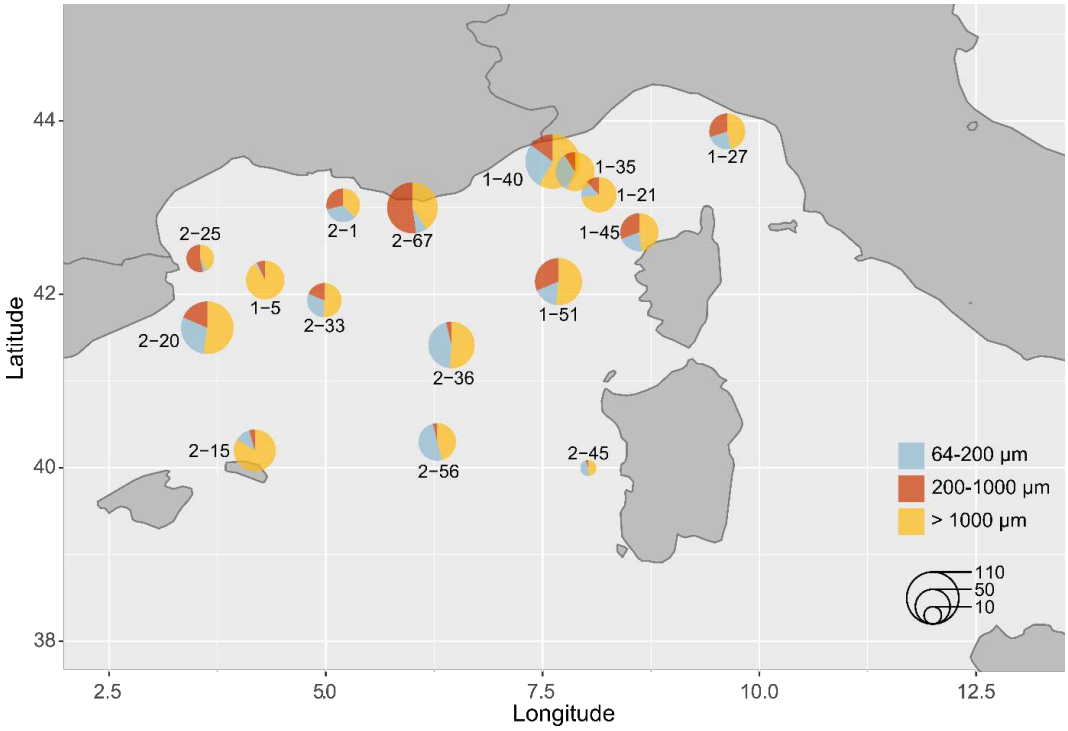

Figure 5. Overview of the bSi biomass of Rhizaria integrated in the upper 500 m of the water column (µmol-Si m^{-2}) in the Mediterranean Sea. Piecharts indicate relative contributions of the three size classes studied to the global bSi at each station and their size is proportional to their Si contribution.

Table 4. Biogenic silica integrated over the 0 – 500 m layer for Rhizaria collected using three different devices corresponding to different size ranges. FlowCAM corresponds to 64-200 µm, Zooscan to >200 µm and UVP to individuals >1000 µm.

Station	Size sampled		
	64-200 µm	>200 µm	>1000 µm
Leg-Stn	bSi Rhizaria (µmol-Si m^{-2})		
leg1-005	1.1	4.3	55.4
leg1-021	7.9	6.1	37.3
leg1-027	12.4	15.9	24.8
leg1-035	21.0	5.7	35.3
leg1-040	33.0	17.7	70.3
leg1-045	12.7	18.1	28.4
leg1-051	15.4	28.2	46.8
leg2-001	15.4	13.4	17.5
leg2-015	8.4	3.1	60.0
leg2-020	32.8	21.0	59.0
leg2-025	1.6	16.4	12.8
leg2-033	14.6	9.1	24.7
leg2-036	39.9	3.3	44.9
leg2-045	4.8	0.5	5.2
leg2-056	28.9	2.1	26.3
leg2-067	7.4	55.2	42.9

Specimens of the Nassellaria order were found at all stations, contributing to the biomass more than 50% in most stations (except stations leg2-001 and leg2-015).

4. Discussion

4.1. Use of imaging data to assess the relative contribution of Rhizaria to the bSi stock in the Mediterranean Sea

Using data obtained from the imaging tools along with the allometric relationship previously established (Llopis Monferrer et al., 2020), we provide a first attempt to determine the contribution of all siliceous Rhizaria, across the entire size spectrum, to the bSi standing stock in the Mediterranean Sea. The NW Mediterranean basin is characterised by oligotrophic conditions. During Fall (September-early November), surface waters are nutrient depleted, and microphytoplankton is generally dominated by non-siliceous organisms (Leblanc et al., 2003). Leblanc et al. (2003) reported bSi integrated stocks from 3.1 to 21.5 mmol-Si m^{-2} in the first 150 m of the water column with the lowest values of bSi corresponding to autumn. During

MOOSE-GE 17 cruise, bSi values integrated over the 0-DCM layer ranged between 1.7 and 6.8 mmol-Si m^{-2}, which are concordant to those found by Leblanc et al. (2003) at a similar period of the year at a station located in the NW Mediterranean basin.

Here, we found that siliceous Rhizaria contributed up to 6% of the total bSi in the water column, considering that phytoplankton bSi under the DCM was null. Values of diatom bSi seem to be very close to 0 under 80 m throughout the year (Leblanc et al., 2003). Assessing whether the highest concentrations of Rhizaria corresponded to the highest concentrations of diatoms is a difficult task. The smallest size class was collected with a plankton net over the first 500 m. With this sampling method, there is no detailed information on vertical distribution of small Rhizaria, and it is difficult to know if they mainly thrive in the euphotic layer, which is generally dominated by diatoms. Investigating metabarcoding from the Niskin bottles would shed light on this issue. For larger individuals, imaged *in situ* with the UVP, highest abundances were found at approximately 100 m depth, below the maximum of bSi found for this area (Leblanc et al., 2003). There is evidence that vertical distribution of some groups of Rhizaria can be associated with several hydrographic features, such as the DCM (Dennett, 2002; Kling and Boltovskoy, 1995). A wider depth coverage would be needed to study in detail the effect of these features on the rhizarians community.

According to Llopis Monferrer et al. (2020), in tropical and subtropical waters (0-40°N/S) the contribution of Rhizaria to the standing stock of silicifiers in the 0-200 m water layer is of the same order of magnitude as their contribution estimated for the 200-1000 m layer. The impact of deeper-living organisms to the Si cycle has not been considered here, as we only analysed rhizarians found in the 0-500 m layer.

In productive areas of the World Ocean, where Rhizaria are less abundant and diatoms concentrations are much higher, the impact of these protists on the bSi biomass in surface waters is much lower, as in the case of the Ross Sea in Antarctica, where Rhizaria account for only 0.1% at most of the total bSi (Llopis Monferrer et al.; in prep).

Different Rhizaria species have different depth preferences (Biard and Ohman, 2020; Boltovskoy et al., 2017). According to this information, Rhizarians living in deeper layers, have been omitted in our estimates. This uneven distribution of organisms would affect the contribution of Rhizaria to the global bSi standing stocks, especially in the waters below the

euphotic layer, where they can be very abundant contributing to the bSi fluxes to the deep ocean (Nakamura et al., 2013).

Our results highlight that the study of the entire size spectrum and vertical distribution of Rhizaria is essential to fully understand the role of these protists in the biogeochemical cycle of silicon. Despite the possible underestimation of cell concentrations, small specimen accounted for up to 50% of the bSi standing stock at some stations. The bSi content was certainly influenced by the taxonomic groups present at each station and their different cell sizes. The size of the individual affects the bSi content (Llopis Monferrer et al., 2020). Small Rhizaria, chiefly represented by polycystine (Nassellaria and Spumellaria) possess solid skeletons and are generally denser (up to 530 µg-Si mm^{-3}) than large phaeodarians (10 µg-Si mm^{-3}) (Llopis Monferrer et al., 2020). Large phaeodarians skeletons are instead porous (Nakamura et al., 2018).

Despite the uncertainties associated with each method employed, results showed that both, small and large Rhizaria are non-negligible contributors to the bSi biomass in the area of study and likely in other oceanic regions, especially in oligotrophic areas. To better understand the global significance of these organisms and to be able to include them in the biogeochemical models, the full extent of siliceous rhizarians should be investigated.

4.2. Rhizaria abundances and diversity: imaging and genomics

Rhizaria are important contributors to bSi production in the global ocean (Biard et al., 2016; Llopis Monferrer et al., 2020; Takahashi et al., 1983). They span a wide size range and occupy a variety of ecosystems which makes difficult to achieve an integrated perspective on their specific contribution to major ecological process such as biogeochemical cycles (Biard and Ohman, 2020; Suzuki and Not, 2015).

This study is one of the few that simultaneously analyses planktonic Rhizaria from the water column spanning several orders of magnitude, from few micrometres to several millimetres.

Imaging technologies give Rhizaria concentrations in the Mediterranean Sea ranging from 0.2 to 61.1 cells m^{-3} in 0-500 m water depth, with small cells being largely dominant (from 5.0 to 61.1 cells m^{-3}) over larger ones (from 0.2 to 4.6 cells m^{-3}). These concentrations are consistent with the size distribution of organisms reported in previous studies where small organisms are generally more abundant than larger ones in the upper water column (Boltovskoy et al., 1993;

Llopis Monferrer et al., 2020). Yet, abundances observed here fall in the lower range of estimates from a worldwide compilation from microscopic observations of net samples deployed the 0-1000 m water layer of the tropical and subtropical waters (40°N/S), which stated that small Rhizaria cell abundances ranged from 79 to 892 cells m^{-3} and from 5 to 20 cells m^{-3} for larger individuals. Low cell densities observed in this study could be due to the seasonality patterns in rhizarians communities as very little is known about the ecology of these organisms as well as the oligotrophic nature of the Mediterranean Sea. Analysis of plankton time series on the northern coast of the Mediterranean Sea shows the highest biomass of Rhizaria (including the non-silicified) in August (Romagnan et al., 2015).

Low cell densities could also be explained by the caveats associated with the use of imaging instruments. Although the combined use of the three instruments covered a broad size spectrum, we observed a size gap between the Flowcam and Zooscan. From 176 µm to 365 µm no specimens were observed (Figure 2), while specimens of the order Spumellaria and genus Challengeria can exceed 176 µm in size (ESD) (Llopis Monferrer et al., 2020). Their absence in the results could be explained by the handling of FlowCAM samples prior to analysis, since these are sieved onto a 200 µm mesh size to prevent instrument clogging. Many siliceous Rhizaria specimens can exhibit a size smaller than 64 µm which was the smallest plankton mesh used (*e.g.*, small size species, juvenile forms), leading to an underestimation of total siliceous Rhizaria abundances. Finally, fixatives used classically (*e.g.* lugol's iodine or formaldehyde) are known to affect organisms leading to potential underestimated cell counts (Choi and Stoecker, 1989, Beers and Stewart, 1970).

Regarding the Zooscan (200 – 1000 µm), its operational size range starts at 240 µm. This instrument may not easily recognize small individuals whose sizes are close to the detection limit. Although all observations reported in this study lie within the range in which reliable quantitative results can be obtained, not all the operational size range is efficient to obtain quantitative results. The Zooscan captured the smallest individuals of the family Aulacanthidae and therefore it was necessary to avoid an even higher gap between different instruments.

Metabarcoding results show that siliceous Rhizaria were present in almost every sample among the different stations and size fractions. The different methods (imaging and molecular) do not match neither in relative abundances nor in the taxonomic groups represented at each station. Molecular results show that the larger individuals had the higher

relative abundances, in contrast to imaging results. DNA copies number increases with cell size, as shown in Collodaria specimens (Biard et al., 2017), which might lead to an overrepresentation in metabarcoding data compared to morphologically cell counting. On the other hand, Nassellaria, which is the dominant group in abundances with imaging techniques, rarely appear in metabarcoding data. Nassellaria possess robust skeletons (Takahashi et al., 1983) and cell breakage may play a crucial role in molecular diversity studies (Méndez-Sandín, 2019; Not et al., 2007). The low representation of Nassellaria could be due to the robust cellular architecture, affecting DNA extraction and amplification. In addition, metabarcoding analyses rely on the reference database and taxa not included in the database may lead to an underestimation (or even an absence) of the relative abundances found in the metabarcoding data.

Although a correlation between rDNA copy number per cell and cell length was established across eukaryotic marine protists (Biard et al., 2017), the comparison of relative abundances and diversity measured by imaging methods and molecular tools is complex and must be made cautiously. Imaging and metabarcoding methods have a great potential and allow a relatively rapid analysis and processing of samples. All these approaches for plankton enumeration have, however, uncertainties when estimating the actual composition and abundance of the community, and a thorough interpretation of the results requires assessment of the limits of each method.

In order to provide reliable comparisons, sampling protocols must be homogeneous between the different methods (*e.g.*, sample the same size class). Single-cell sequencing may avoid the mismatch between the taxonomic groups as it will enrich the database.

4.3. Prospects to better characterize the entire Rhizaria community

Plankton has been traditionally collected by plankton nets, including the closing nets (Ishitani and Takahashi, 2007; Itaki et al., 2003). To sample both, large and small organisms simultaneously, bongo nets can be used, as is the case of the present study. Sampling of Rhizaria can be done filtering water (Boltovskoy et al., 1993). According to our experience, to successfully conduct experiments we need at least 30 individuals of small rhizarians, with an average abundance of 30 cell m^{-3}, we will need to filter 1000 L. For larger rhizarians, although less individuals are needed to conduct experiments, as they are less abundant (average of 1.5

cell m^{-3}), we would need to filter 3300 L. So far, we have assumed that the bSi retained on filters from the seawater collected with the Niskin bottles, do not contain rhizarians. To confirm this assumption and avoid biases in the bSi analyses, the entire content of a Niskin bottle should be analysed by morphological and/or molecular tools. In addition, Rhizaria collected could be associated to a given depth and to physicochemical parameters, providing valuable information on the ecology of each specimen. Plankton could be sampled by traditional closing nets (*e.g.*, Multinet) to take into account different water layers. To sample both, large and small organisms simultaneously, bongo or triple nets can be used, as was the case for this study. Alternatively, the Bottle-Net (BN) is an oceanographic device designed specifically for the Malaspina 2010 Circumnavigation. It could be used as an alternative to traditional plankton net. This instrument is designed to be mounted on a standard rosette and it consists of an external PVC and stainless steel frame, with a 20 µm mesh size inside it. One of the major assets of this device is that it can sample a delimited water layer and it does not concentrate as many organisms as the plankton net, avoiding damage of the organisms. This can be very useful to study the actual distribution and abundances of Rhizaria, since these organisms are known to inhabit from the surface to the deep waters of the ocean (Suzuki and Not, 2015).

To investigate large Rhizaria, the UVP appears as the most adequate instrument. This *in situ* device is attached to the CTD, no extra time is needed for its deployment and environmental parameters can be associated to the organisms imaged. With this information, their ecological preferences and vertical niches can be characterized (Brisbin et al., 2020). Its depth range is 6000 m, therefore, it can study the vertical distribution of Rhizaria up to zones where other tools cannot reach. The size of the resulting dataset is vast, resulting in a complex and time consuming task to manually classify all the images. Despite some drawbacks, the UVP is a performant instrument, and efforts are being made to facilitate and improve the efficiency of the analysis and processing of the large amount of data generated (Schröder et al., 2019).

Molecular methods provide insights into biodiversity but are not quantitative. Gene copies can vary among groups of protists. For example, Collodaria, possess high rDNA copy number which is not representative of their actual abundance in the ecosystem (Biard et al., 2017). Another limitation of molecular methods is that DNA is capable of remaining available even when cells are dead. For most data, this makes it difficult to know whether organisms found

at a certain depth inhabit that same depth or are simply organisms sedimented from surface waters, making it impossible to know whether the DNA comes from a metabolically active cell, a dead cell, or the remnant of a cell (Brisbin et al., 2020). Molecular tools are a promising alternative to morphological observation but still many concepts are yet to be understood, such as cellular architecture, copy number and intragenomic variability.

The combination of imaging and molecular tools may lead to a better understanding of the Rhizaria biology and ecology as it offers an extensive coverage of the size spectrum.

Acknowledgements

The authors are grateful to the MOOSE observation national network (funded by CNRS - INSU and Research Infrastructure ILICO), which supports the annual ship-based hydrographic sections in the northwestern Mediterranean Sea (MOOSE - GE). We also thank the science team and crew of the RV Atalante and Pierre Testor (CNRS, LOCEAN) as head of the MOOSE GE-2017 mission cruise.

Discussion and perspectives

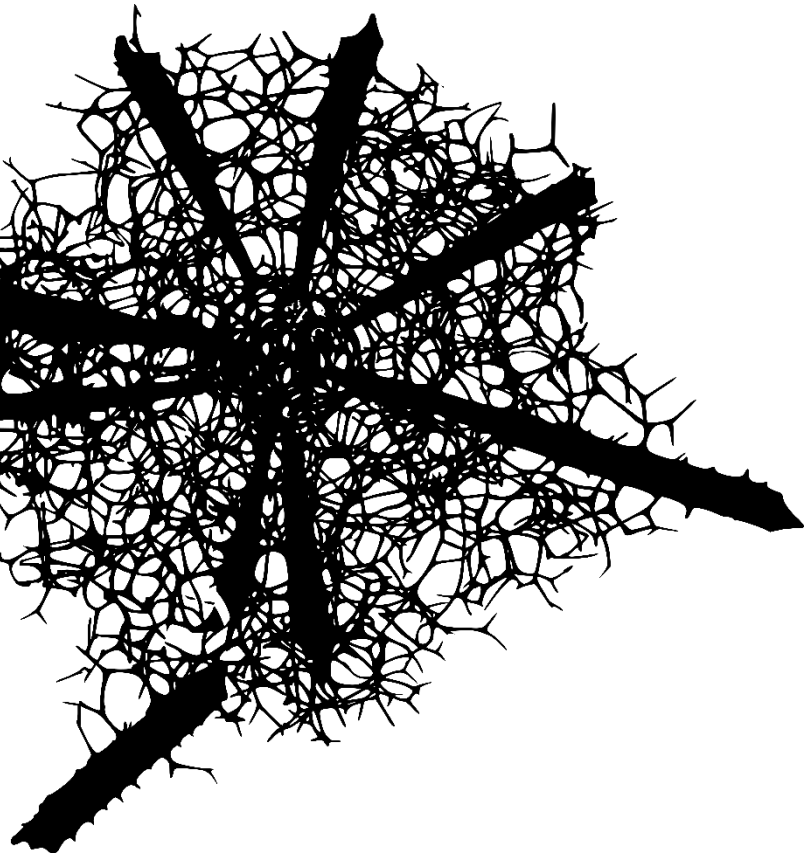

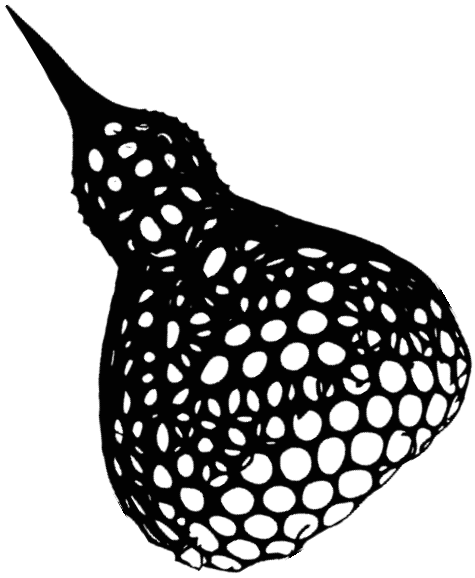

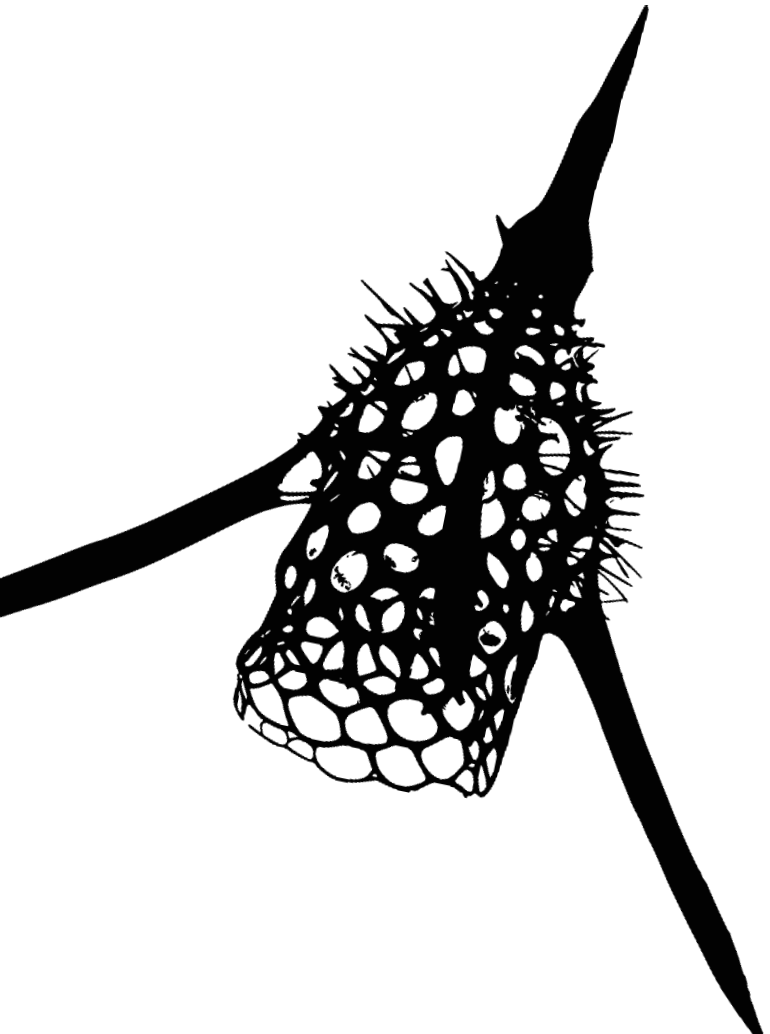

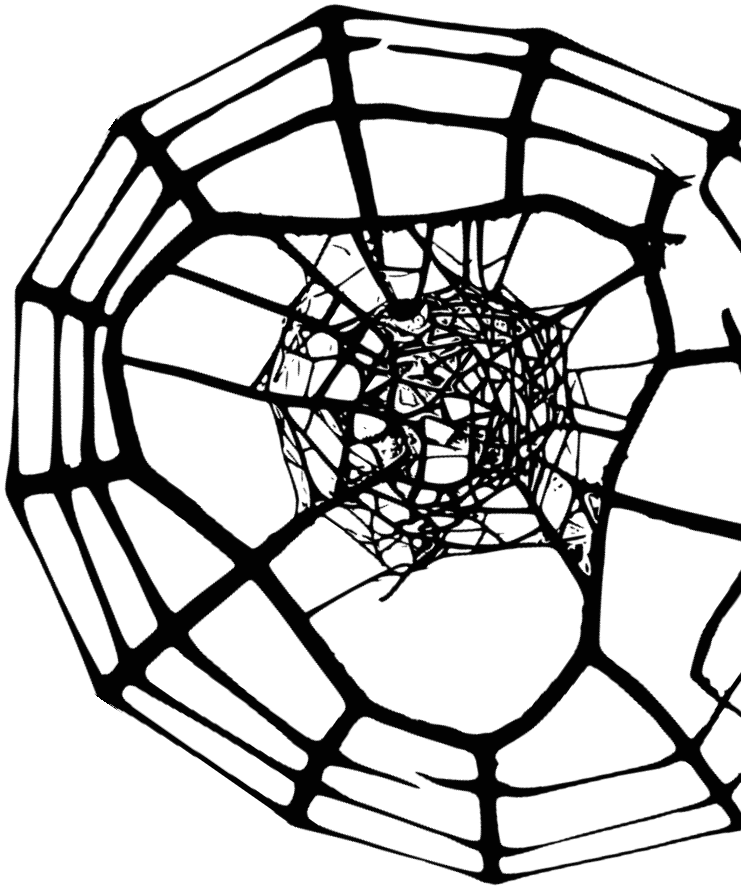

Drawings of Nassellaria and Spumellaria specimens from Miguel Méndez-Sandin pictures.

1. Rhizaria in the silicon cycle: new kids on the block

The global marine Si cycle has evolved through geologic time principally due to the uptake of dSi and its subsequent biomineralisation by silicifier organisms (Siever, 1991). Rhizaria were among the first protists inhabiting the ocean (Suzuki and Oba, 2015). In the Cambrian (~500 Ma), radiolarians were assumed to control the silica output of the oceans together with sponges (Siever, 1991). In the Mesozoic (~186 Ma), diatoms arose in the planktonic realm and became an important competitor to polycystines regarding the access to dissolved silicic acid (dSi). Because of their superior affinity to dSi, diatoms decreased dSi concentrations down to the relatively low levels observed in today's oceans (Conley et al., 2017; Tréguer and De La Rocha, 2013). Today, diatoms are particularly important in the transfer of atmospheric carbon to the deep ocean through the biological sequestration of atmospheric CO_2 (*i.e.* the biological pump, Matsumoto et al., 2002), they are responsible for ~20% of global oxygen production and contribute up to 40% of the export of carbon (Jin et al., 2006).

In recent decades, awareness of the diversity, ecology and contribution of Rhizaria to marine biogeochemical cycles has increased (Biard et al., 2016; Guidi et al., 2016). Large silicified rhizarians are coming into sight as important Si exporters and presumably consumers (Biard et al., 2018), but quantitative information about their dSi consumption is scarce. Most of the published studies on these organisms are indirectly obtained through theoretical approaches (*e.g.*, Takahashi, 1981).

The work carried out during this thesis intended to assess the contribution of Rhizaria to the global Si cycle, focusing on bSi standing stocks and production budgets. I essentially performed direct measurements using the ^{32}Si radioisotope, to evaluate the capacity of individual Rhizaria specimens to consume dSi. In addition to the consumption rates, I investigated the elementary composition (*i.e.*, biogenic silica, carbon and nitrogen) of several taxonomic groups (*i.e.*, polycystines: Nassellaria, Spumellaria, silicified Collodaria and Phaeodaria) from contrasting oceanic areas (*i.e.*, Mediterranean and Ross Sea).

The results of the experiments carried out during my thesis clearly demonstrate that Polycystine and Phaeodaria are highly silicified (up to 9 nmol-bSi $cell^{-1}$) and highly productive (up to 11.85 nmol-Si $cell^{-1}$ d^{-1}) cells. In our attempt to estimate the role of Rhizaria in the global Si cycle, wecombined literature on the distribution and abundances of silicified Rhizaria and

results obtained in the Mediterranean Sea (Chapter 1). Considering two contrasting oceanic regions, warm (0-40° N/S) and cold (>40° N/S) waters, we concluded that these organisms contribute from 0.2 up to 2.2 mmol-Si m^{-2} of the marine standing stock of bSi and up to 19 % of the bSi production in the global ocean. When analysing specimens from other oceanic regions, we observed that rhizarians from the Ross Sea, which were morphologically similar to those found in the Mediterranean Sea, appeared to be more silicified (Chapter 2). In the Southern Ocean (SO), some of the highest dSi concentrations of the World Ocean are observed (Honjo et al., 2008). We included the new values obtained in the SO (Chapter 2) to re-evaluate the contribution of rhizarians in cold waters (>40°N/S), as in Chapter 1, empirical data only came from specimens from the Mediterranean Sea. We observed a slightly higher contribution of specimens from these regions, up to 5% of the total bSi production. Considering these new values, the former 19% of the global bSi production due to rhizarians (Chapter 1) increases up to 22%. With silicified rhizarians possibly being responsible for near a quarter of the global bSi production, the potential role of these organisms cannot be disregarded when studying the Si cycle. Despite the obvious uncertainties associated with such global estimates, these new estimates about Rhizaria production rates and cellular content are valuable to include Rhizaria in subsequent models for Si use and Si cycling in the ocean, models that so far solely focused on diatoms.

2. Rhizaria, throughout the water column down to the sediments

The Antarctic Rhizaria silica paradox. Despite being highly silicified organisms with great potential to impact the global Si cycle in the oceans, Rhizaria contribution to the total bSi standing stocks in the water column is rather low, from less than 0.1% in Antarctic waters up to 6% in oligotrophic zones (Mediterranean Sea). In contrast, much higher percentages have been observed in tropical and Antarctic sediments (Dutkiewicz et al., 2015). A similar paradox (*i.e*., high accumulation rates of opal in the sediment in spite of low production rates in the upper surface waters) has already been described in the Southern Ocean (SO) for the whole phytoplanktonic community (Pondaven et al., 2000).

To solve this paradox (*i.e.* "the low contribution of radiolarians to the production of biogenic silica in the surface layer, but a strong contribution to sedimentary deposits"), we can

reconsider two aspects: either the surface production is underestimated, or the preservation of Rhizaria's bSi is exceptionally high.

Regarding the production rates, we have shown that rhizarians are able to directly take up silica dissolved in seawater. However, the precise mechanism by which silica is absorbed is not known. Other processes such as diatom phagocytosis could also allow them to acquire the silica necessary for their skeleton. Such mechanism has not been taken into account and should be studied further.

Regarding preservation, several factors that contribute to the preservation of Rhizaria's bSi from particles settling in the water column must be examined to explain the paradox. Thermodynamically, the coldest the marine waters of the SO are, the lowest the dissolution of the bSi is (Tréguer et al., 1989).

To investigate if temperature has a similar effect on silicified Rhizaria, experiments are needed to shed light on dissolution rates of these organisms. Considering the difficulty of keeping Rhizaria alive and the impossibility of culturing them in the laboratory, these experiments should be specifically designed for each species, as they can only be maintained from several days to several weeks (Boltovskoy et al., 2017). Incubations using stable isotopes of Si (^{30}Si) could be carried out for 24 to 48 hours, adapting protocols developed to measure the dissolution rates of bSi from diatom frustules (Nelson and Goering, 1977).

Rhizarians skeletons are generally resistant to dissolution and exhibit a very rich and continuous fossil record (Takahashi, 1981). Polycystine Radiolaria and Phaeodaria differ in the robustness of their skeletal structures (Nakamura et al., 2018). While phaeodarians, which are the largest specimens possess porous skeletons prone to dissolution, polycystine radiolarians, the smallest ones, present a more robust and dense skeleton (Takahashi et al., 1983). Polycystine are commonly found in the sediment (Boltovskoy et al., 2017) and are likely important vectors of bSi fluxes to the bottom depth. Radiolarian oozes are commonly found in the SO, certainly associated to a high efficiency of opal preservation in the SO. Large amounts of silicified rhizarians can also be observed in tropical sediments, in the Pacific, Atlantic an Indian oceans (Dutkiewicz et al., 2015), suggesting that other parameters apart from the temperature affect the transfer of Rhizaria from surface layer to the sea bed.

Phaeodarians are rarely found in the sediment, suggesting their role as important nutrient recyclers in the water column, forming an essential link to higher trophic levels by providing enriched organic matter (Stukel et al., 2018). Unfortunately, little is known about the precise mechanisms by which organic matter associated to silicifiers is degraded and how bSi is affected. By studying the elemental composition and uptake rates of rhizarians from several contrasting regions (*e.g*., warm versus cold waters) and different species, we would be able to understand if the contribution of these organisms increases in areas where diatoms are poorly represented.

Along with additional measures of rhizarians' bSi content and uptake rates of silicic acid, accurate estimates of their vertical fluxes across a wider range of cell sizes and of their sinking velocity are required in order to better understand the global significance of silicified rhizarians.

Importance of the twilight zone. In this thesis we have focused on Rhizaria found in the 0-500 m layer of the Mediterranean Sea and in the 0-200 m layer of the Atlantic and Southern Ocean. Rhizaria, unlike diatoms, which are photosynthetic organisms thriving in the euphotic layer, are ubiquitous throughout the pelagic environment (Suzuki and Not, 2015). Although Rhizaria concentrations decrease sharply with depth, depth-integrated values (*i.e*., ind m^{-2}) can be as high, or even higher at depth than in the surface layers (Boltovskoy, 2017; Kling and Boltovskoy, 1995). Therefore, their impact on the biogeochemical cycles under the twilight zone cannot be neglected. For instance, the twilight zone, spanning from 200 m to 1000 m depth, is the habitat of many rhizarians with specific communities thriving at depth (Stukel et al., 2018; Suzuki and Not, 2015). The dark ocean and the underlying deep sea floor represent the largest environment on this planet, comprising about 80% of the oceanic volume (Gooday et al., 2020) and needs to be explored. Deep pelagic environments are difficult to study, with organisms sparsely distributed and often fragile. Not to mention the stress that may be associated with high pressures, which poses problems for laboratory-based experiments at atmospheric pressure (Gooday et al., 2020).

Little is known about the precise mechanisms by which organic matter associated to silicified skeletons is degraded and how silica is affected in this zone. By studying rhizarians from the entire water column, we would be able to understand if the contribution of these organisms in the twilight zone is at least as important as in the euphotic area. Combination of marine

biogeochemistry experiments on Rhizaria, quantitative *in situ* imaging tools, sediment trap fluxes and molecular characterizations of diversity will be needed to study the entire community.

3. Towards a holistic view of Rhizaria community ecology

The comprehensive perspective of Rhizaria contribution to biogeochemical cycles currently suffers a lack of quantitative information regarding various aspects of their basic ecology such as their taxa specific diversity and abundance, trophic modes and relationships, across the broad cell-size spectrum and extended range of habitats Rhizaria occupy throughout the water column (Biard and Ohman, 2020).

In recent years, the rapid development of imaging and molecular techniques has contributed to increase the awareness of planktonic rhizarians as actors in the biogeochemical cycles (Biard et al., 2016; Biard and Ohman, 2020; Faure et al., 2019). Radiolarian molecular sequences are among the most represented environmental diversity survey of eukaryotes (Not et al., 2009).

To investigate the diversity and abundance of the entire cell size spectrum of silicified Rhizaria in the North-Western Mediterranean Sea, we developed a paired approach, bringing together DNA-metabarcoding and imaging tools (FlowCAM, Zooscan and Underwater Vision Profiler 5 – UVP) (Chapter 3).

Regardless of the approach used for plankton quantification, all methods are subject to uncertainties when estimating the actual composition and abundance of the community. Not unexpectedly, diversity and relative contribution of the different taxonomic groups highly differed between the methods used.

In our study, imaging analyses showed higher taxa richness compared to the molecular analyses. Other studies present opposite results, with molecular techniques being very effective in detecting diversity (Schroeder et al., 2020). The accurateness of the reference database used for taxonomic assignation is among the critical requirements for good estimates of diversity and biogeography patterns based on environmental DNA barcode (Guillou et al., 2012). In this respect, it is critically important to maintain expertise and capacity in morphological taxonomic identification to ensure a proper morpho-molecular framework

(Bucklin et al., 2016). Single-cell sequencing of the targeted groups is a valuable approach to complement reference databases to be used for metabarcoding analysis since it could be the missing references in the databases that caused the mismatch in the diversity encountered (Biard et al., 2017; Méndez-Sandín, 2019).

If molecular methods can provide insights into biodiversity they are not quantitative as gene copies can vary among groups of protists. For instance, Collodaria, possess high copy numbers of ribosomal DNA which are not representative of their actual abundance in the ecosystem (Biard et al., 2017) unless proper calibrations are performed. Another limitation of molecular methods is that DNA is capable of remaining in the environment even when cells are dead. For most datasets, it is difficult to know whether organisms found at certain depth actually inhabit that same depth or are simply organisms sedimented from surface waters, making it impossible to know whether the DNA comes from a metabolically active cell, a dead cell, or the remnant of a cell (Brisbin et al., 2020). An alternative could be to use RNA, less stable outside the cells, instead of DNA as template for metabarcoding production (Not et al., 2009).

Regarding the imaging methods, *in situ* imaging systems are non-invasive devices, offering an interesting alternative to quantify Rhizaria without damaging the cells. Although the use of UVP provides an impressive amount of information on the abundances and biomass of silicified Rhizaria, it is restricted to large size-classes >600 µm. Small Rhizaria (*i.e.*, Nassellaria and Spumellaria) are undetectable with the UVP and other alternatives which may damage the cells are used (*i.e*., FlowCAM and Zooscan). With the technology available today, the use of several complementary tools is necessary to assess the entire community. However, biases in imaging methods counts can occur at different steps from the sampling to the final analyses. Appropriate sampling and preservation procedures are required to accurately quantify rhizarians in the environment. Morphology interpretation may be modified by preservation of specimens (Beers and Stewart, 1970), the observation techniques or even the taxonomic expertise of the observer. As for the morpho-molecular reference framework, the images produced in this PhD work will contribute to the richness of the Ecotaxa image database (Picheral et al., 2017) and the training set of expert-classified images are available for future studies. New imaging technologies with higher resolution camera systems are arriving with the potential for analysing small individuals and can better discriminate between rhizarians species.

Despite our attempt of combining several methods, gaps and overlaps between the different instruments for data acquisition were highlighted. Alternative sampling strategies could also be valuable. For instance, the newly developed “bottle net” (Aquatic Biotechnology) could be used as an alternative to a traditional plankton net, as it can sample a delimited water layer without concentrating as many organisms as the plankton net, avoiding the entanglement of the organisms. We could also use the Vertical Multiple Plankton Sampler (VMPS). This net is appropriate for monitoring the vertical distribution of plankton, allowing the collection of living specimens from specific water layers. However, this device will be more suitable for areas with low productivity, where concentrations of individuals are lower.

Another issue encountered during this thesis was that experiments performed were mainly conducted using a limited set of rhizarians species pooled into higher trophic levels. Not being able to culture these organisms (Boltovskoy et al., 2017; Suzuki and Not, 2015), we carried out *in situ* experiments but a minimum number of specimens was required to successfully measure the biomass (*i.e.*, silica, carbon or nitrogen) or production rates. The community composition of natural samples is unpredictable and obtaining enough individuals of the same morphotype is complicated. Rhizaria morphology is very diverse (Boltovskoy et al., 2017), and the individuals required for each taxonomic group is variable. Collecting enough individuals of these unculturable protists to conduct experiments requires a meticulous work in the isolation and a special effort toward collecting replicated taxonomic groups is needed. Still, mid-term maintenance is possible and allows experimental work to investigate Rhizaria physiological ecology (Anderson et al., 1989).

Yet, further studies are required on the ecology and physiology of rhizarians and on the factors controlling their growth, preys’ preferences and skeleton's dissolution rate before we can fully elucidate rhizarians' role in the Si and other marine biogeochemical cycles.

“What we know is a drop, what we don't know is an ocean.”

Isaac Newton

Bibliography

Abelmann, A., Gersonde, R., 1991. Biosiliceous particle flux in the Southern Ocean. Mar. Chem. 35, 503–536. https://doi.org/10.1016/S0304-4203(09)90040-8

Abelmann, A., Gowing, M.M., 1997. Spatial distribution pattern of living polycystine radiolarian taxa — baseline study for paleoenvironmental reconstructions in the Southern Ocean (Atlantic sector). Mar. Micropaleontol. 30, 3–28. https://doi.org/10.1016/S0377-8398(96)00021-7

Aminot, A., Kérouel, R., 2007. Dosage automatique des nutriments dans les eaux marines, Ed. Ifremer, Méthodes d'analyse en milieu marin. ed.

Anderson, O., Gupta, S., 1998. Evidence of Binary Division in Mature Central Capsules of a Collosphaerid Colonial Radiolarians: Implications for Shell Ontogenetic Patterns in Modern and Fossil Species. Palaeontol. Electron. https://doi.org/10.26879/98002

Anderson, O.R., Bennett, P., Bryan, M., 1989. Experimental and observational studies of radiolarian physiological ecology: 1. Growth, abundance and opal productivity of the spongiose radiolarianSpongaster tetras tetras. Mar. Micropaleontol. 14, 257–265. https://doi.org/10.1016/0377-8398(89)90012-1

Anderson, O.R., Moss, M.L., Skalak, R., 1987. The Cytoskeletal and Biomineralized Supportive Structures in Radiolaria, in: Cytomechanics. The Mechanical Basis of Cell Form and Structure. Spreinger-Verlag Berlin Heidelberg.

Baines, S.B., Twining, B.S., Brzezinski, M.A., Nelson, D.M., Fisher, N.S., 2010. Causes and biogeochemical implications of regional differences in silicification of marine diatoms: diatom silicification and marine biogeochemistry. Glob. Biogeochem. Cycles 24, n/a-n/a. https://doi.org/10.1029/2010GB003856

Beers, J.R., Stewart, G.L., 1970. THE PRESERVATION OF ACANTHARIANS IN FIXED PLANKTON SAMPLES1. Limnol. Oceanogr. 15, 825–827. https://doi.org/10.4319/lo.1970.15.5.0825

Benfield, M., Grosjean, P., Culverhouse, P., Irigolen, X., Sieracki, M., Lopez-Urrutia, A., Dam, H., Hu, Q., Davis, C., Hanson, A., Pilskaln, C., Riseman, E., Schulz, H., Utgoff, P., Gorsky, G., 2007. RAPID: Research on Automated Plankton Identification. Oceanography 20, 172–187. https://doi.org/10.5670/oceanog.2007.63

Biard, T., Bigeard, E., Audic, S., Poulain, J., Gutierrez-Rodriguez, A., Pesant, S., Stemmann, L., Not, F., 2017. Biogeography and diversity of Collodaria (Radiolaria) in the global ocean. ISME J. 11, 1331–1344. https://doi.org/10.1038/ismej.2017.12

Biard, T., Krause, J.W., Stukel, M.R., Ohman, M.D., 2018. The Significance of Giant Phaeodarians (Rhizaria) to Biogenic Silica Export in the California Current Ecosystem. Glob. Biogeochem. Cycles 32, 987–1004. https://doi.org/10.1029/2018GB005877

Biard, T., Ohman, M.D., 2020. Vertical niche definition of test-bearing protists (Rhizaria) into the twilight zone revealed by in situ imaging. Limnol. Oceanogr. lno.11472. https://doi.org/10.1002/lno.11472

Biard, T., Pillet, L., Decelle, J., Poirier, C., Suzuki, N., Not, F., 2015. Towards an Integrative Morpho-molecular Classification of the Collodaria (Polycystinea, Radiolaria). Protist 166, 374–388. https://doi.org/10.1016/j.protis.2015.05.002

Biard, T., Stemmann, L., Picheral, M., Mayot, N., Vandromme, P., Hauss, H., Gorsky, G., Guidi, L., Kiko, R., Not, F., 2016. In situ imaging reveals the biomass of giant protists in the global ocean. Nature 532, 504–507. https://doi.org/10.1038/nature17652

Boltovskoy, 2003. First record of a brackish radiolarian (Polycystina): Lophophaena rioplatensis n. sp. in the Rio de la Plata estuary. J. Plankton Res. 25, 1551–1559. https://doi.org/10.1093/plankt/fbg107

Boltovskoy, D., 2017. Vertical distribution patterns of Radiolaria Polycystina (Protista) in the World Ocean: living ranges, isothermal submersion and settling shells. J. Plankton Res. 39, 330–349. https://doi.org/10.1093/plankt/fbx003

Boltovskoy, D., Alder, V.A., Abelmann, A., 1993. Annual flux of radiolaria and other shelled plankters in the eastern equatorial atlantic at 853 m: seasonal variations and polycystine species-specific responses. Deep Sea Res. Part Oceanogr. Res. Pap. 40, 1863–1895. https://doi.org/10.1016/0967-0637(93)90036-3

Boltovskoy, D., Anderson, O.R., Correa, N., 2017. Handbook of the protists, Springer. Archibald, John M., Simpson, Alastair G.B., Slamovits, Claudio H. (Eds.), Cham (Switzerland).

Boltovskoy, D., Anderson, O.R., Correa, N., 1990. Radiolaria and Phaeodaria, in: Handbook of the Protists. Springer.

Boltovskoy, D., Correa, N., 2016. Biogeography of Radiolaria Polycystina (Protista) in the World Ocean. Prog. Oceanogr. 149, 82–105. https://doi.org/10.1016/j.pocean.2016.09.006

Boltovskoy, D., Kling, S.A., Takahashi, K., Bjørklund, K., 2010. World Atlas of Distribution of recent Polycystina (Radiolaria) 230.

Breiman, L., 2001. Random Forests. Machine Learning 45, 5–32.

Brisbin, M.M., Brunner, O.D., Grossmann, M.M., Mitarai, S., 2020. Paired high-throughput, in-situ imaging and high-throughput sequencing illuminate acantharian abundance and vertical distribution (preprint). Microbiology. https://doi.org/10.1101/2020.02.27.967349

Brzezinski, M.A., 1985. The Si:C:N ratio of marine diatoms: Interspecific variability and the effect of some environmental variables. J. Phycol.

Brzezinski, M.A., Nelson, D.M., 1989. Seasonal changes in the silicon cycle within a Gulf Stream warm-core ring. Deep Sea Res. Part Oceanogr. Res. Pap. 36, 1009–1030. https://doi.org/10.1016/0198-0149(89)90075-7

Brzezinski, M.A., Phillips, D.R., 1997. Evaluation of ^{32} Si as a tracer for measuring silica production rates in marine waters. Limnol. Oceanogr. 42, 856–865. https://doi.org/10.4319/lo.1997.42.5.0856

Bucklin, A., Lindeque, P.K., Rodriguez-Ezpeleta, N., Albaina, A., Lehtiniemi, M., 2016. Metabarcoding of marine zooplankton: prospects, progress and pitfalls. J. Plankton Res. 38, 393–400. https://doi.org/10.1093/plankt/fbw023

Buitenhuis, E., Le Quéré, C., Aumont, O., Beaugrand, G., Bunker, A., Hirst, A., Ikeda, T., O'Brien, T., Piontkovski, S., Straile, D., 2006. Biogeochemical fluxes through mesozooplankton: BIOGEOCHEMICAL FLUXES THROUGH MESOZOOPLANKTON. Glob. Biogeochem. Cycles 20, n/a-n/a. https://doi.org/10.1029/2005GB002511

Callahan, B.J., McMurdie, P.J., Rosen, M.J., Han, A.W., Johnson, A.J.A., Holmes, S.P., 2016. DADA2: High-resolution sample inference from Illumina amplicon data. Nat. Methods 13, 581–583. https://doi.org/10.1038/nmeth.3869

Carrasco, J.F., Bromwich, D.H., Monaghan, A.J., 2003. Distribution and Characteristics of Mesoscale Cyclones in the Antarctic: Ross Sea Eastward to the Weddell Sea. Mon. WEATHER Rev. 131, 13.

Claquin, P., Leynaert, A., Sferratore, A., Garnier, J., Ragueneau, O., 2006. Physiological Ecology of Diatoms Along the River-Sea Continuum., in: The Silicon Cycle. Human Perturbations and Impacts on Aquatic Systems. pp. 121–138.

Conley, D.J., Frings, P.J., Fontorbe, G., Clymans, W., Stadmark, J., Hendry, K.R., Marron, A.O., De La Rocha, C.L., 2017. Biosilicification Drives a Decline of Dissolved Si in the Oceans through Geologic Time. Front. Mar. Sci. 4, 397. https://doi.org/10.3389/fmars.2017.00397

Conley, D.J., Kilham, S.S., Theriot, E., 1989. Differences in silica content between marine and freshwater diatoms. Limnol. Oceanogr. 34, 205–212. https://doi.org/10.4319/lo.1989.34.1.0205

de Vargas, C., Audic, S., Henry, N., Decelle, J., Mahe, F., Logares, R., Lara, E., Berney, C., Le Bescot, N., Probert, I., Carmichael, M., Poulain, J., Romac, S., Colin, S., Aury, J.-M., Bittner, L., Chaffron, S., Dunthorn, M., Engelen, S., Flegontova, O., Guidi, L., Horak, A., Jaillon, O., Lima-Mendez, G., Luke, J., Malviya, S., Morard, R., Mulot, M., Scalco, E., Siano, R., Vincent, F., Zingone, A., Dimier, C., Picheral, M., Searson, S., Kandels-Lewis, S., Tara Oceans Coordinators, Acinas, S.G., Bork, P., Bowler, C., Gorsky, G., Grimsley, N., Hingamp, P., Iudicone, D., Not, F., Ogata, H., Pesant, S., Raes, J., Sieracki, M.E., Speich, S., Stemmann, L., Sunagawa, S., Weissenbach, J., Wincker, P., Karsenti, E., Boss, E., Follows, M., Karp-Boss, L., Krzic, U., Reynaud, E.G., Sardet, C., Sullivan, M.B., Velayoudon, D., 2015. Eukaryotic plankton diversity in the sunlit ocean. Science 348, 1261605–1261605. https://doi.org/10.1126/science.1261605

Decelle, J., Colin, S., Foster, R.A., 2015. Photosymbiosis in Marine Planktonic Protists, in: Marine Protists. Springer, Tokyo; New York, pp. 465–500.

Del Amo, Y.D., Brzezinski, M.A., 1999. The chemical form of dissolved Si taken up by marine diatoms. J. Phycol. 35, 1162–1170. https://doi.org/10.1046/j.1529-8817.1999.3561162.x

Dennett, M.R., 2002. Video plankton recorder reveals high abundances of colonial Radiolaria in surface waters of the central North Pacific. J. Plankton Res. 24, 797–805. https://doi.org/10.1093/plankt/24.8.797

Donoso, K., Carlotti, F., Pagano, M., Hunt, B.P.V., Escribano, R., Berline, L., 2017. Zooplankton community response to the winter 2013 deep convection process in the NWMediterranean Sea: ZOOPLANKTON AND WINTER DEEP CONVECTION. J. Geophys. Res. Oceans 122, 2319–2338. https://doi.org/10.1002/2016JC012176

Dutkiewicz, A., Müller, R.D., O'Callaghan, S., Jónasson, H., 2015. Census of seafloor sediments in the world's ocean. Geology 43, 795–798. https://doi.org/10.1130/G36883.1

Edwards, M., Beaugrand, G., Helaouët, P., Alheit, J., Coombs, S., 2013. Marine Ecosystem Response to the Atlantic Multidecadal Oscillation. PLoS ONE 8, e57212. https://doi.org/10.1371/journal.pone.0057212

Faure, E., Not, F., Benoiston, A.-S., Labadie, K., Bittner, L., Ayata, S.-D., 2019. Mixotrophic protists display contrasted biogeographies in the global ocean. ISME J. 13, 1072–1083. https://doi.org/10.1038/s41396-018-0340-5

Finkel, Z.V., Kotrc, B., 2010. Silica Use Through Time: Macroevolutionary Change in the Morphology of the Diatom Fustule. Geomicrobiol. J. 27, 596–608. https://doi.org/10.1080/01490451003702941

Flynn, K.J., Skibinski, D.O.F., Lindemann, C., 2018. Effects of growth rate, cell size, motion, and elemental stoichiometry on nutrient transport kinetics. PLOS Comput. Biol. 14, e1006118. https://doi.org/10.1371/journal.pcbi.1006118

Garcia, N.S., Sexton, J., Riggins, T., Brown, J., Lomas, M.W., Martiny, A.C., 2018. High Variability in Cellular Stoichiometry of Carbon, Nitrogen, and Phosphorus Within Classes of Marine Eukaryotic Phytoplankton Under Sufficient Nutrient Conditions. Front. Microbiol. 9, 543. https://doi.org/10.3389/fmicb.2018.00543

Gloor, G.B., Macklaim, J.M., Pawlowsky-Glahn, V., Egozcue, J.J., 2017. Microbiome Datasets Are Compositional: And This Is Not Optional. Front. Microbiol. 8, 2224. https://doi.org/10.3389/fmicb.2017.02224

Goering, J.J., Nelson, D.M., Carter, J.A., 1973. Silicic acid uptake by natural populations of marine phytoplankton. Deep Sea Res. Oceanogr. Abstr. 20, 777–789. https://doi.org/10.1016/0011-7471(73)90001-6

Gooday, A.J., Schoenle, A., Dolan, J.R., Arndt, H., 2020. Protist diversity and function in the dark ocean – Challenging the paradigms of deep-sea ecology with special emphasis on foraminiferans and naked protists. Eur. J. Protistol. 75, 125721. https://doi.org/10.1016/j.ejop.2020.125721

Gorsky, G., Ohman, M.D., Picheral, M., Gasparini, S., Stemmann, L., Romagnan, J.-B., Cawood, A., Pesant, S., Garcia-Comas, C., Prejger, F., 2010. Digital zooplankton image analysis using the ZooScan integrated system. J. Plankton Res. 32, 285–303. https://doi.org/10.1093/plankt/fbp124

Gowing, M.M., 1989. Abundance and feeding ecology of Antarctic phaeodarian radiolarians. Mar. Biol. 103, 107–118. https://doi.org/10.1007/BF00391069

Gowing, M.M., 1986. Trophic biology of phaeodarian radiolarians and flux of living radiolarians in the upper 2000 m of the North Pacific central gyre. Deep Sea Res. Part Oceanogr. Res. Pap. 33, 655–674. https://doi.org/10.1016/0198-0149(86)90059-2

Gowing, M.M., Coale, S.L., 1989. Fluxes of living radiolarians and their skeletons along a northeast Pacific transect from coastal upwelling to open ocean waters. Deep Sea Res. Part Oceanogr. Res. Pap. 36, 561–576. https://doi.org/10.1016/0198-0149(89)90006-X

Guidi, L., Chaffron, S., Bittner, L., Eveillard, D., Larhlimi, A., Roux, S., Darzi, Y., Audic, S., Berline, L., Brum, J.R., Coelho, L.P., Espinoza, J.C.I., Malviya, S., Sunagawa, S., Dimier, C., Kandels-Lewis, S., Picheral, M., Poulain, J., Searson, S., Stemmann, L., Not, F., Hingamp, P., Speich, S., Follows, M., Karp-Boss, L., Boss, E., Ogata, H., Pesant, S., Weissenbach, J., Wincker, P., Acinas, S.G., Bork, P., de Vargas, C., Iudicone, D., Sullivan, M.B., Raes, J., Karsenti, E., Bowler, C., Gorsky, G., 2016. Plankton networks driving carbon export in the oligotrophic ocean. Nature 532, 465–470. https://doi.org/10.1038/nature16942

Guillou, L., Bachar, D., Audic, S., Bass, D., Berney, C., Bittner, L., Boutte, C., Burgaud, G., de Vargas, C., Decelle, J., del Campo, J., Dolan, J.R., Dunthorn, M., Edvardsen, B., Holzmann, M., Kooistra, W.H.C.F., Lara, E., Le Bescot, N., Logares, R., Mahé, F., Massana, R., Montresor, M., Morard, R., Not, F., Pawlowski, J., Probert, I., Sauvadet, A.-L., Siano, R., Stoeck, T., Vaulot, D., Zimmermann, P., Christen, R., 2012. The Protist Ribosomal Reference database (PR2): a catalog of unicellular eukaryote Small Sub-Unit rRNA sequences with curated taxonomy. Nucleic Acids Res. 41, D597–D604. https://doi.org/10.1093/nar/gks1160

Haeckel, E., 1887. Report on the Radiolaria collected by H. M. S. Challenger during the years 1873-1876. Rep Voyage Chall. Zool 18, 1–1803.

Hamm, C.E., Merkel, R., Springer, O., Jurkojc, P., Maier, C., Prechtel, K., Smetacek, V., 2003. Architecture and material properties of diatom shells provide effective mechanical protection. Nature 421, 841–843. https://doi.org/10.1038/nature01416

Heath, G.R., 1974. Dissolved Silica in Deep-Sea Sediments, in: Studies in Paleo-Oceanography, Society of Economic Paleontology and Mineralogy Special Publication. pp. 77–93.

Hendry, K.R., Marron, A.O., Vincent, F., Conley, D.J., Gehlen, M., Ibarbalz, F.M., Quéguiner, B., Bowler, C., 2018. Competition between Silicifiers and Non-silicifiers in the Past and Present Ocean and Its Evolutionary Impacts. Front. Mar. Sci. 5, 22. https://doi.org/10.3389/fmars.2018.00022

Honjo, S., Manganini, S.J., Krishfield, R.A., Francois, R., 2008. Particulate organic carbon fluxes to the ocean interior and factors controlling the biological pump: A synthesis of global sediment trap programs since 1983. Prog. Oceanogr. 76, 217–285. https://doi.org/10.1016/j.pocean.2007.11.003

Ishitani, Y., Takahashi, K., 2007. The vertical distribution of Radiolaria in the waters surrounding Japan. Mar. Micropaleontol. 65, 113–136. https://doi.org/10.1016/j.marmicro.2007.06.002

Itaki, T., Ito, M., Narita, H., Ahagon, N., Sakai, H., 2003. Depth distribution of radiolarians from the Chukchi and Beaufort Seas, western Arctic. Deep Sea Res. Part Oceanogr. Res. Pap. 50, 1507–1522. https://doi.org/10.1016/j.dsr.2003.09.003

Jin, X., Gruber, N., Dunne, J.P., Sarmiento, J.L., Armstrong, R.A., 2006. Diagnosing the contribution of phytoplankton functional groups to the production and export of particulate organic carbon, $CaCO_3$, and opal from global nutrient and alkalinity distributions: DIAGNOSING PHYTOPLANKTON FUNCTIONAL GROUPS. Glob. Biogeochem. Cycles 20, n/a-n/a. https://doi.org/10.1029/2005GB002532

Keeling, P.J., Burki, F., 2019. Progress towards the Tree of Eukaryotes. Curr. Biol. 29, R808–R817. https://doi.org/10.1016/j.cub.2019.07.031

Kling, S.A., Boltovskoy, D., 1995. Radiolarian vertical distribution patterns across the Southern California current. Deep Sea Res. Part Oceanogr. Res. Pap. 42, 191–231. https://doi.org/10.1016/0967-0637(94)00038-T

Krabberød, A.K., Bråte, J., Dolven, J.K., Ose, R.F., Klaveness, D., Kristensen, T., Bjørklund, K.R., Shalchian-Tabrizi, K., 2011. Radiolaria Divided into Polycystina and Spasmaria in Combined 18S and 28S rDNA Phylogeny. PLoS ONE 6, e23526. https://doi.org/10.1371/journal.pone.0023526

Krause, J.W., Brzezinski, M.A., Baines, S.B., Collier, J.L., Twining, B.S., Ohnemus, D.C., 2017. Picoplankton contribution to biogenic silica stocks and production rates in the Sargasso Sea: Picoplankton bSi Stock and Production. Glob. Biogeochem. Cycles 31, 762–774. https://doi.org/10.1002/2017GB005619

Lampitt, R.S., Salter, I., Johns, D., 2009. Radiolaria: Major exporters of organic carbon to the deep ocean: Radiolaria export carbon to the deep ocean. Glob. Biogeochem. Cycles 23, n/a-n/a. https://doi.org/10.1029/2008GB003221

Latasa, M., 2014. A simple method to increase sensitivity for RP-HPLC phytoplankton pigment analysis: Increased HPLC sensitivity. Limnol. Oceanogr. Methods 12, 46–53. https://doi.org/10.4319/lom.2014.12.46

Lazarus, D.B., Kotrc, B., Wulf, G., Schmidt, D.N., 2009. Radiolarians decreased silicification as an evolutionary response to reduced Cenozoic ocean silica availability. Proc. Natl. Acad. Sci. 106, 9333–9338. https://doi.org/10.1073/pnas.0812979106

Le Queré, C., Harrison, S.P., Colin Prentice, I., Buitenhuis, E.T., Aumont, O., Bopp, L., Claustre, H., Cotrim Da Cunha, L., Geider, R., Giraud, X., Klaas, C., Kohfeld, K.E., Legendre, L., Manizza, M., Platt, T., Rivkin, R.B., Sathyendranath, S., Uitz, J., Watson, A.J., Wolf-Gladrow, D., 2005. Ecosystem dynamics based on plankton functional types for global ocean biogeochemistry models. Glob. Change Biol. 0, 051013014052005-??? https://doi.org/10.1111/j.1365-2486.2005.1004.x

Leblanc, K., Quéguiner, B., Garcia, N., Rimmelin, P., Raimbault, P., 2003. Silicon cycle in the NW Mediterranean Sea: seasonal study of a coastal oligotrophic site. Oceanol. Acta 26, 339–355. https://doi.org/10.1016/S0399-1784(03)00035-5

Leynaert, A., 1993. La production de la silice biogénique dans l'océan: de la Mer de Weddell à l'Océan Antartique. P. et M. Curie, Paris.

Leynaert, A., Bucciarelli, E., Claquin, P., Dugdale, R.C., Martin-Jézéquel, V., Pondaven, P., Ragueneau, O., 2004. Effect of iron deficiency on diatom cell size and silicic acid uptake kinetics. Limnol. Oceanogr. 49, 1134–1143. https://doi.org/10.4319/lo.2004.49.4.1134

Leynaert, A., Tréguer, P., Nelson, D.M., Del Amo, Y., 1996. 32 Si as a tracer of biogenic silica production: methodological improvements, in: Integrated Marine System Analysis. pp. 29–35.

Llopis Monferrer, N., Boltovskoy, D., Tréguer, P., Sandin, M.M., Not, F., Leynaert, A., 2020. Estimating Biogenic Silica Production of Rhizaria in the Global Ocean. Glob. Biogeochem. Cycles 34. https://doi.org/10.1029/2019GB006286

Lombard, F., Boss, E., Waite, A.M., Vogt, M., Uitz, J., Stemmann, L., Sosik, H.M., Schulz, J., Romagnan, J.-B., Picheral, M., Pearlman, J., Ohman, M.D., Niehoff, B., Möller, K.O., Miloslavich, P., Lara-Lpez, A., Kudela, R., Lopes, R.M., Kiko, R., Karp-Boss, L., Jaffe, J.S., Iversen, M.H., Irisson, J.-O., Fennel, K., Hauss, H., Guidi, L., Gorsky, G., Giering, S.L.C., Gaube, P., Gallager, S., Dubelaar, G., Cowen, R.K., Carlotti, F., Briseño-Avena, C., Berline, L., Benoit-Bird, K., Bax, N., Batten, S., Ayata, S.D., Artigas, L.F., Appeltans, W., 2019. Globally Consistent Quantitative Observations of Planktonic Ecosystems. Front. Mar. Sci. 6, 196. https://doi.org/10.3389/fmars.2019.00196

Maldonado, M., López-Acosta, M., Sitjà, C., García-Puig, M., Galobart, C., Ercilla, G., Leynaert, A., 2019. Sponge skeletons as an important sink of silicon in the global oceans. Nat. Geosci. 12, 815–822. https://doi.org/10.1038/s41561-019-0430-7

Marron, A.O., Ratcliffe, S., Wheeler, G.L., Goldstein, R.E., King, N., Not, F., de Vargas, C., Richter, D.J., 2016. The Evolution of Silicon Transport in Eukaryotes. Mol. Biol. Evol. 33, 3226–3248. https://doi.org/10.1093/molbev/msw209

Martin-Jezequel, V., Hildebrand, M., Brzezinski, M.A., 2000. SILICON METABOLISM IN DIATOMS: IMPLICATIONS FOR GROWTH. J. Phycol. 36, 821–840. https://doi.org/10.1046/j.1529-8817.2000.00019.x

Matsumoto, K., Sarmiento, J.L., Brzezinski, M.A., 2002. Silicic acid leakage from the Southern Ocean: A possible explanation for glacial atmospheric *p* CO_2: SOUTHERN OCEAN SILICIC ACID LEAKAGE. Glob. Biogeochem. Cycles 16, 5-1-5–23. https://doi.org/10.1029/2001GB001442

Matsuzaki, K.M., Nishi, H., Suzuki, N., Cortese, G., Eynaud, F., Takashima, R., Kawate, Y., Sakai, T., 2014. Paleoceanographic history of the Northwest Pacific Ocean over the past 740kyr, discerned from radiolarian fauna. Palaeogeogr. Palaeoclimatol. Palaeoecol. 396, 26–40. https://doi.org/10.1016/j.palaeo.2013.12.036

Mayot, N., D'Ortenzio, F., Taillandier, V., Prieur, L., de Fommervault, O.P., Claustre, H., Bosse, A., Testor, P., Conan, P., 2017. Physical and Biogeochemical Controls of the Phytoplankton Blooms in North Western Mediterranean Sea: A Multiplatform Approach Over a Complete Annual Cycle (2012–2013 DEWEX Experiment). J. Geophys. Res. Oceans 122, 9999–10019. https://doi.org/10.1002/2016JC012052

Méndez-Sandín, M., 2019. Diversité et évolution des nassellaires et spumellaires (radiolaires). Station Biologique de Roscoff.

Michaels, A.F., Caron, D.A., Swanberg, N.R., Howse, F.A., Michaels, C.M., 1995. Planktonic sarcodines (Acantharia, Radiolaria, Foraminifera) in surface waters near Bermuda: abundance, biomass and vertical flux. J. Plankton Res. 17, 131–163. https://doi.org/10.1093/plankt/17.1.131

Milligan, A.J., 2002. A Proton Buffering Role for Silica in Diatoms. Science 297, 1848–1850. https://doi.org/10.1126/science.1074958

Moore, T.C., 1978. The distribution of radiolarian assemblages in the modern and ice-age Pacific. Mar. Micropaleontol. 3, 229–266. https://doi.org/10.1016/0377-8398(78)90030-0

Morley, J.J., Stepien, J.C., 1985. Antarctic Radiolaria in Late Winter/Early Spring Weddell Sea Waters. Micropaleontology 31, 365. https://doi.org/10.2307/1485593

Mortlock, R.A., Froelich, P.N., 1989. A simple method for the rapid determination of biogenic opal in pelagic marine sediments. Deep Sea Res. Part Oceanogr. Res. Pap. 36, 1415–1426. https://doi.org/10.1016/0198-0149(89)90092-7

Nakamura, Y., Imai, I., Yamaguchi, A., Tuji, A., Suzuki, N., 2013. Aulographis japonica sp. nov. (Phaeodaria, Aulacanthida, Aulacanthidae), an abundant zooplankton in the deep sea of the Sea of Japan. Plankton Benthos Res. 8, 107–115. https://doi.org/10.3800/pbr.8.107

Nakamura, Y., Iwata, I., Hori, R.S., Uchiyama, N., Tuji, A., Fujita, M.J., Honda, D., Ohfuji, H., 2018. Elemental composition and ultrafine structure of the skeleton in shell-bearing protists—A case study of phaeodarians and radiolarians. J. Struct. Biol. 204, 45–51. https://doi.org/10.1016/j.jsb.2018.06.008

Nelson, D., DeMaster, D., Dunbar, R., 1994. sedimentary fluxes on the Ross Sea continental shelf 14.

Nelson, D.M., Anderson, R.F., Barber, R.T., Brzezinski, M.A., Buesseler, K.O., Chase, Z., Collier, R.W., Dickson, M.-L., François, R., Hiscock, M.R., Honjo, S., Marra, J., Martin, W.R., Sambrotto, R.N., Sayles, F.L., Sigmon, D.E., 2002. Vertical budgets for organic carbon and biogenic silica in the Pacific sector of the Southern Ocean, 1996–1998. Deep Sea Res. Part II Top. Stud. Oceanogr. 49, 1645–1674. https://doi.org/10.1016/S0967-0645(02)00005-X

Nelson, D.M., Brzezinski, M.A., Sigmon, D.E., Franck, V.M., 2001. A seasonal progression of Si limitation in the Pacific sector of the Southern Ocean. Deep Sea Res. Part II Top. Stud. Oceanogr. 48, 3973–3995. https://doi.org/10.1016/S0967-0645(01)00076-5

Nelson, D.M., Goering, J.J., 1977. A stable isotope tracer method to measure silicic acid uptake by marine phytoplankton. Anal. Biochem. 78, 139–147. https://doi.org/10.1016/0003-2697(77)90017-3

Nelson, D.M., Gordon, L.I., 1982. Production and pelagic dissolution of biogenic silica in the Southern Ocean. Geochim. Cosmochim. Acta 46, 491–501. https://doi.org/10.1016/0016-7037(82)90153-3

Nelson, D.M., Tréguer, P., 1992. Role of silicon as a limiting nutrient to Antarctic diatoms: evidence from kinetic studies in the Ross Sea ice-edge zone. Mar. Ecol. Prog. Ser. 80, 255–264.

Nelson, D.M., Tréguer, P., Brzezinski, M.A., Leynaert, A., Quéguiner, B., 1995. Production and dissolution of biogenic silica in the ocean: Revised global estimates, comparison with regional data and relationship to biogenic sedimentation. Global Biogeochemical Cycle 9, 359–372.

Nimmergut, A., Abelmann, A., 2002. Spatial and seasonal changes of radiolarian standing stocks in the Sea of Okhotsk. Deep Sea Res. Part Oceanogr. Res. Pap. 49, 463–493. https://doi.org/10.1016/S0967-0637(01)00074-7

Not, F., del Campo, J., Balagué, V., de Vargas, C., Massana, R., 2009. New Insights into the Diversity of Marine Picoeukaryotes. PLoS ONE 4, e7143. https://doi.org/10.1371/journal.pone.0007143

Not, F., Gausling, R., Azam, F., Heidelberg, J.F., Worden, A.Z., 2007. Vertical distribution of picoeukaryotic diversity in the Sargasso Sea. Environ. Microbiol. 9, 1233–1252. https://doi.org/10.1111/j.1462-2920.2007.01247.x

Ogane, K., Suzuki, N., Tuji, A., Hori, R.S., 2014. Pseudopodial silica absorption hypothesis (PSA hypothesis): a new function of pseudopodia in living radiolarian polycystine cells. J. Micropalaeontology 33, 143–148. https://doi.org/10.1144/jmpaleo2013-028

Ogane, K., Tuji, A., Suzuki, N., Kurihara, T., Matsuoka, A., 2009. First application of PDMPO to examine silicification in polycystine Radiolaria. Plankton Benthos Res. 4, 89–94. https://doi.org/10.3800/pbr.4.89

Ogane, K., Tuji, A., Suzuki, N., Matsuoka, A., Kurihara, T., Hori, R.S., 2010. Direct observation of the skeletal growth patterns of polycystine radiolarians using a fluorescent marker. Mar. Micropaleontol. 77, 137–144. https://doi.org/10.1016/j.marmicro.2010.08.005

Olenina, I., Hadju, S., Edler, L., Andersoon, A., Wasmund, N., Busch, S., Göbel, J., Gromisz, S., Huseby, S., Huttunen, M., Jaanus, A., Kokkonen, P., Ledaine, I., Niemkiewicz, E., 2006. Biovolumes and size-classes of phytoplankton in the Baltic Sea, Baltic Sea Environment Proceedings N°106. Helsinki Commision. Baltic Marine Environment Protection Commission.

Picheral, M., Colin, S., Irisson, J.-O., 2017. EcoTaxa [WWW Document]. Httpecotaxaobs-Vlfrfr. URL https://ecotaxa.obs-vlfr.fr/ (accessed 6.29.20).

PIQv [WWW Document], n.d. URL https://sites.google.com/view/piqv (accessed 7.1.20).

Polet, S., 2004. Small-Subunit Ribosomal RNA Gene Sequences of Phaeodarea Challenge the Monophyly of Haeckel's Radiolaria. Protist 155, 53–63. https://doi.org/10.1078/1434461000164

Pondaven, P., Ragueneau, O., Tréguer, P., Hauvespre, A., Dezileau, L., Reyss, J.L., 2000. Resolving the 'opal paradox' in the Southern Ocean. Nature 405, 168–172. https://doi.org/10.1038/35012046

Ragueneau, O., Savoye, N., Del Amo, Y., Cotten, J., Tardiveau, B., Leynaert, A., 2005. A new method for the measurement of biogenic silica in suspended matter of coastal waters: using Si:Al ratios to correct for the mineral interference. Cont. Shelf Res. 25, 697–710. https://doi.org/10.1016/j.csr.2004.09.017

Reynolds, C.S., 2001. Emergence in pelagic communities. Sci. Mar. 65, 5–30. https://doi.org/10.3989/scimar.2001.65s25

Riedel, G.F., Nelson, D.M., 1985. Silicon uptake by algae with no known Si requirement. II. Strong pH dependence of uptake kinetic parameters in Phaeodactylum tricornutum (Bacillariophyceae). J. Phycol. 21, 168–171.

Robinson, A.R., Leslie, W.G., Theocharis, A., Lascaratos, A., 2001. Mediterranean Sea Circulation, in: Encyclopedia of Ocean Sciences. Elsevier, pp. 1689–1705. https://doi.org/10.1006/rwos.2001.0376

Rognes, T., Flouri, T., Nichols, B., Quince, C., Mahé, F., 2016. VSEARCH: a versatile open source tool for metagenomics. PeerJ 4, e2584. https://doi.org/10.7717/peerj.2584

Romagnan, J.-B., Legendre, L., Guidi, L., Jamet, J.-L., Jamet, D., Mousseau, L., Pedrotti, M.-L., Picheral, M., Gorsky, G., Sardet, C., Stemmann, L., 2015. Comprehensive Model of Annual Plankton Succession Based on the Whole-Plankton Time Series Approach. PLOS ONE 10, e0119219. https://doi.org/10.1371/journal.pone.0119219

Safi, K.A., Brian Griffiths, F., Hall, J.A., 2007. Microzooplankton composition, biomass and grazing rates along the WOCE SR3 line between Tasmania and Antarctica. Deep Sea Res. Part Oceanogr. Res. Pap. 54, 1025–1041. https://doi.org/10.1016/j.dsr.2007.05.003

Schröder, S.-M., Kiko, R., Irisson, J.-O., Koch, R., 2019. Low-Shot Learning of Plankton Categories, in: Brox, T., Bruhn, A., Fritz, M. (Eds.), Pattern Recognition. Springer International Publishing, Cham, pp. 391–404. https://doi.org/10.1007/978-3-030-12939-2_27

Schroeder, A., Stanković, D., Pallavicini, A., Gionechetti, F., Pansera, M., Camatti, E., 2020. DNA metabarcoding and morphological analysis - Assessment of zooplankton biodiversity in transitional waters. Mar. Environ. Res. 160, 104946. https://doi.org/10.1016/j.marenvres.2020.104946

Shipe, R.F., Brzezinski, M.A., 2001. A time series study of silica production and flux in an eastern boundary region: Santa Barbara Basin, California. Glob. Biogeochem. Cycles 15, 517–531. https://doi.org/10.1029/2000GB001297

Siever, R., 1991. Silica in the oceans: biological-geochemical interplay, in: Scientis on Gaia. S. H. Schneider and P. J. Boston, (Cambridge, MA: MIT Press), pp. 287–295.

Smith, W.O., Kaufman, D.E., 2018. Climatological temporal and spatial distributions of nutrients and particulate matter in the Ross Sea. Prog. Oceanogr. 168, 182–195. https://doi.org/10.1016/j.pocean.2018.10.003

Stoeck, T., Bass, D., Nebel, M., Christen, R., Jones, M.D.M., Breiner, H.-W., Richards, T.A., 2010. Multiple marker parallel tag environmental DNA sequencing reveals a highly complex eukaryotic community in marine anoxic water. Mol. Ecol. 19, 21–31. https://doi.org/10.1111/j.1365-294X.2009.04480.x

Stukel, M.R., Biard, T., Krause, J., Ohman, M.D., 2018. Large Phaeodaria in the twilight zone: Their role in the carbon cycle: Phaeodarian ecology in the twilight zone. Limnol. Oceanogr. 63, 2579–2594. https://doi.org/10.1002/lno.10961

Sun, J., 2003. Geometric models for calculating cell biovolume and surface area for phytoplankton. J. Plankton Res. 25, 1331–1346. https://doi.org/10.1093/plankt/fbg096

Suzuki, N., Not, F., 2015. Biology and Ecology of Radiolaria, in: Marine Protists: Diversity and Dynamics. Springer, Tokyo; New York, pp. 179–222.

Suzuki, N., Oba, M., 2015. Oldest Fossil Records of Marine Protists and the Geologic History Toward the Establishment of the Modern-Type Marine Protist World, in: Marine Protists: Diversity and Dynamics. Springer, Tokyo; New York, pp. 359–394.

Takahashi, K., 1983. Radiolaria: sinking population, standing stock, and production rate. Marine Micropaleontology 8, 171–181.

Takahashi, K., 1981. Vertical flux, Ecology and dissolution of radiolaria in Tropical Oceans: Implications for the Silica cycle. Massachusetts Institute of Technology and Woods Hole Oceanographic Institution.

Takahashi, K., Hurd, D.C., Honjo, S., 1983. Phaeodarian Skeletons: Their Role in Silica Transport to the Deep Sea. Science 222, 616–618. https://doi.org/10.1126/science.222.4624.616

Tanaka, S., Takahashi, K., 2008. Detailed vertical distribution of radiolarian assemblage (0-3000 m, fifteen layers) in the central subarctic Pacific, June 2006 24.

Thamatrakoln, K., Hildebrand, M., 2008. Silicon Uptake in Diatoms Revisited: A Model for Saturable and Nonsaturable Uptake Kinetics and the Role of Silicon Transporters. Plant Physiol. 146, 1397–1407.

Toullec, J., Vincent, D., Frohn, L., Miner, P., Le Goff, M., Devesa, J., Moriceau, B., 2019. Copepod Grazing Influences Diatom Aggregation and Particle Dynamics. Front. Mar. Sci. 6, 751. https://doi.org/10.3389/fmars.2019.00751

Tréguer, De La Rocha, C.L., 2013. The World Ocean Silica Cycle. Annu. Rev. Mar. Sci. 5, 477–501. https://doi.org/10.1146/annurev-marine-121211-172346

Tréguer, P., Kamatani, A., Gueneley, S., Quéguiner, B., 1989. Kinetics of dissolution of Antarctic Diatom Frustules and the Biogeocheical Cycle in the Southern Ocean 397–403.

Tréguer, P., Lindner, L., van Bennekom, A.J., Leynaert, A., Panouse, M., Jacques, G., 1991. Production of biogenic silica in the Weddell-Scotia Seas measured with ^{32} Si. Limnol. Oceanogr. 36, 1217–1227. https://doi.org/10.4319/lo.1991.36.6.1217

Tréguer, P., Nelson, D.M., Van Bennekom, A.J., DeMaster, D.J., Leynaert, A., Queguiner, B., 1995. The Silica Balance in the World Ocean: A Reestimate. Science 268, 375–379. https://doi.org/10.1126/science.268.5209.375

Tréguer, P.J., 2014. The Southern Ocean silica cycle. Comptes Rendus Geosci. 346, 279–286. https://doi.org/10.1016/j.crte.2014.07.003

Uitz, J., Claustre, H., Morel, A., Hooker, S.B., 2006. Vertical distribution of phytoplankton communities in open ocean: An assessment based on surface chlorophyll. J. Geophys. Res. 111, C08005. https://doi.org/10.1029/2005JC003207

Utermohl, H., 1958. Zur Ver vollkommung der quantitativen phytoplankton-methodik. Mitt int verein. theor. amgew. Limnol. 1–38.

White, K.K., Dugdale, R.C., 1997. Silicate and nitrate uptake in the Monterey Bay upwelling system. Cont. Shelf Res. 17, 455–472. https://doi.org/10.1016/S0278-4343(96)00042-8

Annexes

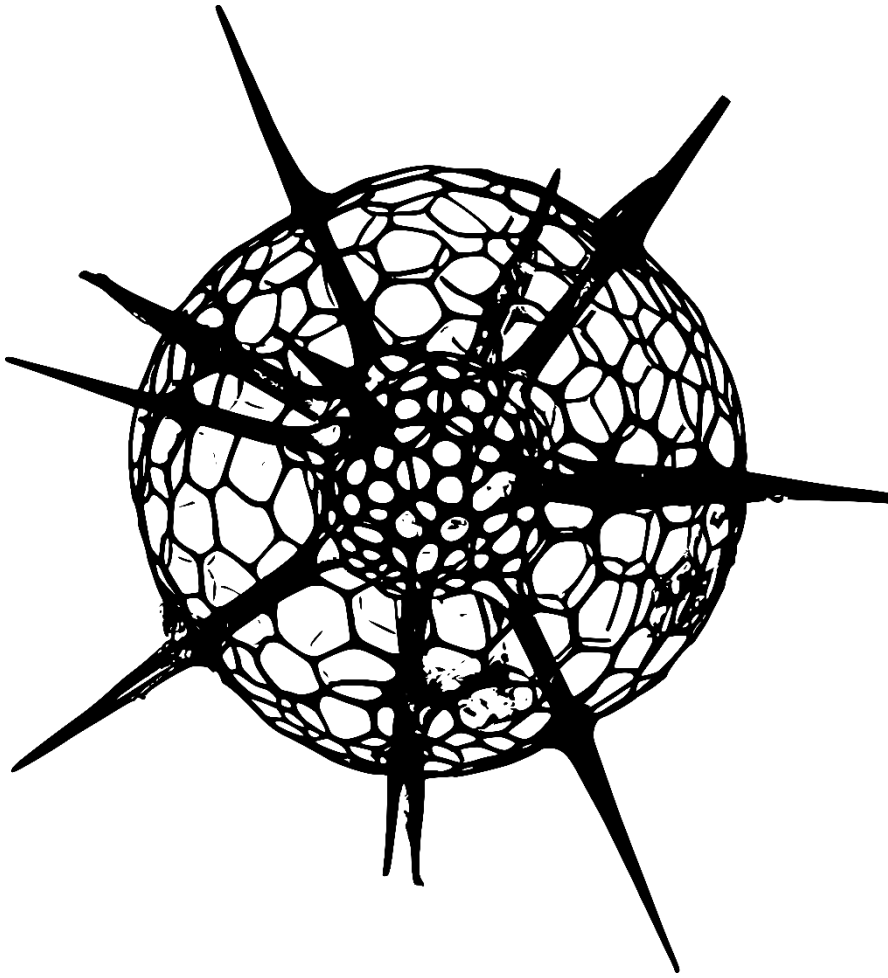

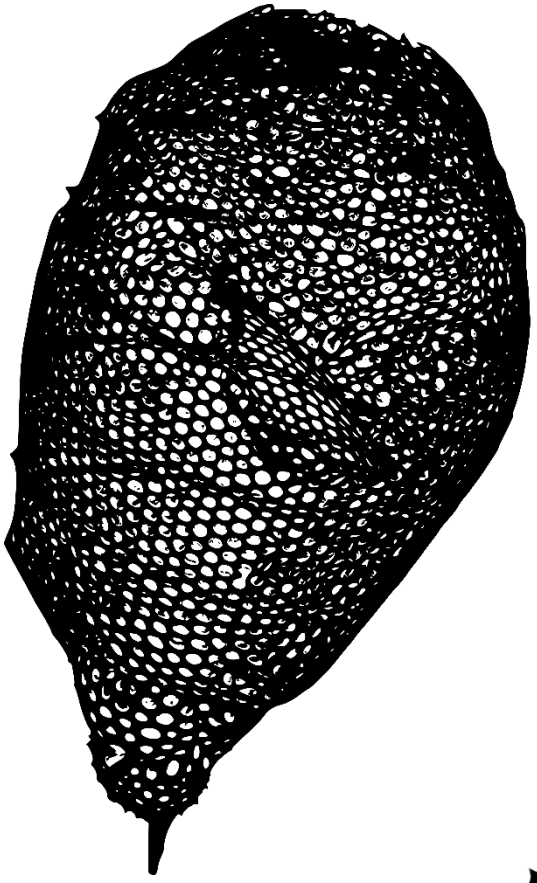

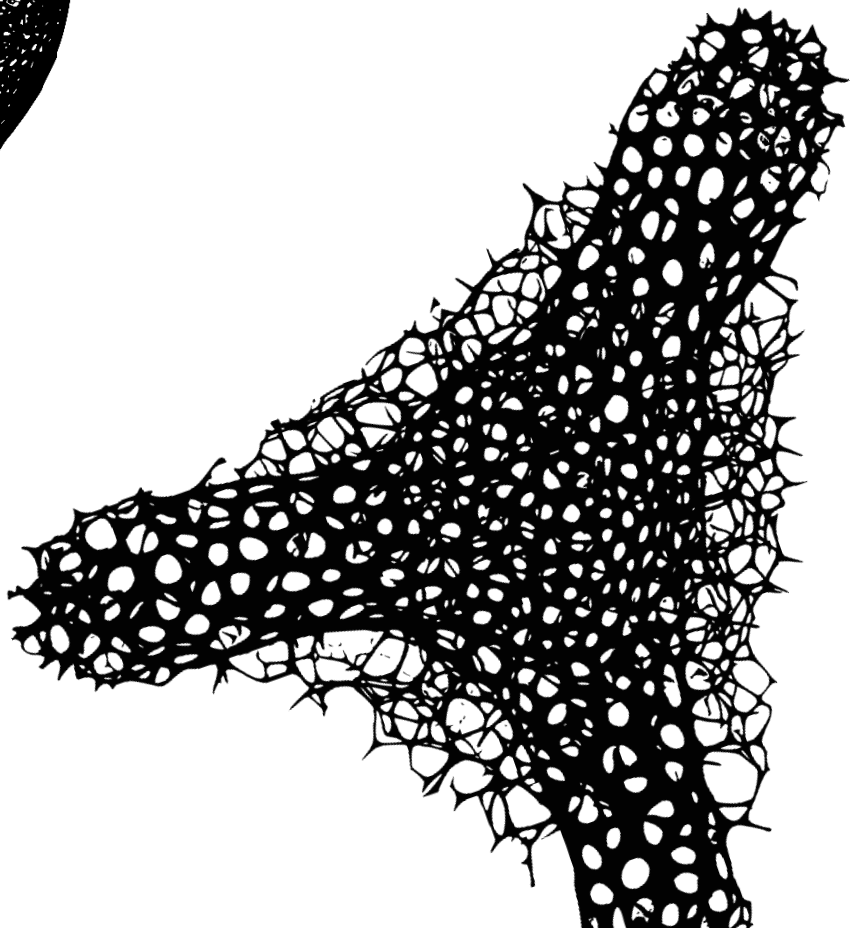

Drawings of Nassellaria and Spumellaria specimens from Miguel Méndez-Sandin pictures.

AMT28 Cruise – Preliminary results

This annex presents the preliminary results of the AMT28 cruise (23 September – 29 October 2018), from Harwich to the Falkland Islands aboard the Royal Research Ship James Clark Ross.

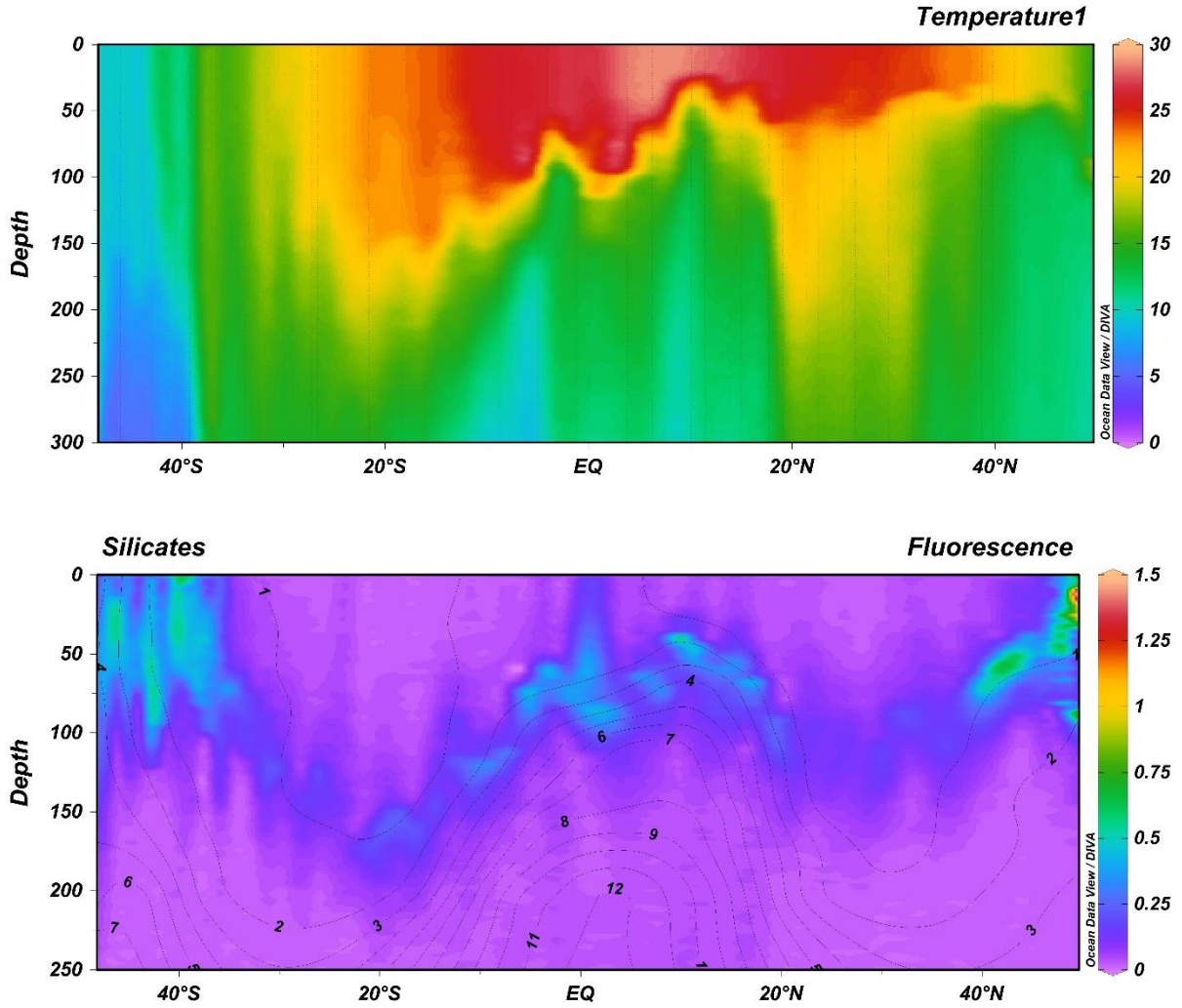

Figure 1. Basin-scale patterns of seawater temperature in °C and fluorescence with silicates concentrations in µM (black lines) in the upper 300 m of the water column along the AMT28.

Table 1. Biogenic silica (bSi) and silica production rates of individuals collected along the AMT28 cruise. *Cruise_Station_type of sample_taxonomic.group_filter.number.

Bongo	Latitude	Longitude	Station_ID*	bSi nmol Si cell $^{-1}$	Si poduction nmol Si cell^{-1} d^{-1}
2	46.0291	-12.7325	AMT28_st3_Bsi_phaeo#2	2.23	NA
2	46.0291	-12.7325	AMT28_st3_Bsi_phaeo#4	21.04	NA
2	46.0291	-12.7325	AMT28_st4_Bsi_phaeo#1	3.09	NA
4	39.7193	-17.7161	AMT28_st8_Bsi_spum#4	3.01	NA
4	39.7193	-17.7161	AMT28_st8_Bsi_spum#8	37.12	NA
4	39.7193	-17.7161	AMT28_st8_32Si_spum#5	6.30	0.18
4	39.7193	-17.7161	AMT28_st8_32Si_spum#6	1.52	2.61
4	39.7193	-17.7161	AMT28_st8_32Si_spum#7	8.50	0.79
5	36.4139	-20.1215	AMT28_st10_Bsi_Aulas#4	19.00	NA
5	36.4139	-20.1215	AMT28_st10_Bsi_Aulac#8	19.88	NA
5	36.4139	-20.1215	AMT28_st10_Si32_spum#2	12.57	1.28
6	33.0469	-22.1368	AMT28_st12_Si32_phaeoc#2	22.08	0.32
6	33.0469	-22.1368	AMT28_st12_Si32_spum#1	0.87	0.23
7	29.4883	-23.9325	AMT28_st14_Bsi_phaeo#4	7.47	NA
9	22.5997	-27.2134	AMT28_st18_Si32_phaeocalp#3	50.59	0.65
9	22.5997	-27.2134	AMT28_st18_Si32_spum#1	1.78	0.27
9	22.5997	-27.2134	AMT28_st18_Si32_spum#2	14.07	0.93
10	19.0778	-28.8168	AMT28_st20_Si32_spum#1	2.01	0.06
10	19.0778	-28.8168	AMT28_st20_Si32_spum#7	2.35	0.14
12	11.4470	-27.7087	AMT28_st24_32Si_paheo#1	3.80	0.16
12	11.4470	-27.7087	AMT28_st24_32Si_spum#2	4.46	0.35
12	11.4470	-27.7087	AMT28_st24_32Si_spum#3	1.57	0.12
12	11.4470	-27.7087	AMT28_st24_32Si_spum#8	8.58	0.31
13	7.4713	-26.6501	AMT28_st27_BSi_phaeo#1	9.66	NA
13	7.4713	-26.6501	AMT28_st27_BSi_phaeo#4	14.09	NA
13	7.4713	-26.6501	AMT28_st27_BSi_spum#5	15.47	NA
13	7.4713	-26.6501	AMT28_st27_BSi_spum#9	13.00	NA
13	7.4713	-26.6501	AMT28_st27_BSi_phaeo#10	16.13	NA
15	0.0005	-24.9992	AMT28_st30_BSi_spum#6	9.47	NA
16	-3.6918	-24.9774	AMT28_st32_BSi_nass#1	4.42	NA
18	-11.2623	-24.9374	AMT28_st36_Si32_phaeo#5	13.20	0.51
18	-11.2623	-24.9374	AMT28_st36_Si32_spum#3	3.72	0.63
19	-14.7798	-24.9847	AMT28_st38_Si32_phaeo#2	27.90	0.52
20	-18.3390	-25.0858	AMT28_st41_Si32_nass#7	22.76	0.88
20	-18.3393	-25.0857	AMT28_st41_Si32_phaeo#6	70.59	4.93

20	-18.3393	-25.0857	AMT28_st41_Si32_spum#2	1.27	0.25
21	-20.3793	-25.0595	AMT28_st43_Si32_nass#3	11.94	0.57
21	-20.3793	-25.0595	AMT28_st43_Si32_spum#9	2.33	0.29
22	-24.0000	-25.0000	AMT28_st45_Si32_nass#1	13.17	0.2
22	-23.9995	-24.9993	AMT28_st45_Si32_spum#2	1.64	0.79
22	-23.9995	-24.9993	AMT28_st45_Si32_spum#3	2.50	3.58
22	-23.9995	-24.9993	AMT28_st45_Si32_spum#6	1.58	3.77
22	-23.9995	-24.9993	AMT28_st45_Si32_spum#7	0.46	0.13
22	-23.9995	-24.9993	AMT28_st45_Si32_spum#8	13.82	0.41
23	-26.6280	-27.6554	AMT28_st47_Si32_spum#4	0.88	0.52
23	-26.6280	-27.6554	AMT28_st47_Si32_spum#5	1.37	0.68
23	-26.6280	-27.6554	AMT28_st47_Si32_spum#10	3.34	7.72
24	-29.1280	-30.2230	AMT28_st49_Si32_nass#5	10.12	0.76
24	-29.1276	-30.2235	AMT28_st49_Si32_spum#2	10.45	3.08
24	-29.1276	-30.2235	AMT28_st49_Si32_spum#3	2.40	1.04
24	-29.1276	-30.2235	AMT28_st49_Si32_spum#6	3.22	0.64
24	-29.1276	-30.2235	AMT28_st49_Si32_spum#7	2.14	7.08
27	-43.0060	-45.9817	AMT28_st61_BSi_nass#1	4.01	NA
27	-43.0060	-45.9817	AMT28_st61_BSi_spum#2	7.67	NA
27	-43.0060	-45.9817	AMT28_st61_BSi_spum#3	11.67	NA
27	-43.0060	-45.9817	AMT28_st61_BSi_phaeo#4	25.83	NA
28	-45.2975	-48.8964	AMT28_st63_Si32_nass#4	2.20	0.77
28	-45.2976	-48.8965	AMT28_st63_Si32_phaeo#2	11.56	0.68
28	-45.2976	-48.8965	AMT28_st63_Si32_spum#3	7.08	2.80
28	-45.2976	-48.8965	AMT28_st63_Si32_spum#9	56.86	5.32
29	-47.5618	-51.7740	AMT28_st65_Si32_phaeo#3	2.10	0.38
29	-47.5618	-51.7740	AMT28_st65_Si32_phaeo#4	2.92	0.57
29	-47.5618	-51.7740	AMT28_st65_Si32_phaeo#7	47.11	15.98

Table 2. Average biogenic silica stocks and production rates of siliceous Rhizaria per cell, over the entire cruise. ESD is the equivalent spherical diameter; n, denotes the number of samples analysed; and cells corresponds to the number of specimens analysed.

Taxonomic group	**n**	**cells**	**bSi** **nmol-Si cell^{-1}**	**Si production** **nmol-Si cell^{-1} d^{-1}**	**ESD** **µm**
Phaeodaria (> 300 µm)	6	45	17.1 ± 16.6	4.4 ± 7.7	787.5 ± 156.4
Phaeodaria (< 300 µm)	14	118	20.5 ± 19.2	1.2 ± 1.8	129.3 ± 46.8
Nassellaria	8	29	9.0 ± 6.9	0.6 ± 0.2	142.0 ± 24.6
Spumellaria	35	570	7.8 ± 11.1	1.6 ± 2.1	154.4 ± 55.5

Table 3. Biogenic silica stocks and production rates of phytoplankton community.

CTD	Depth m	Longitude	Latitude	Temperature °C	Fluorescence	Salinity PSU	bSi µM	bSi production nmol Si d^{-1}	Nitrite µM	Phosphate µM	Silicate µM
CTD002	25	-8.8365	48.4693	16.4	1.0	35.5	0.25	0.10	0.1	0.1	0.3
CTD002	10	-8.8365	48.4693	16.4	0.4	35.5	0.35	16.37	0.1	0.1	0.3
CTD002	5	-8.8365	48.4693	16.4	0.6	35.5	0.32	1.38	0.1	0.1	0.2
CTD006	23	-15.2132	42.9670	19.7	0.1	35.8	0.06	0.11	0.0	0.0	0.3
CTD006	7	-15.2132	42.9670	NA	NA	NA	0.08	0.28	NA	NA	NA
CTD006	5	-15.2132	42.9670	19.7	0.1	35.8	0.12	0.15	0.0	0.1	0.3
CTD010	45	-20.1215	36.4140	20.4	0.1	36.4	0.02	0.05	0.0	0.0	0.3
CTD010	14	-20.1215	36.4140	23.2	0.0	36.6	0.02	0.18	0.0	0.0	0.3
CTD010	5	-20.1215	36.4140	23.2	0.0	36.6	0.02	0.18	0.0	0.0	0.2
CTD014	45	-23.9325	29.4883	22.1	0.0	36.9	0.02	0.13	0.0	0.0	0.3
CTD014	15	-23.9325	29.4883	24.8	0.0	37.3	0.04	0.27	0.0	0.0	0.3
CTD014	5	-23.9325	29.4883	25.0	0.0	37.2	0.03	0.21	0.0	0.0	0.3
CTD018	41	-27.2133	22.5997	25.5	0.1	37.2	0.01	0.11	0.0	0.0	0.3
CTD018	13	-27.2133	22.5997	25.8	0.0	37.2	0.01	0.18	0.0	0.0	0.4
CTD018	5	-27.2133	22.5997	25.8	0.0	37.2	0.01	0.49	0.0	0.0	0.3
CTD022	25	-28.6127	15.0760	26.9	0.1	36.3	0.03	0.71	0.0	0.1	0.9
CTD022	7	-28.6127	15.0760	27.1	0.1	36.3	0.02	0.62	0.0	0.0	0.8
CTD022	5	-28.6127	15.0760	27.1	0.1	36.3	0.02	0.99	0.0	0.0	0.8
CTD027	30	-26.3800	6.2560	NA	NA	NA	0.02	0.54	NA	NA	NA
CTD027	9	-26.3800	6.2560	NA	NA	NA	0.04	0.45	NA	NA	NA
CTD027	5	-26.3800	6.2560	28.7	0.1	35.0	0.08	0.58	0.0	0.0	1.0
CTD030	26	-24.9907	-1.1518	26.8	0.1	36.0	0.06	7.54	0.0	0.0	1.4
CTD030	8	-24.9907	-1.1518	27.0	0.0	36.0	0.05	3.33	0.0	0.0	1.4
CTD030	5	-24.9907	-1.1518	27.0	0.0	36.0	0.06	4.81	0.0	0.0	1.4
CTD034	47	-24.9485	-8.7632	26.0	0.0	36.4	0.02	1.78	0.0	0.0	1.1
CTD034	15	-24.9485	-8.7632	NA	NA	NA	0.02	1.57	NA	NA	NA
CTD034	5	-24.9485	-8.7632	26.0	0.0	36.4	0.02	2.54	0.0	0.0	1.0
CTD038	62	-24.9485	-8.7632	NA	NA	NA	0.02	0.32	NA	NA	NA
CTD038	20	-25.0235	-16.0323	23.8	0.0	37.1	0.01	0.52	0.0	0.1	0.6
CTD038	5	-25.0235	-16.0323	23.8	0.0	37.1	0.01	0.47	0.0	0.1	0.7
CTD043	70	-25.9033	-24.9058	22.0	0.1	36.7	0.01	0.26	0.0	0.0	0.8
CTD043	25	-25.9033	-24.9058	NA	NA	NA	0.02	0.58	NA	NA	NA
CTD043	5	-25.9033	-24.9058	22.0	0.0	36.7	0.02	0.65	0.0	0.0	0.9
CTD047	56	-31.1497	-30.0060	18.9	0.0	35.9	0.02	1.57	0.0	0.0	1.0
CTD047	17	-31.1497	-30.0060	19.6	0.0	36.1	0.01	0.44	0.0	0.0	1.1
CTD047	5	-31.1497	-30.0060	19.6	0.0	36.1	0.02	0.89	0.0	0.0	0.9
CTD051	56	-36.0915	-34.5805	16.4	0.1	35.6	0.02	4.35	0.0	0.1	0.8
CTD051	17	-36.0915	-34.5805	NA	NA	NA	0.03	0.62	NA	NA	NA
CTD051	5	-36.0915	-34.5805	16.4	0.1	35.6	0.03	0.87	0.0	0.1	0.7
CTD055	30	-41.4750	-39.2093	12.6	0.5	35.0	0.09	3.31	0.3	0.6	1.5
CTD055	10	-41.4750	-39.2093	12.6	0.3	35.0	0.08	2.94	0.3	0.5	1.4
CTD055	5	-41.4750	-39.2093	NA	NA	NA	0.10	5.01	NA	NA	NA
CTD059	40	-46.9552	-43.7905	9.6	0.4	34.5	0.13	16.52	0.2	0.8	2.2
CTD059	8	-46.9552	-43.7905	NA	NA	NA	0.11	14.28	NA	NA	NA
CTD059	5	-46.9552	-43.7905	9.6	0.2	34.5	0.12	17.98	0.2	0.8	2.3
CTD063	24	-52.6893	-48.1988	9.9	0.2	34.8	0.09	9.32	0.5	0.8	3.9
CTD063	7	-52.6893	-48.1988	10.0	0.1	34.8	0.12	11.12	0.5	0.8	4.4
CTD063	5	-52.6893	-48.1988	NA	NA	NA	0.11	14.75	NA	NA	NA

Oral and poster presentations

February 2020	Rhizaria and Diatoms: their relative impact on the silicon cycle in the Southern Ocean. OSM San Diego, USA. Poster presentation
June 2019	Contribution of siliceous Rhizaria in the marine silica and carbon cycles. IMBER in Brest, France. Oral presentation
February 2018	Rhizaria: unexpected role in the marine ecosystem and in the silica cycle. OSM ASLO in Portland, USA. Oral presentation

Oceanographic cruises

January 2020	Ross Sea Environment and Ecosystem Voyage 2019 - TAN1901 **(40 days)** Estimate biogenic silica (bSi), carbon and nitrogen stock in Rhizaria and diatoms as well as their production. ^{32}Si, ^{13}C and ^{15}N incubations.
September 2018	Atlantic Meridional Transect - AMT28 **(36 days)** Estimate bSi in Rhizaria and diatoms as well as their Si production. ^{32}Si incubations.
September 2017	Mediterranean Ocean Observing System for the Environment Grande Echélle MOOSE-GE 17 **(12 days)** Estimate bSi and production in Rhizaria.

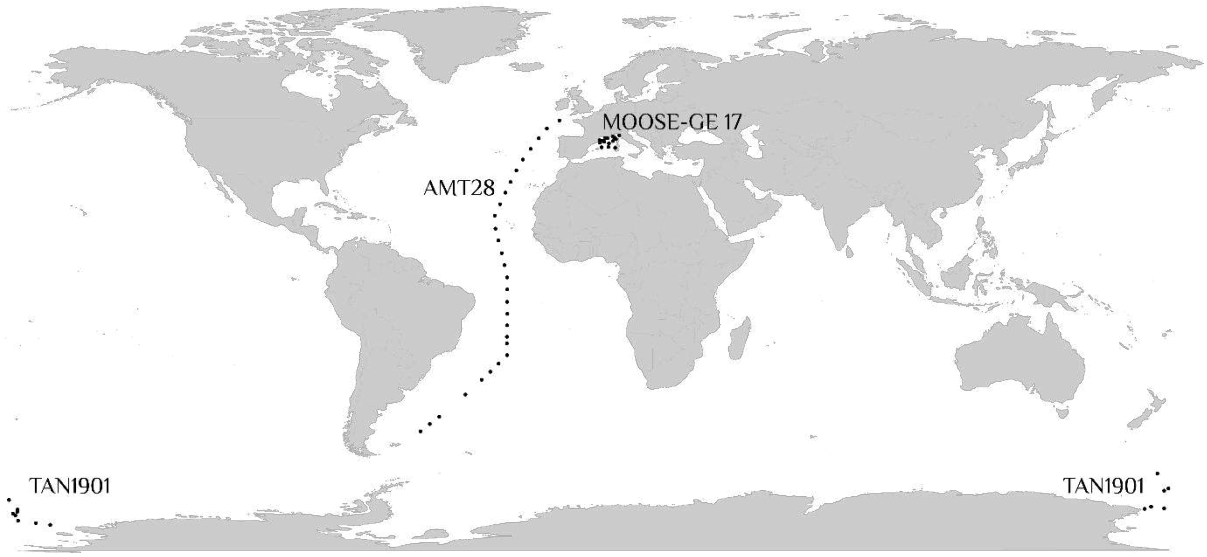

Others

2020 Cover image of *Global Biogeochemical Cycles*, March 2020, Volume 34, Issue 3. The paper “Estimating biogenic silica production of Rhizaria in the global ocean" was selected to be featured as a Research Spotlight on https://Eos.org and on the journal’s website.

2019-2020 Teaching assistance, Biology at Université de Bretagne Occidentale (UBO), Brest, France – 49 h

March 2019 Project *Jeunes Chercheurs*. Science exchange programme investigating plankton diversity with French (Brest) and British (Plymouth) kids

July 2018 Radiation protection course at Laboratoire des sciences de l’Environnement Marin, Brest, France

July 2018 Training in personal survival techniques at Centre Européen de formation continie maritime, Concarneau, France

March 2018 Imaging technologies course (Zooscan and Flowcam) at the Observatoire Océanologique de Villefranche-sur-mer, France

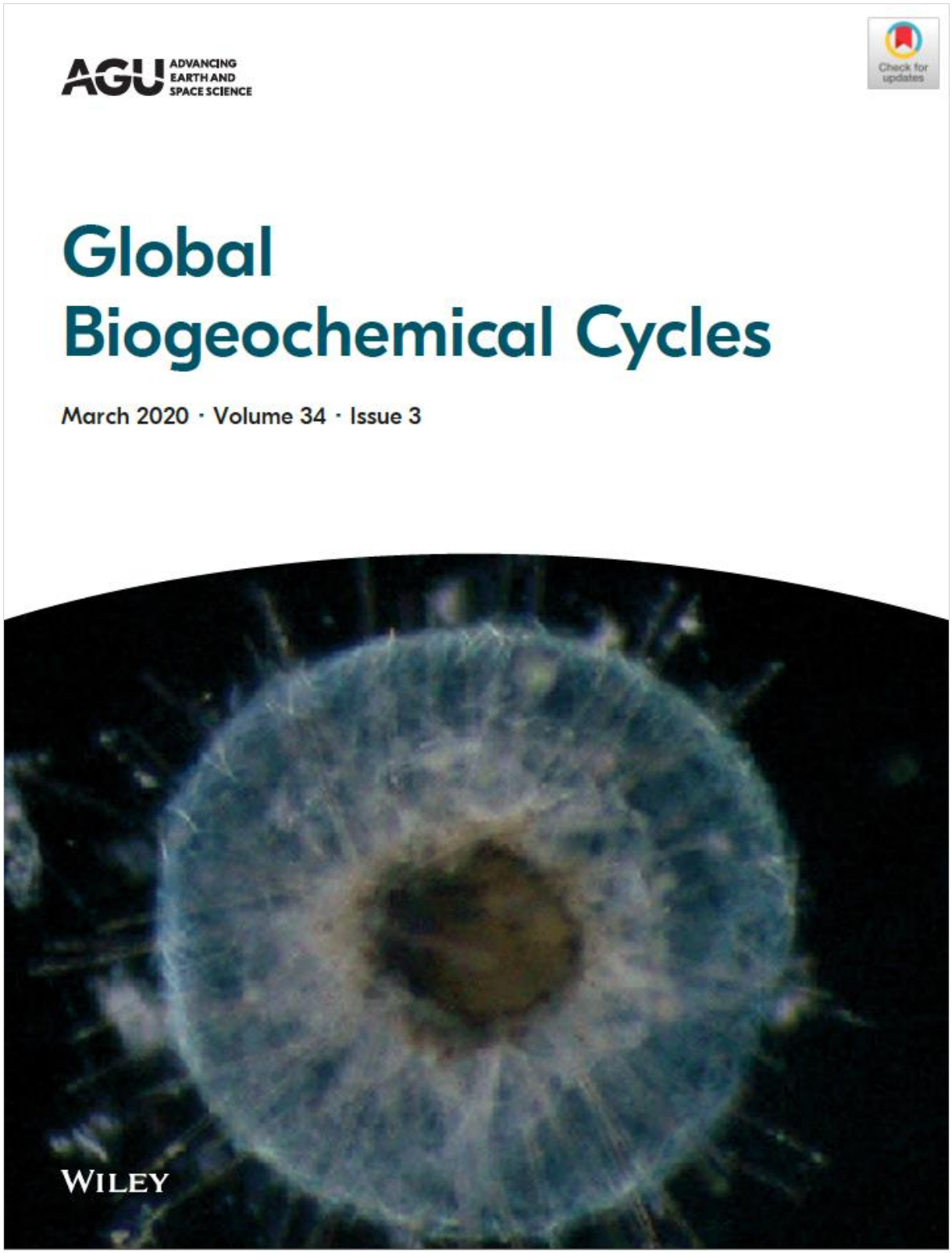

Copy of the original copy of *Global Biogeochemical Cycles*, March 2020, Volume 34, Issue 3

Collaborations

Carbon and nitrogen biomass to volume relation for larger protists – Rhizaria

Joost Samir Mansour[1*], Andreas Norlin[2,3], **Natalia Llopis Monferrer** [4], Stéphane L'Helguen[4] Fabrice Not[1]

[1] Sorbonne University, CNRS, UMR7144 Adaptation and Diversity in Marine Environment (AD2M) laboratory, Ecology of Marine Plankton team, Station Biologique de Roscoff, Place Georges Teissier, 29680 Roscoff, France, [2] Biosciences, Swansea University, Swansea SA2 8PP, UK, [3] Université Libre de Bruxelles, Boulevard du Triomphe, B-1050, Belgium, [4] Univ Brest, CNRS, IRD, Ifremer, LEMAR, F-29280 Plouzane, France

In preparation: Limnology and Oceanography Letters

Abstract

Rhizaria have been shown to be a major component of the protistan community and contribute significantly to carbon flux, silicification and calcification. However, unlike for many other protist, limited data is available on their cellular carbon and nitrogen biomass and biovolume. Data that is important for estimating biomass and for characterizing planktic ecosystems. As previously published biomass to volume (C:vol) equations and ratios are inadequate for large protist, we present such novel data for several Rhizaria (Radiolaria and Phaeodaria). The C:vol and nitrogen to volume (N:vol) of Collodaria central capsules (cc) was significantly correlated and can be accurately estimated from the C:vol equation ngC cc^{-1} = -13.51 + 0.1524 x volume (μm^3) or N:vol. ngN cc^{-1} = -4.33 + 0.0249 x volume (μm^3). Significant biomass to volume correlations were also identified, and corresponding equations are proposed, for C:vol and N:vol of Collodaria colonies, and C:vol of Protocystis. Furthermore, average biomass (C and N) densities are given for all studied Rhizaria, *i.e.* Collodaria, Acantharia, Nassellaria, Spumellaria, *Aulacantha*, *Protocystis* and *Challengeria*. Using the biomass densities and ratios proposed here could show that, with the exception of *Aulacantha*, biomass of these Rhizaria would have been underestimated using previously published generic protist C:vol ratios. Our data will prove valuable for model input and ecological studies of oceanic ecosystems.

The silica cycle in the modern ocean

Paul J. Tréguer[1,2*], Jill N. Sutton[1], Mark Brzezinski[3], Matthew A. Charette[4], Timothy Devries[5], Stephanie Dutkiewicz[6], Claudia Ehlert[7], Jon Hawkings[8], Aude Leynaert[1], Su Mei Liu[9,10], **Natalia Llopis Monferrer**[1], María López-Acosta[11], Manuel Maldonado[11], Shaily Rahman[12], Lihua Ran[13], Olivier Rouxel[14]

[1]Univ Brest, CNRS, IRD, Ifremer, Institut Universitaire Européen de la Mer, LEMAR, Rue Dumont d'Urville, 29280, Plouzané, France; [2]State Key Laboratory of Satellite Ocean Dynamics (SOED), Ministry of Natural Resource, Hangzhou 310012, China; [3]Marine Science Institute, University of California, Santa Barbara, CA, USA; [4]Department of Marine Chemistry and Geochemistry, Woods Hole Oceanographic Institution, Woods Hole, MA 02543 USA; [5]Department of Geography, University of California, Santa Barbara, California, USA; [6]Department of Earth, Atmospheric and Planetary Sciences (DEAPS), Massachusetts Institute of Technology (MIT), Cambridge, MA 02139, USA; [7]Research Group for Marine Isotope Geochemistry, Institute for Chemistry and Biology of the Marine Environment (ICBM), Carl-von Ossietzky University Oldenburg, Germany; [8]National High Magnetic Field Lab and Earth, Ocean and Atmospheric Sciences, Florida State University, USA; [9] Key Laboratory of Marine Chemistry Theory and Technology MOE/ Institute for Advanced Ocean Study, Ocean University of China, Qingdao 266100, China ; [10] Laboratory for Marine Ecology and Environmental Science, Qingdao National Laboratory for Marine Science and Technology, Qingdao 266237, China; [11] Center for Advanced Studies of Blanes (CEAB-CSIC), Acceso Cala St. Francesc 14, Blanes 17300, Girona, Spain; [12] Department of Marine Science, University of Southern Mississippi, Stennis Space Center, MS 39529, USA; [13] Second Institute of Oceanography, Ministry of Natural Resources, P. R. China; [14] IFREMER, Centre de Brest, Technopôle Brest Iroise, Plouzané, France

In preparation: Biogeosciences

Abstract

The element silicon (Si) is required for the growth of silicified organisms, such as diatoms, which globally consume vast amounts of Si concomitantly with N, P, and C, connecting the biogeochemical cycles via processes such as atmospheric CO_2 sequestration. Thus, understanding the Si cycle in the world ocean is a crucial issue for marine biogeochemistry. In this review, we show that recent advances in process studies indicate that total Si inputs and outputs, to and from the world ocean, are ca. 63% and 35% higher, respectively, than previous estimates. These changes are significant, modifying factors such as the geochemical residence time of Si, previously assumed to be >10,000 years, to ca. 6000 years. In addition, new data based on field studies and model outputs allow an updated value of the total annual pelagic biogenic silica production (255 Tmol-Si yr^{-1}) to be calculated. Given these important modifications, we discuss the steady state hypothesis of the Si cycle for past and modern oceans, propose a possible steady state scenario for the global ocean (inputs = outputs = 15.4 Tmol-Si yr^{-1}) and boundary exchange zone, and discuss potential impacts of global change *sensu lato* on the marine Si cycle.

DOCTORAT SCIENCES BRETAGNE DE LA MER LOIRE ET DU LITTORAL

UBO Université de Bretagne Occidentale

Titre : Rôle des Rhizaria dans le cycle biogéochimique du silicium

Mots clés : cycle de la silice, silice biogénique, production de silice, Rhizaria, polycystines, Phaeodaria

Résumé : Les Rhizaria sont des protistes planctoniques présents à la surface et dans l'ensemble des océans. Certains taxons (*i.e.*, polycystines, Phaeodaria) construisent des squelettes siliceux complexes et robustes. Les connaissances de base telles que l'abondance, la diversité, le contenu cellulaire (silice biogénique - bSi, carbone et azote) et les taux d'absorption du silicium (Si) par les Rhizaria sont méconnus, rendant difficile l'évaluation de leur contribution au cycle biogéochimique du Si. Pour y remédier, les taux d'absorption d'acide silicique —en utilisant le radio-isotope ^{32}Si— et le contenu cellulaire en Si ont été mesurés au cours de trois campagnes océanographiques en mer Méditerranée, mer de Ross et dans l'océan Atlantique. Des taux de production élevés (jusqu'à 9 nmol-Si cell^{-1}d^{-1}) et une importante teneur en Si (jusqu'à 11,9 nmol-Si cell-1) ont été observées, par rapport aux microalgues diatomées. En combinant ces résultats avec des données d'abondance publiées, la contribution de ces organismes a permis d'estimer que les Rhizaria contribuent jusqu'à 22 % de la production océanique de bSi. L'abondance, la biomasse et la diversité des Rhizaria ont été quantifiées dans le nord-ouest de la Méditerranée par des outils d'imagerie (FlowCAM, Zooscan et UVP) et des techniques de biologie moléculaire pour couvrir la large gamme de taille des Rhizaria. Cette approche intégrative a révélé que les Rhizaria représentent jusqu'à 6% de la bSi dans les 500 premiers mètres de la colonne d'eau. Ces travaux fournissent des données quantitatives originales qui mettent en évidence l'impact des Rhizairia dans le cycle du Si dans l'océan mondial. Ils révèlent notamment la nécessité d'explorer davantage les couches profondes de l'océan pour affiner les estimations de leur contribution au cycle du Si.

Title : Unveiling the role of Rhizaria in the silicon cycle

Keywords : silicon cycle, biogenic silica, silicic acid uptake, Rhizaria, Polycystina, Phaeodaria

Abstract : Rhizaria are ubiquitous planktonic protists, thriving from surface waters to bathypelagic ecosystems. A number of rhizarians taxa (*i.e.*, polycystines, phaeodarians) build complex and robust siliceous skeletons. Yet, basic knowledge such as abundances, diversity, cellular content (biogenic silica-bSi, carbon and nitrogen) and silicon (Si) uptake rates of rhizarians are poorly known. This lack of knowledge prevents an accurate estimate of their contribution to the Si biogeochemical cycle. To address this issue, Si uptake rates —using the ^{32}Si radioisotope— and cellular content were measured during three research cruises (Mediterranean Sea, Ross Sea and Atlantic Ocean). High individual production rates (up to 9 nmol-Si cell^{-1}d^{-1}) and Si content (up to 11.9 nmol-Si cell^{-1}) were reported, as compared to diatoms. Combining these first results with previously published abundance data, the contribution of these organisms to the biogeochemical cycling of Si was assessed, revealing that Rhizaria contribute up to 22% of the bSi production in the global ocean. Additionally, the abundance, biomass and diversity of Rhizaria were quantified by pairing imaging tools (FlowCAM, Zooscan and UVP) and molecular barcode techniques to cover the wide size range represented by Rhizaria in the NW Mediterranean Sea. This integrative approach revealed that Rhizaria represent up to 6% of the bSi in the first 500 metres of the water column. Overall, this work provides unique quantitative data that highlight the impact of rhizarians in the cycling of Si in the ocean. This thesis work also emphasizes the need to explore further the deep ocean to refine our first estimates of Rhizarian contribution to the Si biogeochemical cycle at local and global scales.